Mesoscale Meteorology

Downbursts and Sting Jets

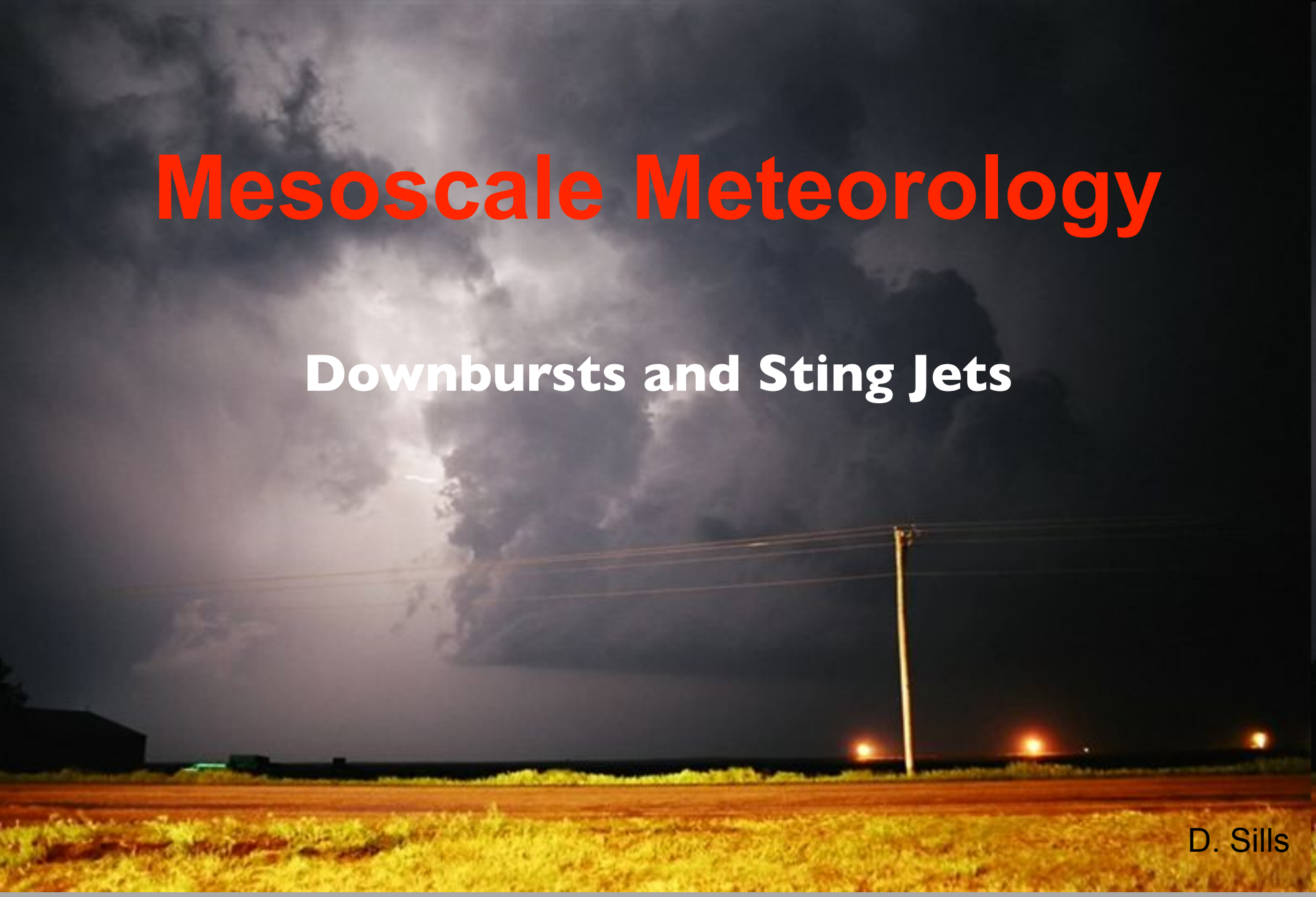

Downbursts

- Introduction to downbursts
- Aircraft hazards
- Downbursts vs microbursts
- Dry vs wet microbursts
- Downbursts on radar
- Downbursts vs derechoes
- Sting Jets

Origin of the Conceptual Model

- Dr. T. Fujita - aerial surveys of damage caused by 3-4 April 1974 ‘super-outbreak’ (148 tornadoes), found strange ‘starburst’ patterns of tree damage.
- While investigating an aircraft accident in 1975, he hypothesized that wind system that caused plane to go down was the same that caused starburst damage pattern in trees.
- Called new wind system a ‘downburst.’

‘Starburst’ Tree Damage

Microbursts & Background Winds

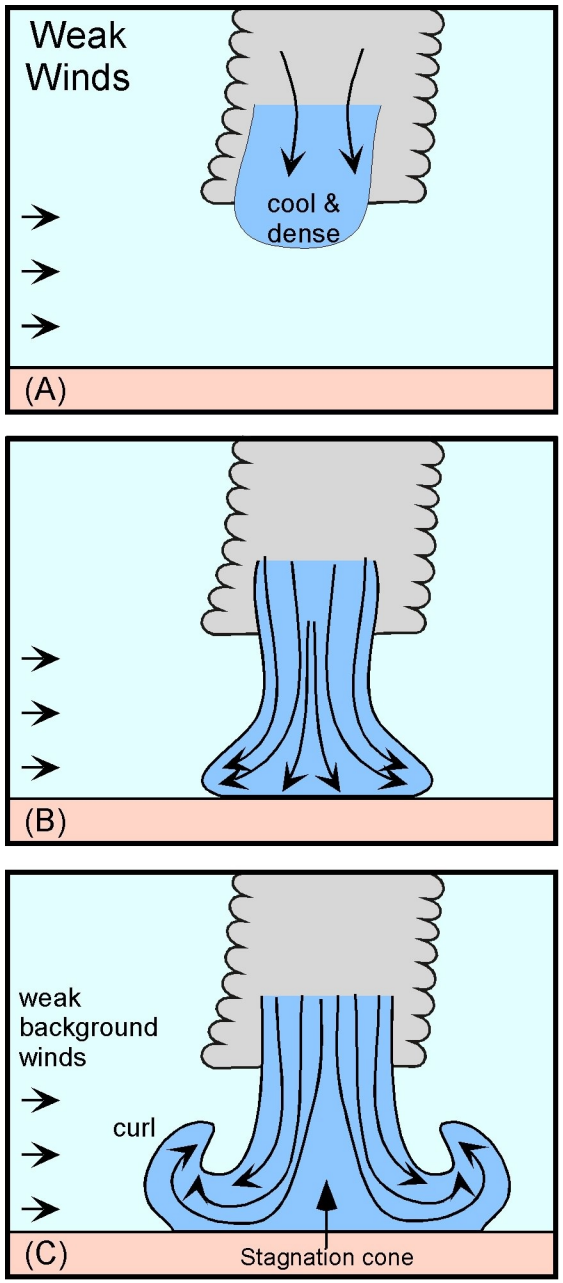

Microbursts & Background Winds

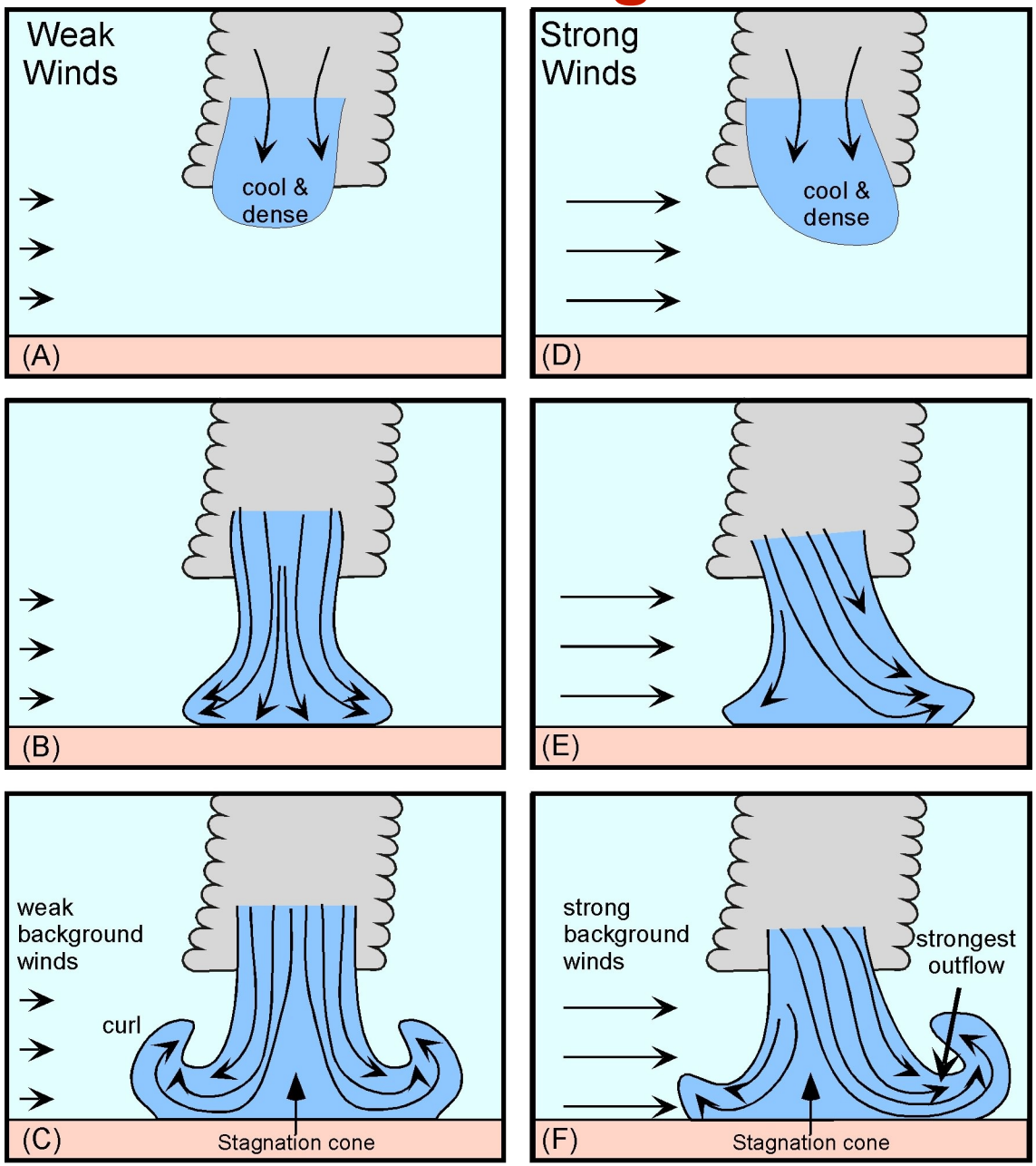

Downburst Video

Pakwash Blowdown 18 Jul 1991

Airport Winds

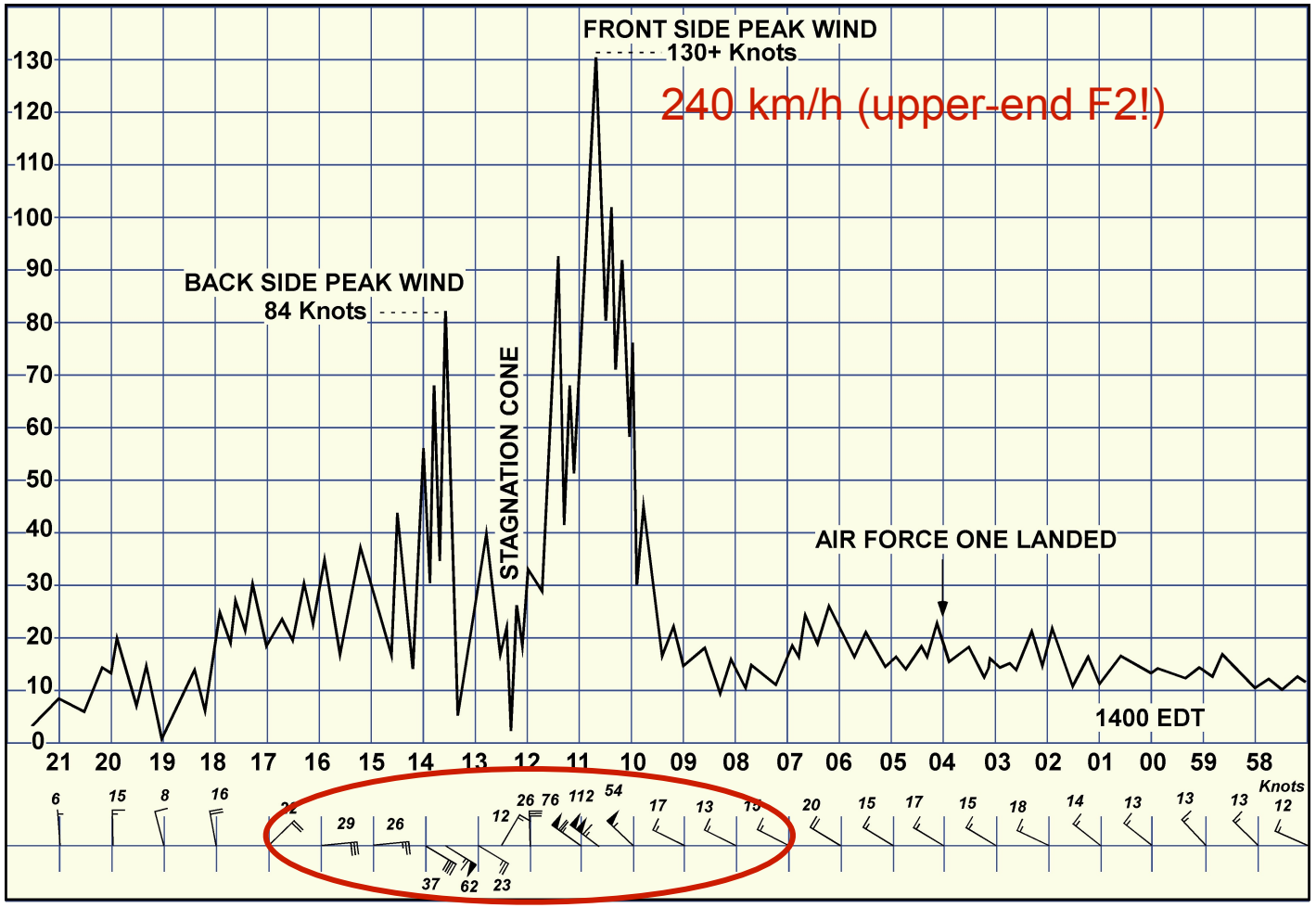

Courtesy of the Theodore Fujita Family

Hazards to Aircraft

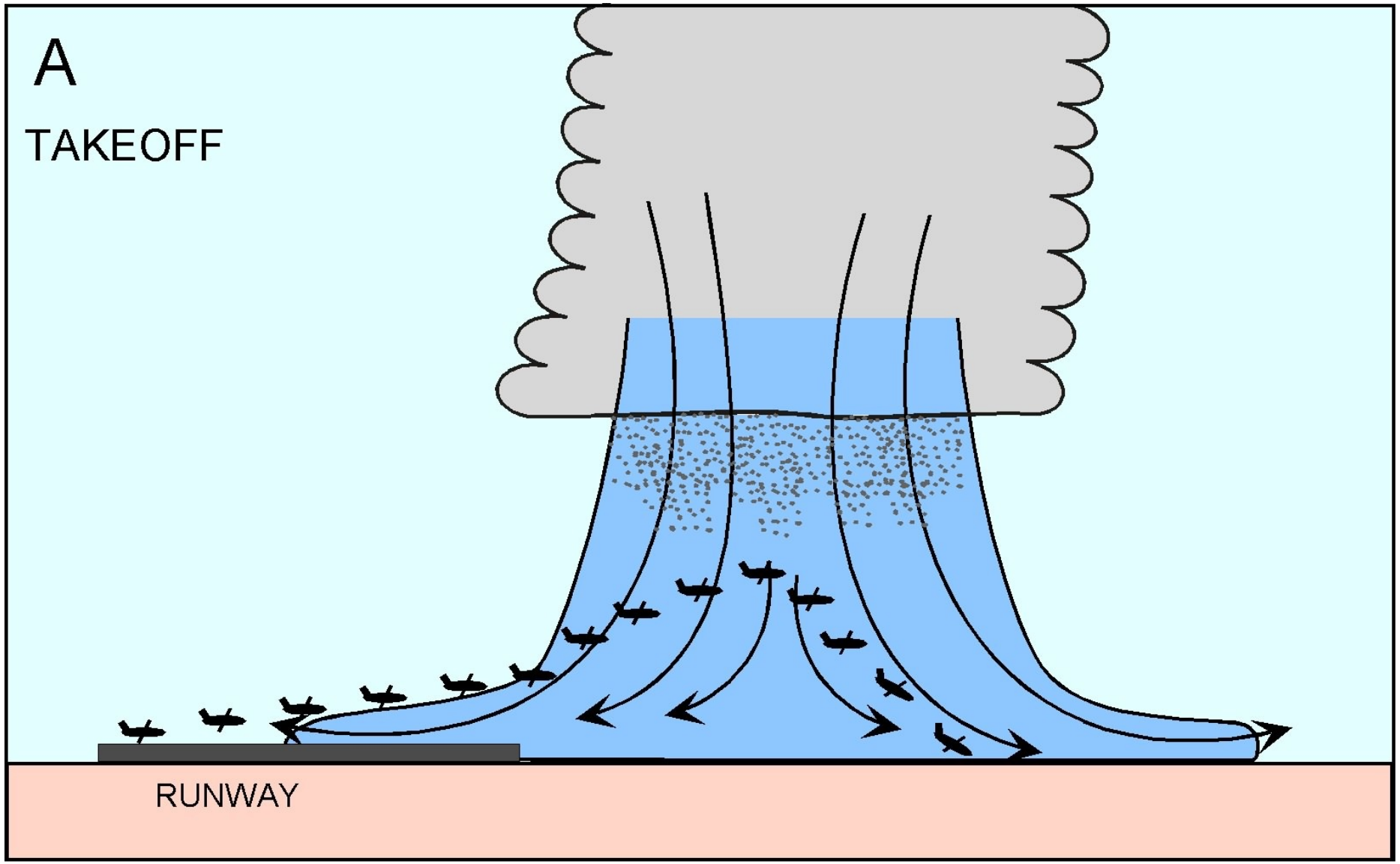

Hazards to Aircraft

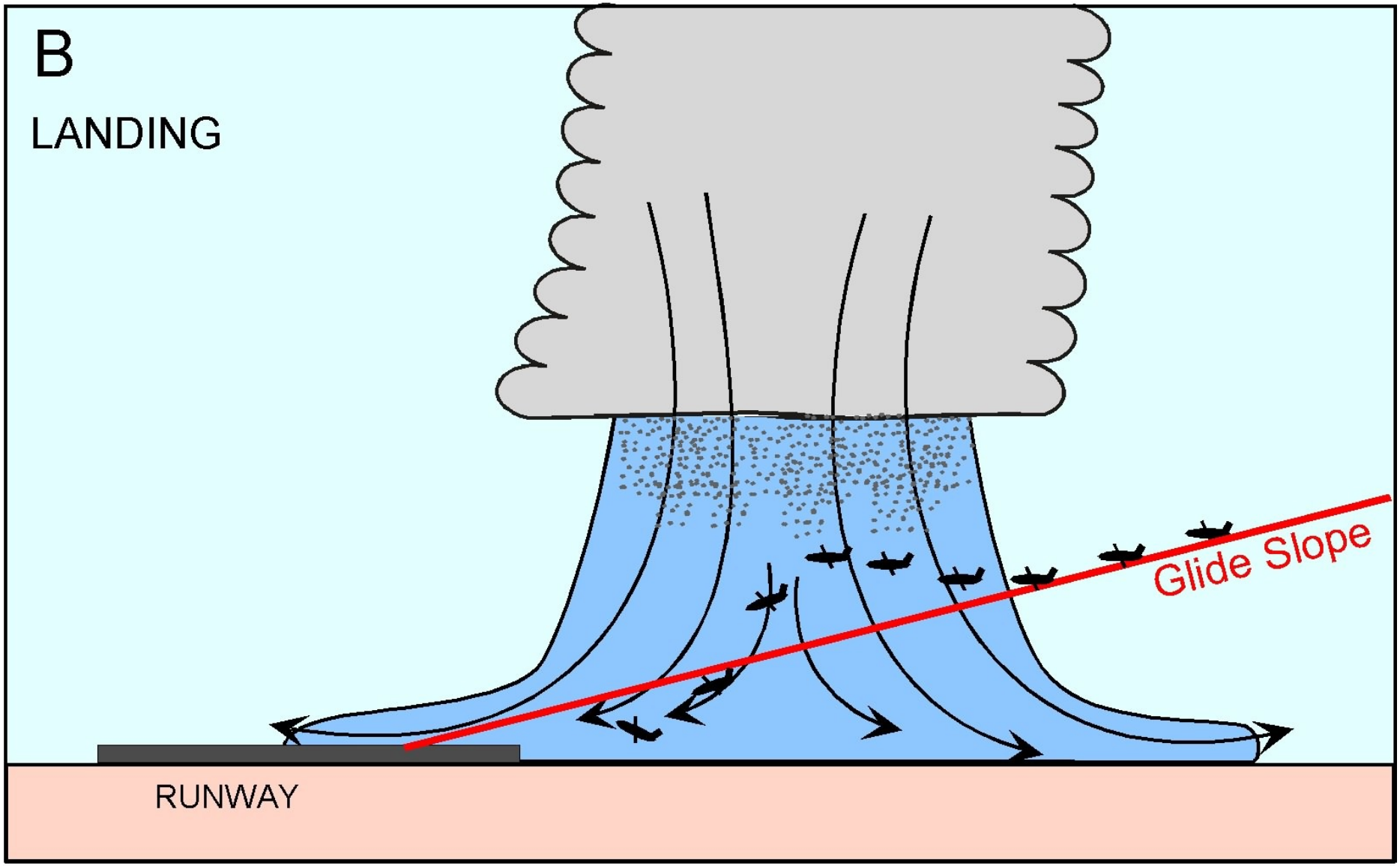

Hazards to Aircraft

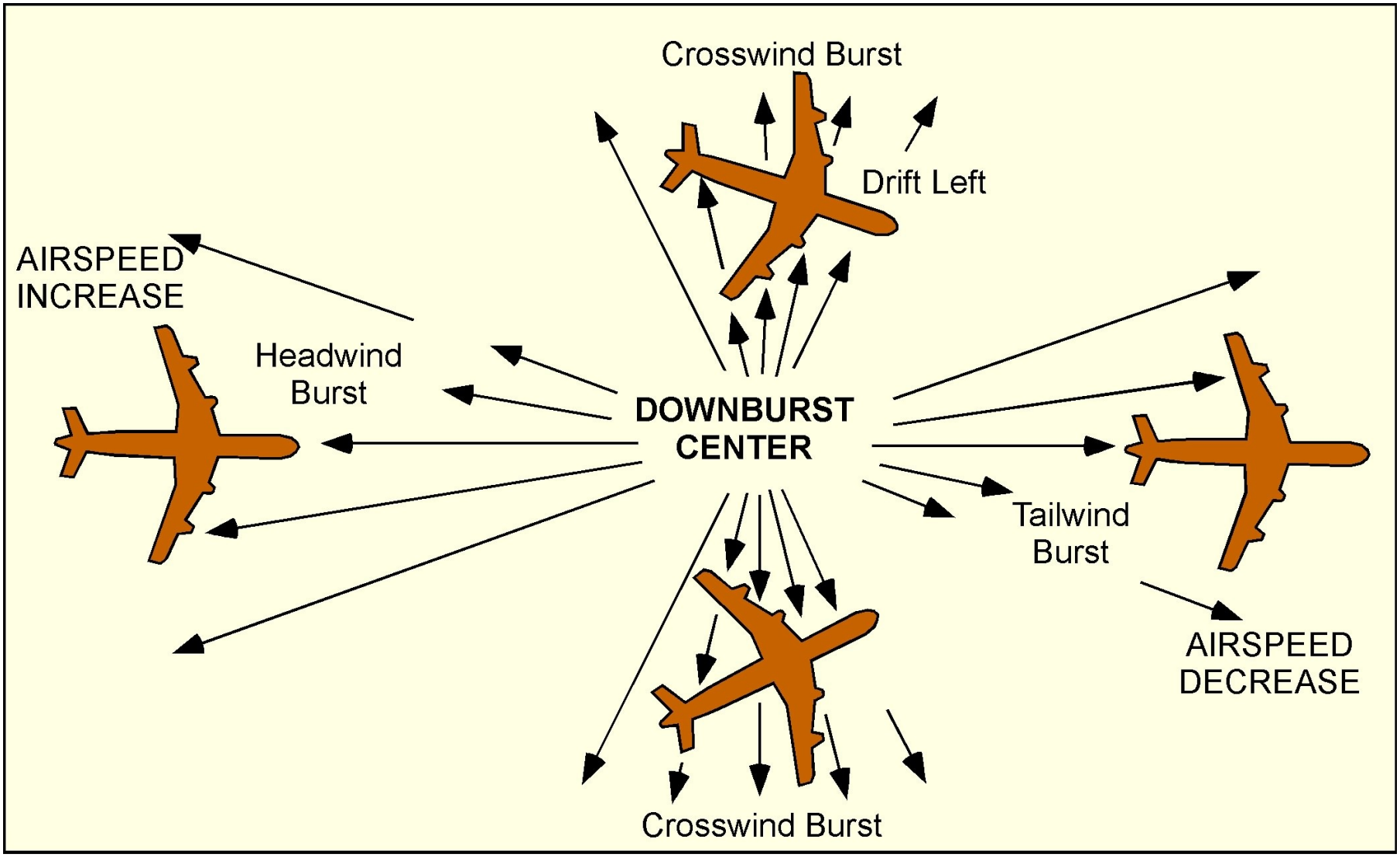

Courtesy of the Theodore Fujita Family

Fujita and Downbursts

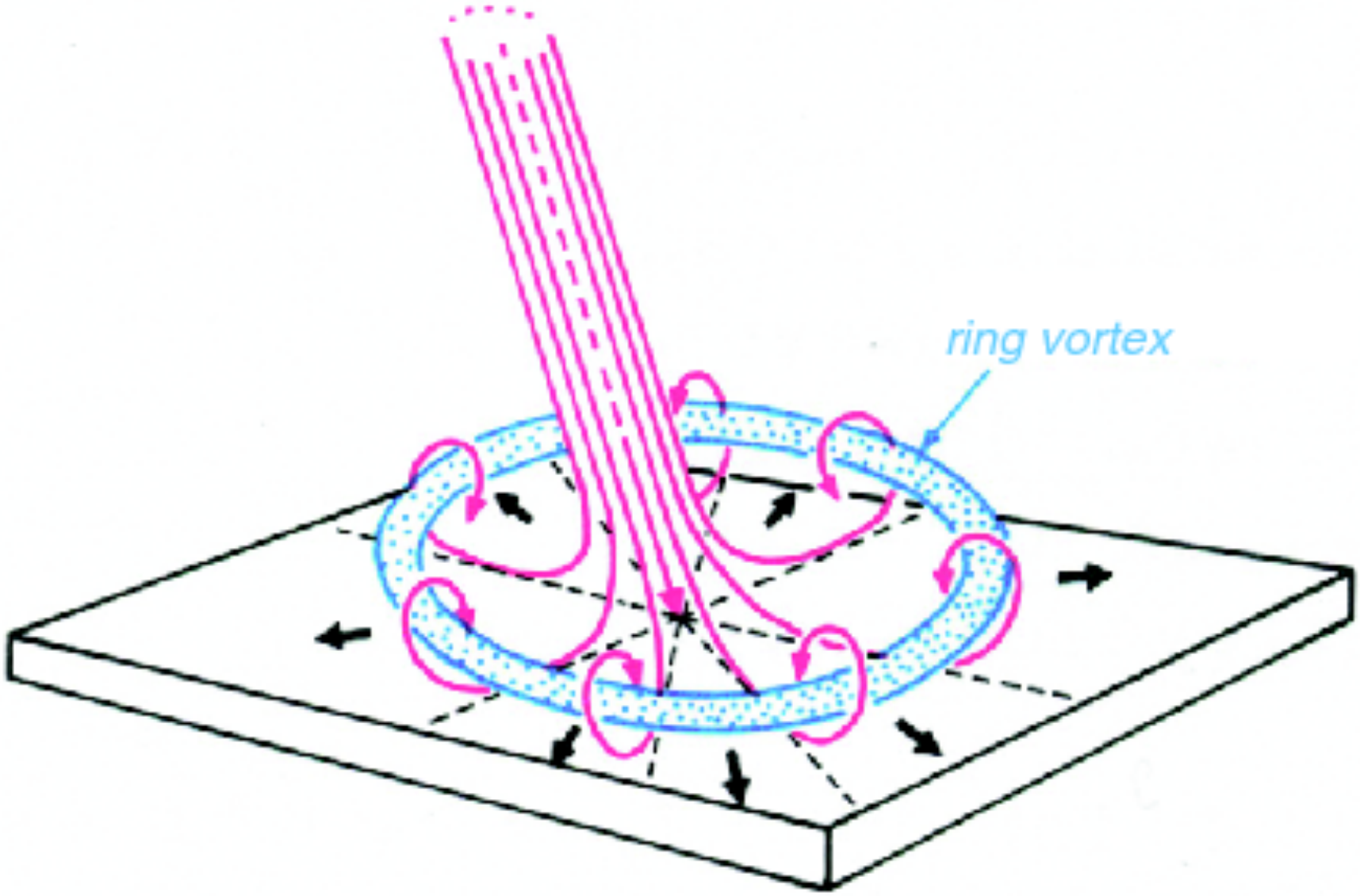

Microburst vs. Tornado

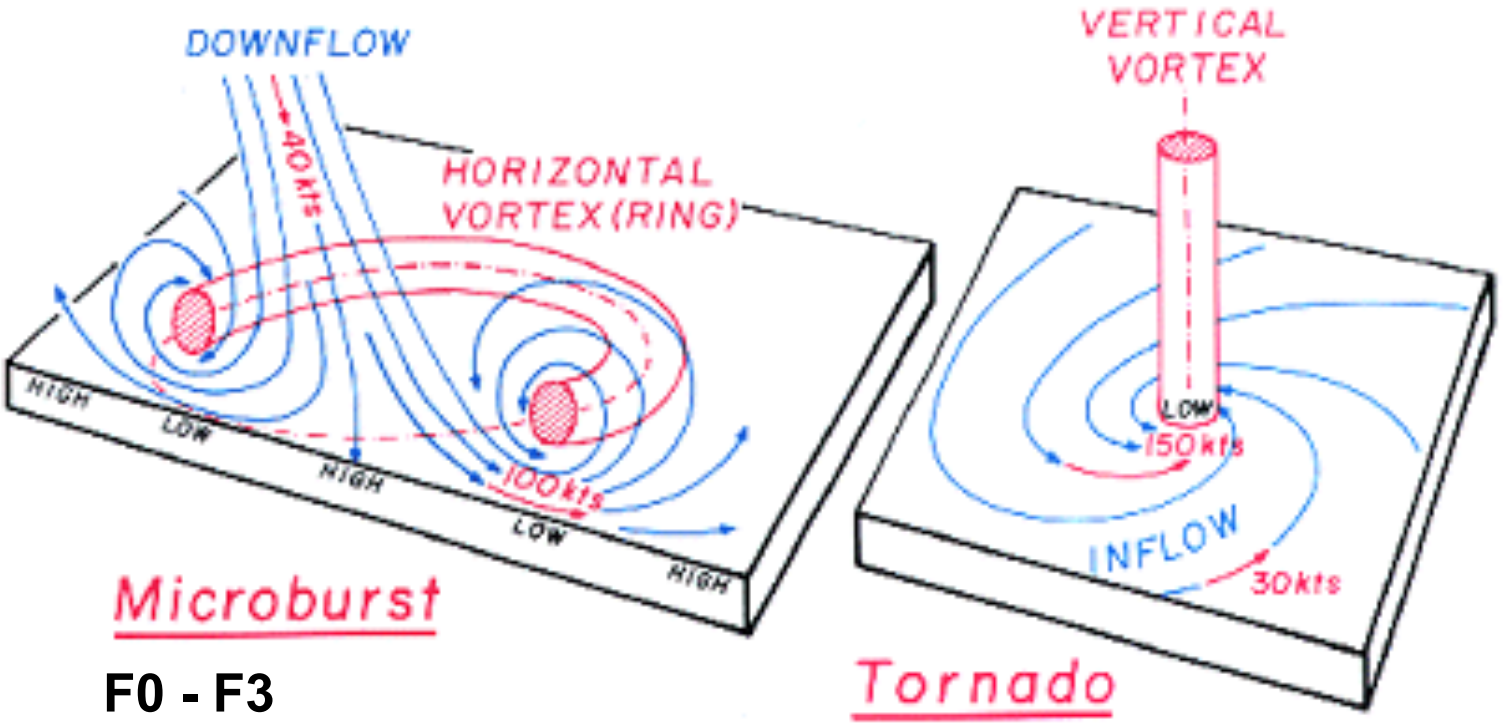

F0 - F3

F0 - F5

The Vortex Ring

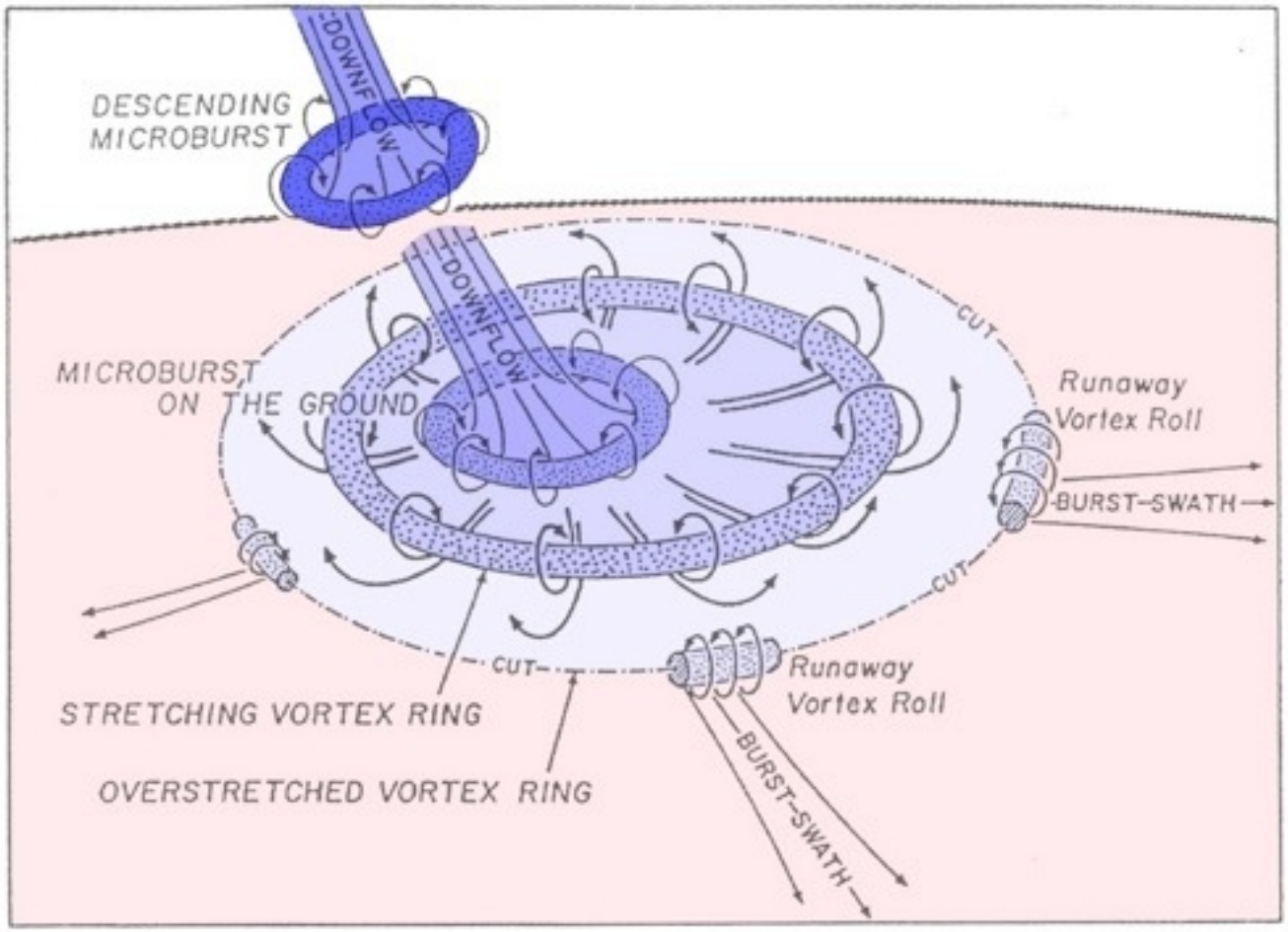

Courtesy of the T. Theodore Fujita Family

Portions of the vortex ring sometimes break away from the remainder of the ring, resulting in runaway vortex rolls that can produce very narrow burst swaths of damages equivalent to that caused by a F0 to F1 tornado.

The Burst Swath

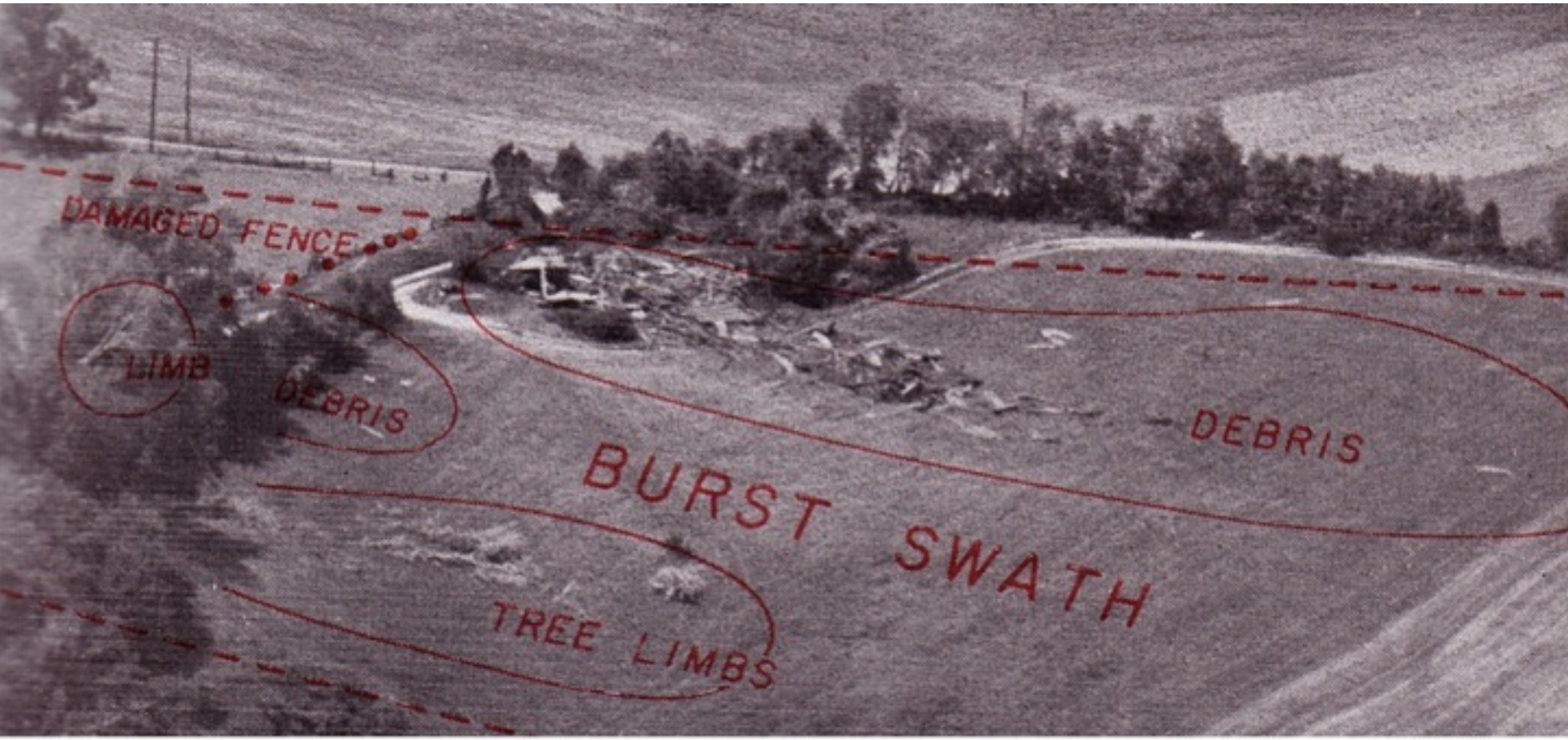

USAF Photo

Downburst damages can be different from a tornado, because debris is blown in one direction, while in tornadoes debris is typically distributed in swirl patterns.

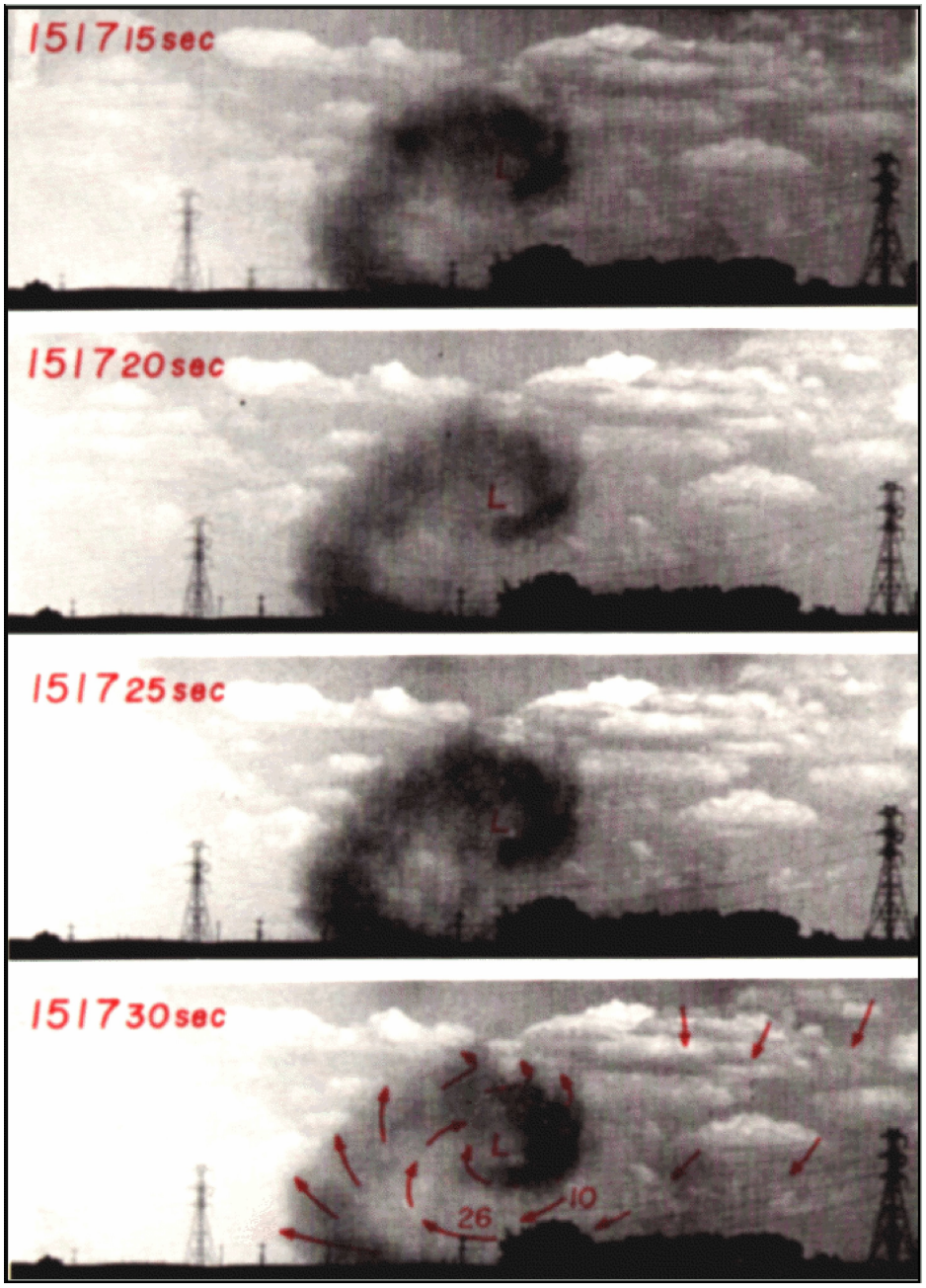

Courtesy of the NOAA Photo Library

Downburst Animation

Cool air descending in a simulation of a downburst-producing thunderstorm

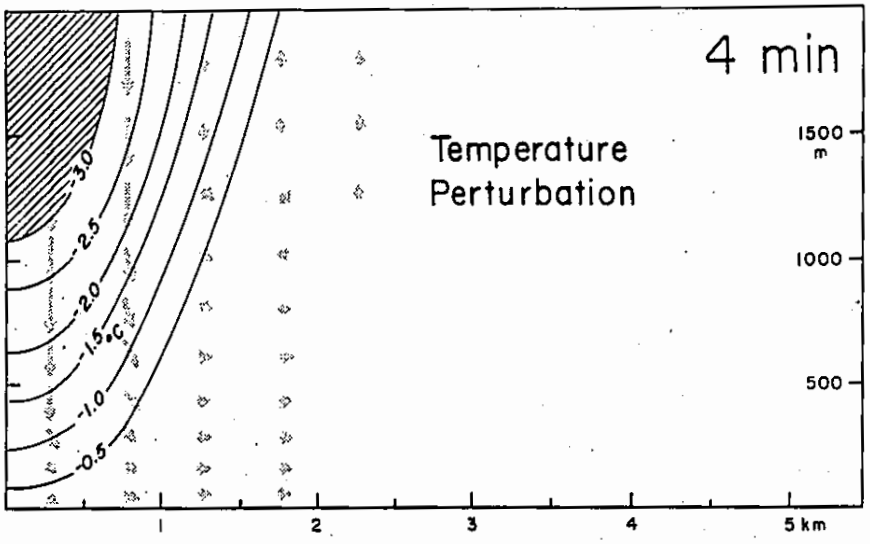
4 min
Temperature
Perturbation
-3.0
-2.5
-2.0
-1.5°C
-1.0
-0.5
1500 m
1000
500
1
2
3
4
5 km

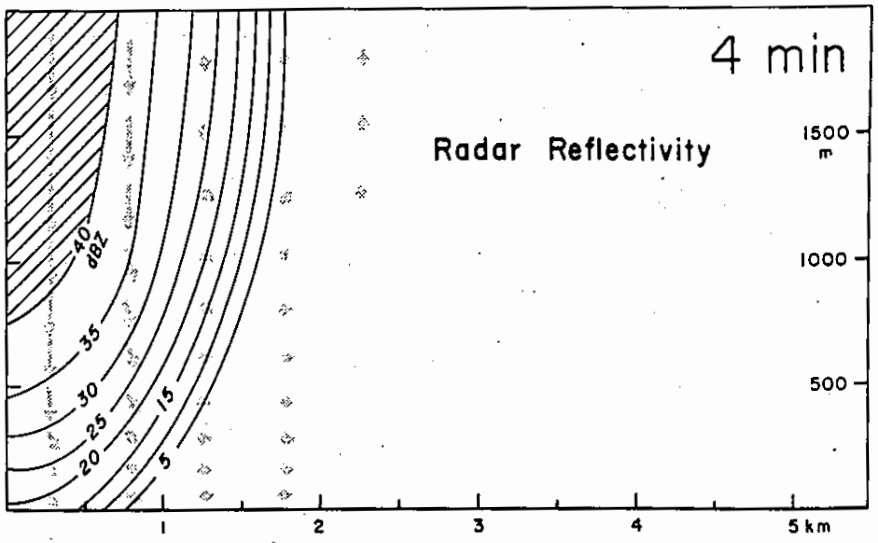
4 min
Radar Reflectivity
40 dBZ
35
30
25
20
15
5
1500 m
1000
500
1
2
3
4
5 km

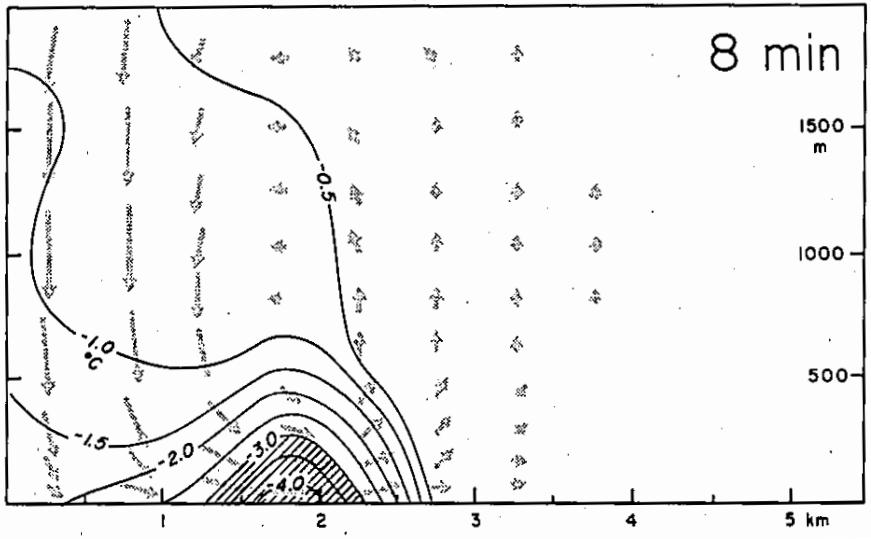
8 min
-0.5
-1.0
-1.5°C
-2.0
-3.0
-4.0
1500 m
1000
500
1
2
3
4
5 km

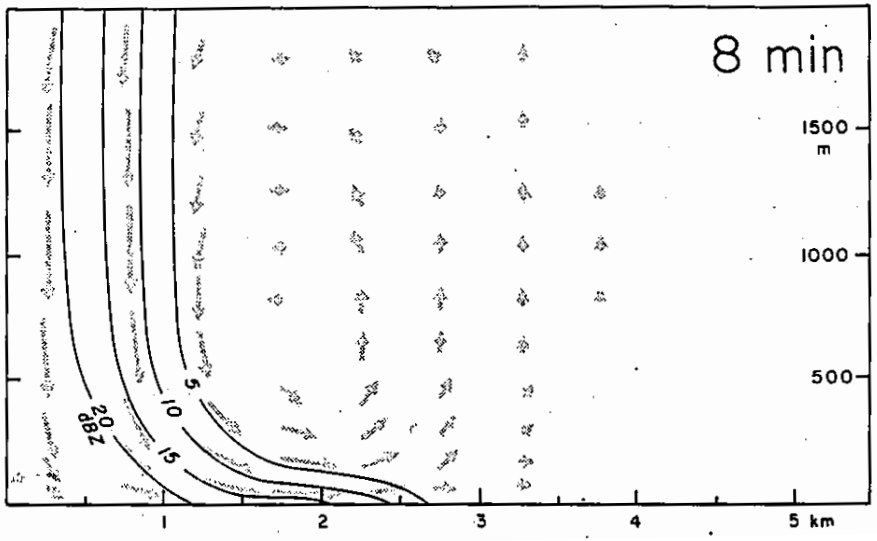
8 min
20 dBZ
15
10
5
1500 m
1000
500
1
2
3
4
5 km

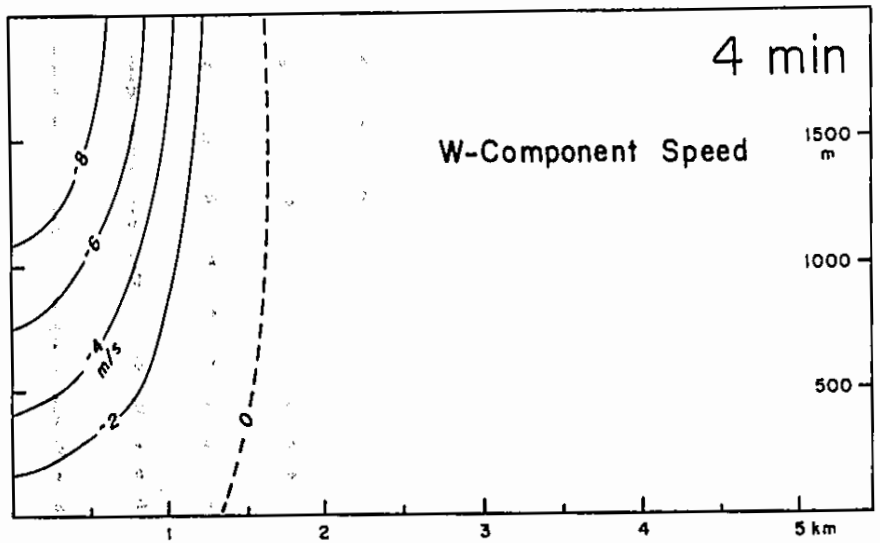
4 min
W-Component Speed
1500 m
1000
500
-8
-6
-4
m/s
-2
0
1
2
3
4
5 km

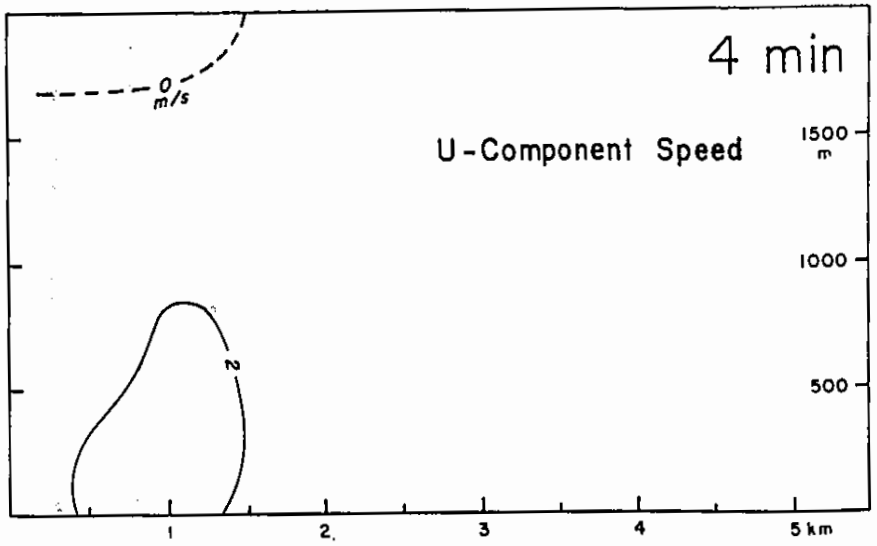
4 min
U-Component Speed
1500 m
1000
500
0 m/s
2
1
2
3
4
5 km

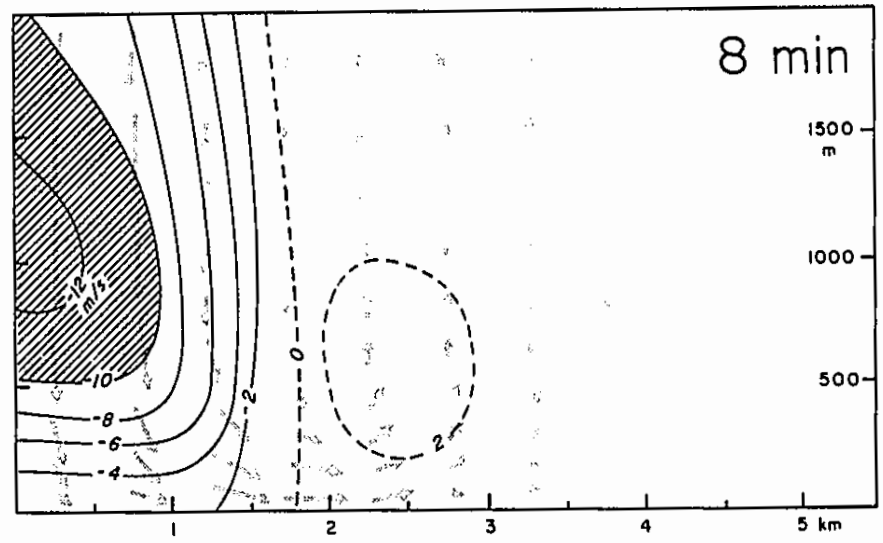
8 min
1500 m
1000
500
-12 m/s
-10
-8
-6
-4
2
0
2
1
2
3
4
5 km

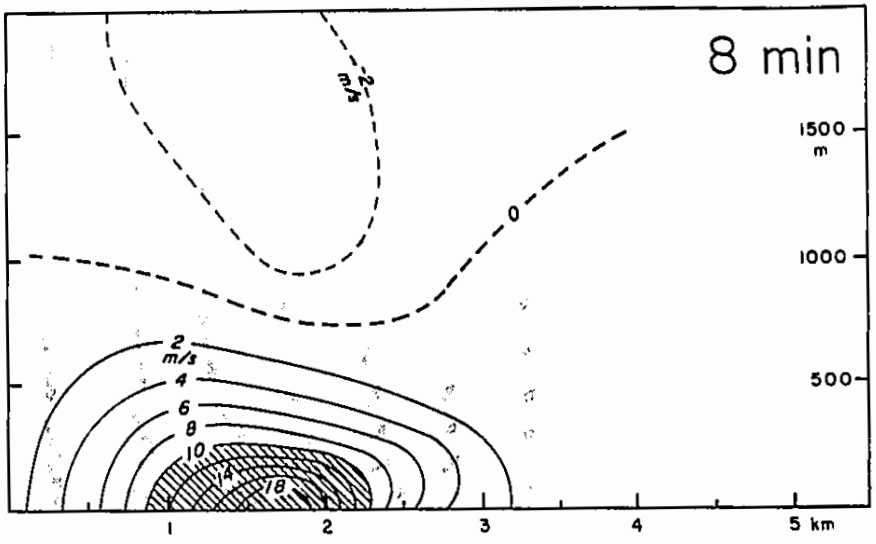
8 min
1500 m
1000
500
-2 m/s
0
2 m/s
4
6
8
10
14
18
1
2
3
4
5 km

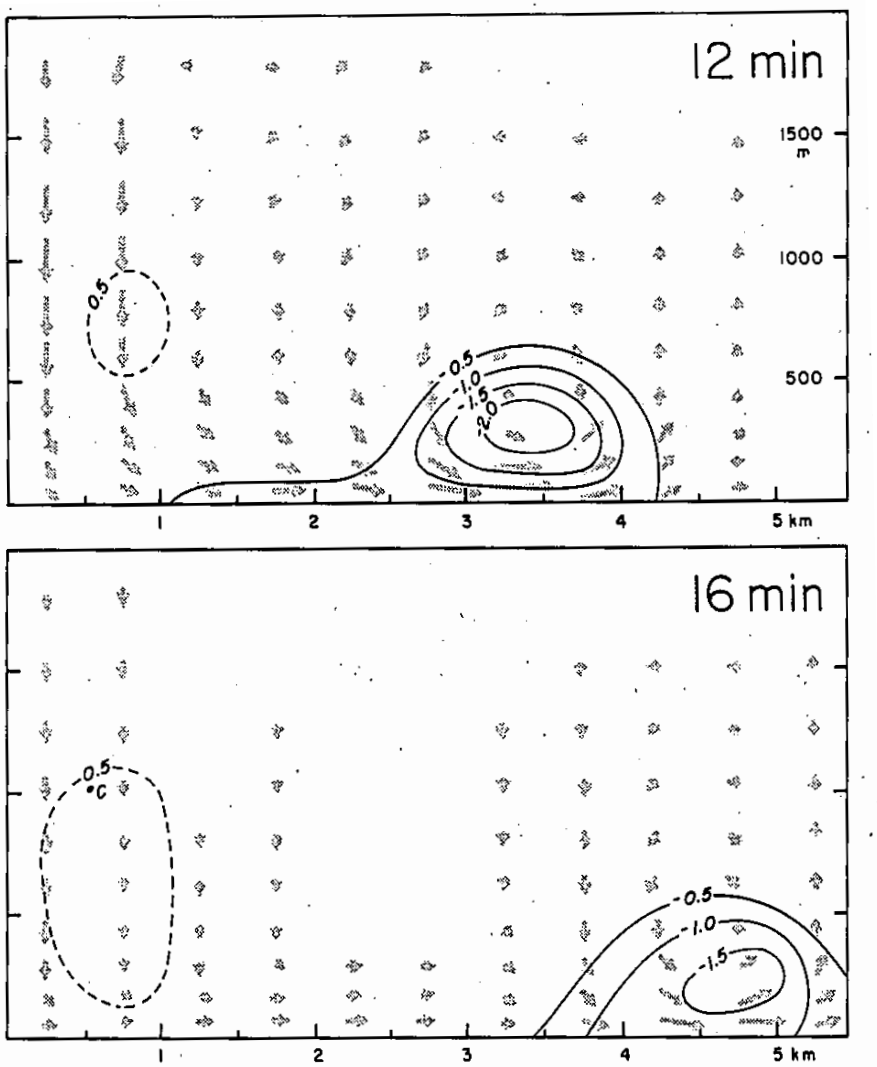

Fig. 3. As in Fig. 1 except contours show temperature departure from the environment.

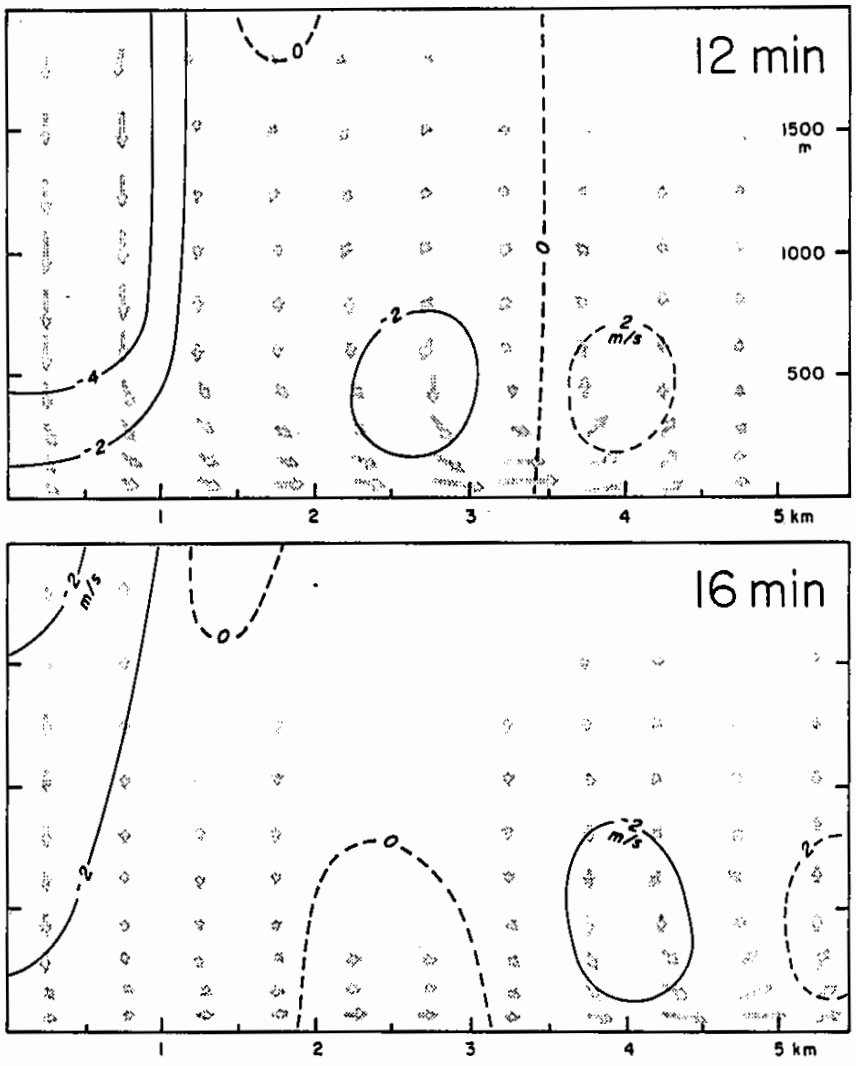

Fig. 1. Radius-height cross sections of vector wind velocity (arrows) and vertical velocity component (contours).

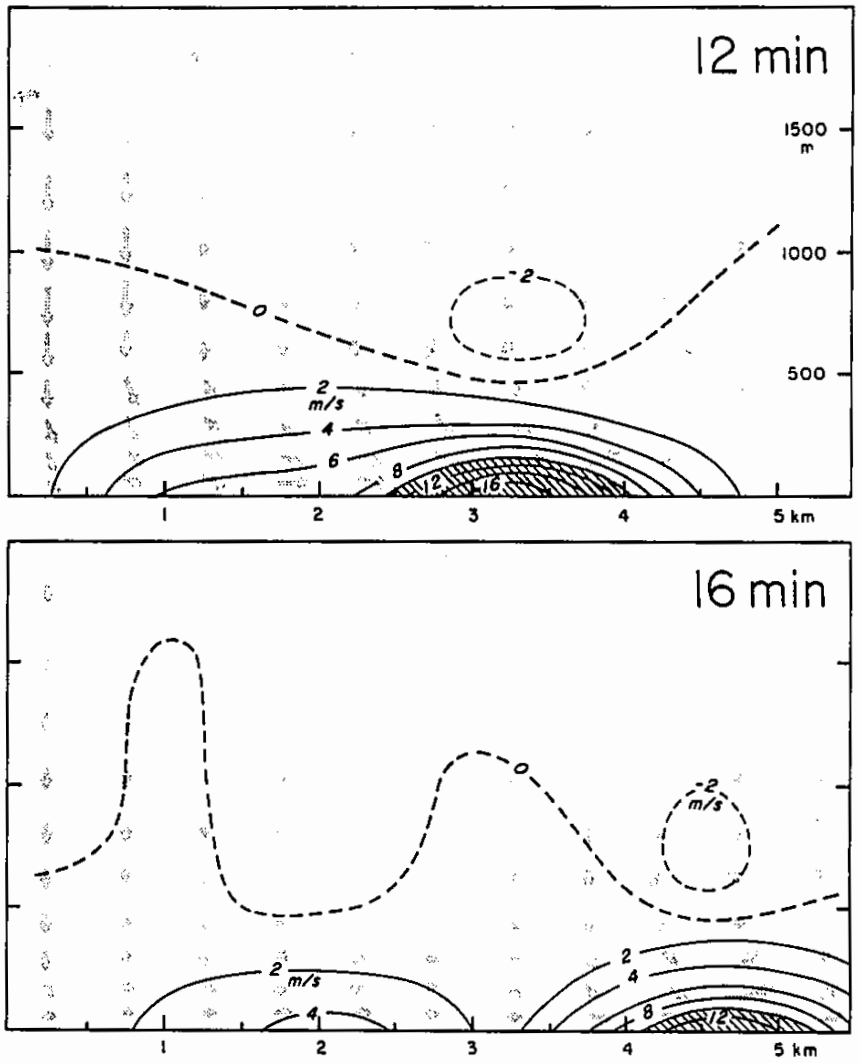

Fig. 2. As in Fig. 1 except contours show horizontal velocity component.

Refinement of Conceptual Model

- Initially regarded as controversial but Fujita presented incontrovertible evidence of downburst damage
- NIMROD project in Chicago in 1978 using mesonet and Doppler radar – found larger ‘macrobursts’ and smaller, more intense ‘microbursts’

Modern Definitions

From AMS Glossary (latest online):

- **Downburst** — An area of strong, often damaging winds produced by one or more convective downdrafts over an area from less than 1 to 400 km in horizontal dimensions. *(Downburst cluster?)*
- **Microburst** — A *downburst* that covers an area less than 4 km along a side with peak winds that last 2–5 minutes.

Downbursts typically F0-F1, microbursts up to F3

Downbursts vs Microbursts

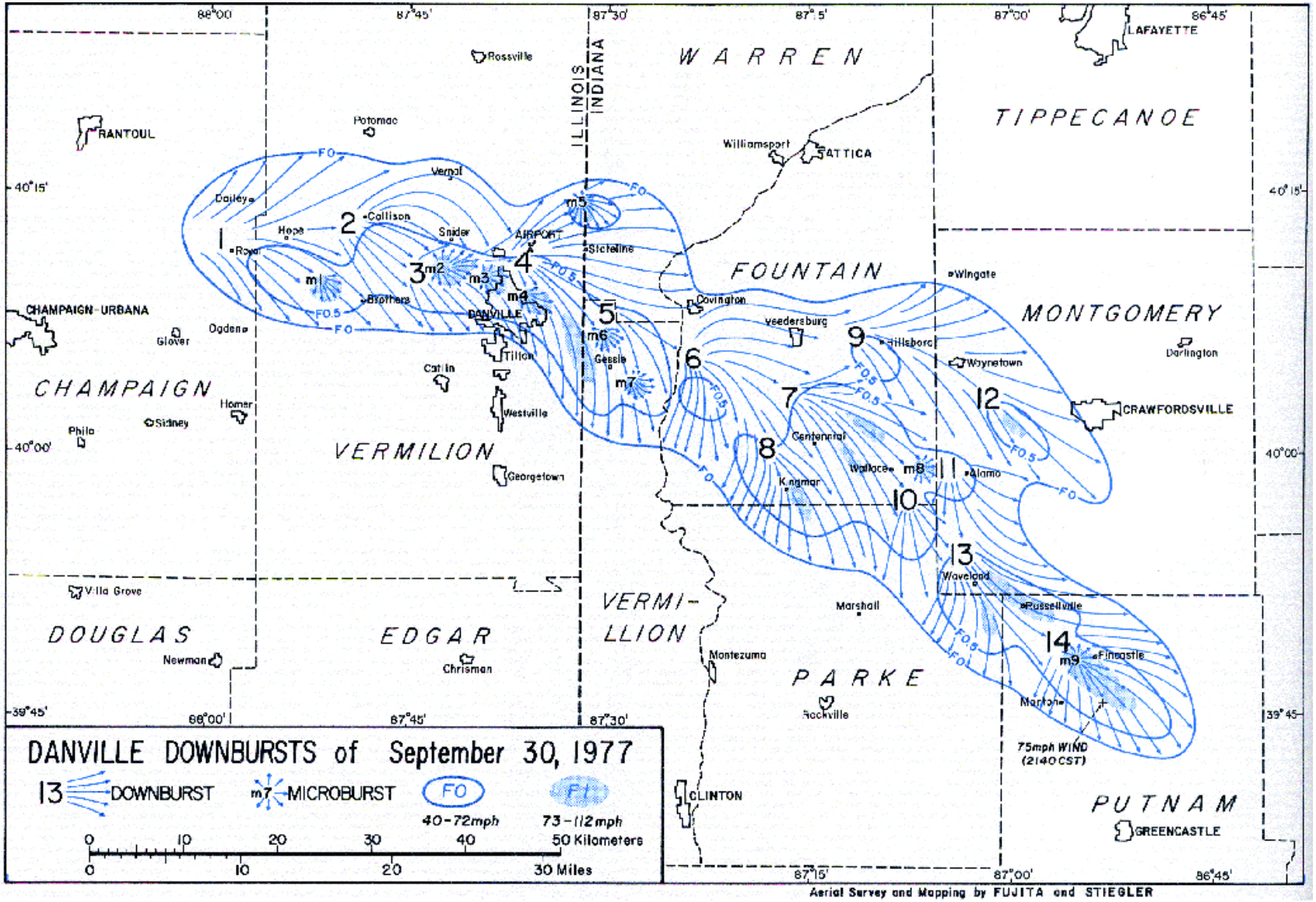

Downbursts vs Microbursts

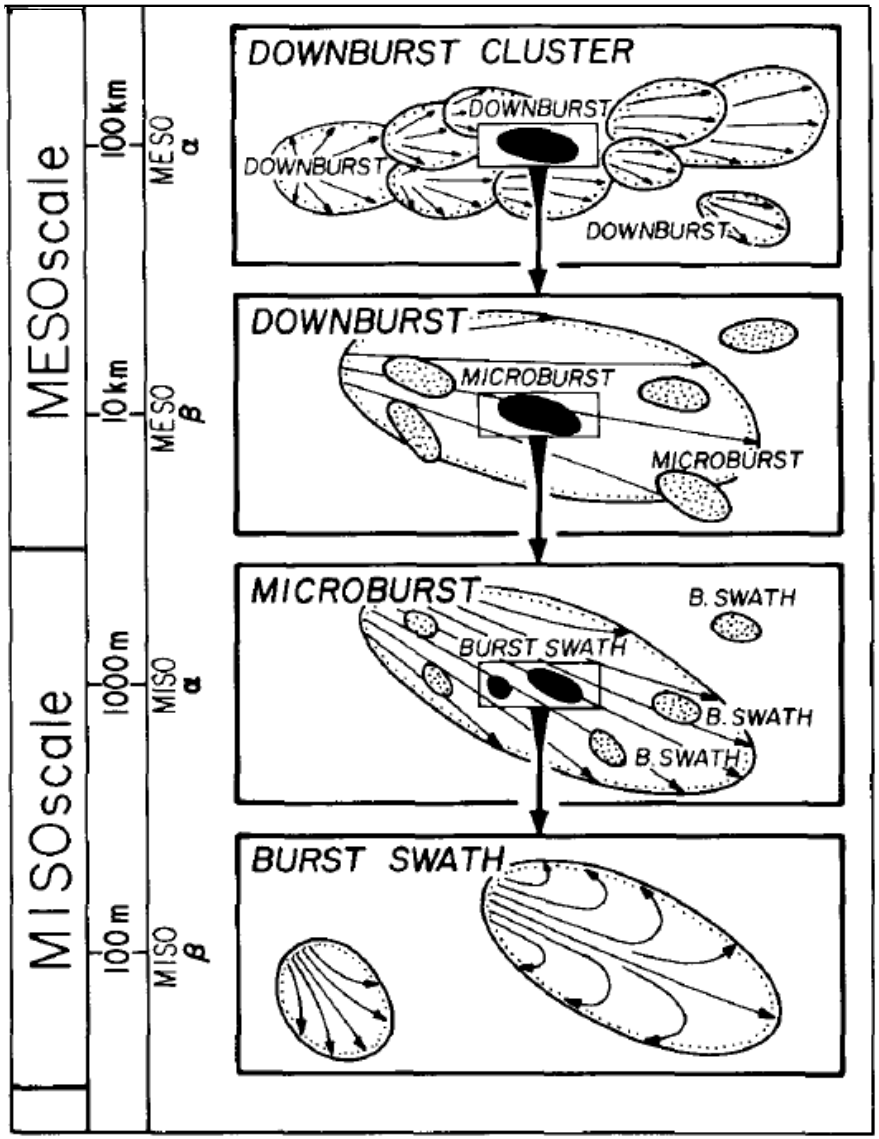

Fujita and Wakimoto, 1981

Refinement of Conceptual Model

- Initially regarded as controversial but Fujita presented incontrovertible evidence of downburst damage
- NIMROD project in Chicago in 1978 using mesonet and Doppler radar – found larger ‘macrobursts’ and smaller, more intense ‘microbursts’
- Similar JAWS project near Denver in 1982 resulted in distinction between ‘wet’ and ‘dry’ microbursts.
- Let to Doppler radars and surface wind shear detection systems being installed at major airports.

Wet Microburst

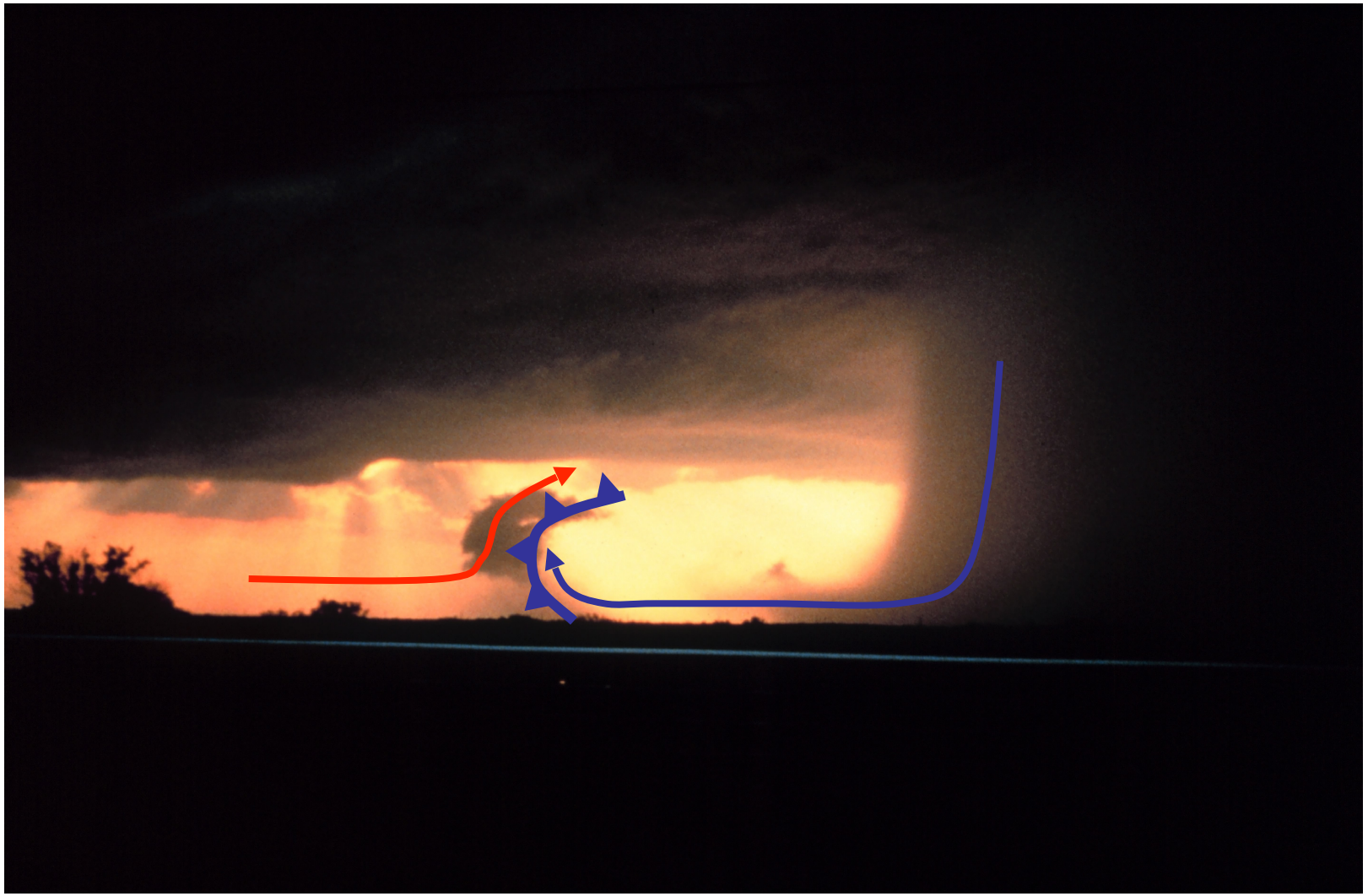

Courtesy of NOAA/NSSL Photo Library

Wet Microburst over Tucson, AZ

https://vimeo.com/135811823

Dry Microburst

Dry Microburst

Courtesy of the National Center for Atmospheric Research

Time-lapse movie

Salt Lake City, Salt Lake City International Airport, UT (KSLC)

25 Aug 6:05 pm	97	30	10	CALM		10.00		CLR		29.77	25.500						OK
25 Aug 6:00 pm	97	30	10	CALM		10.00		CLR		29.78	25.509						OK
25 Aug 5:55 pm	95	30	10	CALM		10.00		CLR		29.78	25.509						OK
25 Aug 5:53 pm	95	30	10	CALM		10.00		FEW040 SCT090 SCT200		1001.7	29.78	25.509		98	91		
	OK																
25 Aug 5:50 pm	95	31	10	SSW	5	10.00		CLR	1001.7	29.78	25.509		98	91			OK
25 Aug 5:45 pm	97	30	10	WSW	6	10.00		CLR		29.78	25.509						OK
25 Aug 5:40 pm	97	32	10	SW	7	10.00		CLR		29.79	25.518						OK
25 Aug 5:35 pm	95	30	10	SSW	6	10.00		CLR		29.79	25.518						OK
25 Aug 5:30 pm	97	30	10	SW	5	10.00		CLR		29.79	25.518						OK
25 Aug 5:25 pm	97	30	10	VRBL	3	10.00		CLR		29.79	25.518						OK
25 Aug 5:20 pm	97	30	10	VRBL	6	10.00		CLR		29.79	25.518						OK
25 Aug 5:15 pm	97	30	10	VRBL	5	10.00		CLR		29.79	25.518						OK
25 Aug 5:10 pm	97	30	10	SSW	7	10.00		CLR		29.79	25.518						OK
25 Aug 5:05 pm	97	30	10	VRBL	7	10.00		CLR		29.80	25.526						OK
25 Aug 5:00 pm	99	29	8	VRBL	3	10.00		CLR		29.80	25.526						OK
25 Aug 4:55 pm	97	29	9	VRBL	6	10.00		CLR		29.80	25.526						OK
25 Aug 4:53 pm	97	29	9	ENE	3	10.00		FEW050 SCT090 SCT200		1002.2	29.80	25.526					
	OK																
25 Aug 4:50 pm	97	29	9	ENE	6	10.00		FEW050 SCT090 SCT200		1002.2	29.80	25.526					
	OK																
25 Aug 4:45 pm	99	29	8	NE	7	10.00		CLR		29.80	25.526						OK
25 Aug 4:40 pm	99	29	8	VRBL	3	10.00		CLR		29.81	25.535						OK
25 Aug 4:35 pm	97	30	10	VRBL	3G17	10.00		CLR		29.81	25.535						OK
25 Aug 4:30 pm	97	30	10	SSW	5G22	10.00		CLR		29.81	25.535						OK
25 Aug 4:25 pm	97	30	10	SE	13G23	10.00		CLR		29.82	25.544						OK
25 Aug 4:20 pm	97	30	10	SE	15G23	10.00		CLR		29.82	25.544						OK
25 Aug 4:15 pm	97	30	10	S	15	10.00		FEW001		29.83	25.553						OK
25 Aug 4:10 pm	93	30	11	S	15G28	10.00		FEW001		29.84	25.562						OK
25 Aug 4:05 pm	93	30	11	S	23G41	6.00	HZ	FEW001 SCT040 SCT090			29.84	25.562					
	OK																
25 Aug 4:00 pm	91	30	11	S	24G45	4.00	HZ	FEW001 SCT040 SCT090			29.84	25.562					
	OK																
25 Aug 3:55 pm	91	30	11	S	33G47	1.25	HZ	FEW001		29.84	25.562						OK
25 Aug 3:53 pm	92	30	11	S	36G47	1.50	HZ	FEW040 SCT090 SCT130 SCT200		1003.8	29.84	25.562					
		OK															
25 Aug 3:50 pm	92	31	11	S	33G47	2.00	HZ	FEW040 SCT090 SCT130 SCT200		1003.8	29.84	25.562					
		OK															
25 Aug 3:45 pm	93	28	10	SSW	17G23	10.00		CLR		29.84	25.562						OK
25 Aug 3:40 pm	93	28	10	SSW	12G17	10.00		CLR		29.84	25.562						OK
25 Aug 3:35 pm	93	34	12	S	7G20	10.00		CLR		29.84	25.562						OK
25 Aug 3:30 pm	95	36	13	S	13G20	10.00		CLR		29.84	25.562						OK
25 Aug 3:25 pm	99	36	11	SSE	15G20	10.00		CLR		29.84	25.562						OK
25 Aug 3:20 pm	97	36	12	SSE	8	10.00		CLR		29.84	25.562						OK
25 Aug 3:15 pm	97	36	12	S	12	10.00		CLR		29.84	25.562						OK
25 Aug 3:10 pm	97	36	12	SE	8G20	10.00		CLR		29.84	25.562						OK
25 Aug 3:05 pm	97	36	12	E	10G20	10.00		CLR		29.84	25.562						OK
25 Aug 3:00 pm	97	34	11	SE	10	10.00		CLR		29.85	25.571						OK
25 Aug 2:55 pm	95	34	12	VRBL	3	10.00		CLR		29.85	25.571						OK
25 Aug 2:53 pm	96	34	11	SSW	6	10.00		FEW030 SCT090CB SCT130 SCT200		1003.9	29.85	25.571					
		OK															
25 Aug 2:50 pm	96	34	11	SSE	8	10.00		CLR	1004.0	29.85	25.571						OK
25 Aug 2:45 pm	95	34	12	S	9	10.00		CLR		29.86	25.579						OK
25 Aug 2:40 pm	97	34	11	SSE	13G17	10.00		CLR		29.86	25.579						OK
25 Aug 2:35 pm	97	34	11	SE	6	10.00		CLR		29.86	25.579						OK
25 Aug 2:30 pm	95	34	12	S	9	10.00		CLR		29.86	25.579						OK
25 Aug 2:25 pm	95	34	12	SSW	7	10.00		CLR		29.87	25.588						OK
25 Aug 2:20 pm	95	34	12	SSW	6G16	10.00		CLR		29.87	25.588						OK
25 Aug 2:15 pm	95	36	13	SSE	13G16	10.00		CLR		29.87	25.588						OK
25 Aug 2:10 pm	95	36	13	SE	10	10.00		CLR		29.88	25.597						OK
25 Aug 2:05 pm	95	34	12	S	7	10.00		CLR		29.88	25.597						OK

72572 SLC Salt Lake City

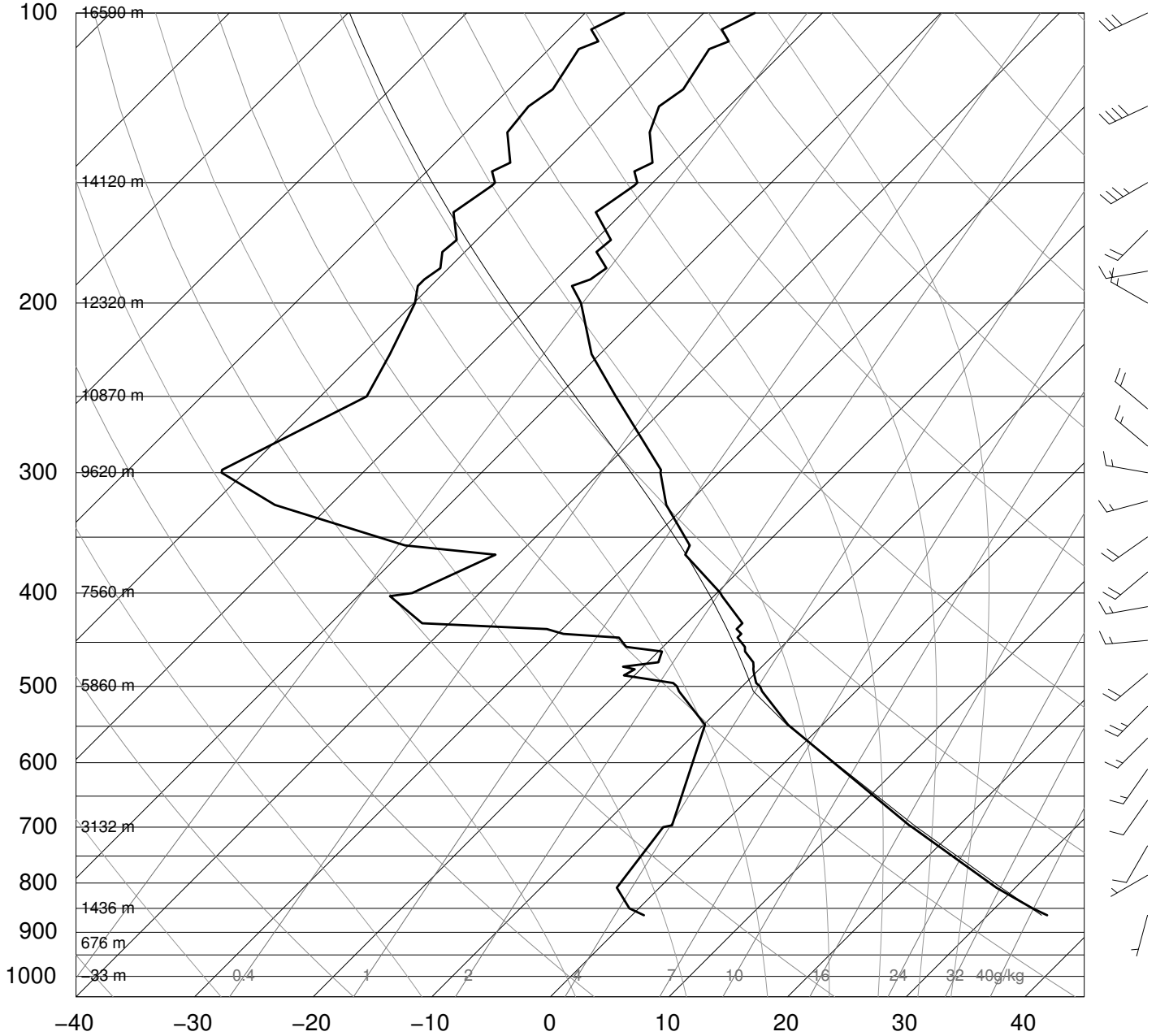

SLAT	40.78
SLON	
SELV	1288.
SHOW	0.46
LIFT	0.67
LFTV	0.42
SWET	32.64
KINX	19.90
CTOT	7.70
VTOT	41.70
TOTL	49.40
CAPE	22.11
CAPV	29.02
CINS	−89.7
CINV	−59.0
EQLV	364.2
EQTV	362.7
LFCT	367.8
LFCV	373.5
BRCH	3.69
BRCV	4.85
LCLT	265.2
LCLP	514.2
MLTH	320.8
MLMR	4.16
THCK	5893.
PWAT	14.77

00Z 26 Aug 2008

University of Wyoming

Downburst Formation

- Two processes are important for generation of negative buoyancy
  - Diabatic cooling: includes evaporation of liquid water, melting of ice, sublimation of ice (upper levels especially)
  - Precipitation loading: the drag force of falling hydrometeors drives the air downward
- Diabatic cooling is more important overall, but precip loading often crucial in initiation

Dry Microburst Sounding

Deep mixed layer (dry adiabatic lapse rate).
Air is precipitation free or contains virga.

Wet Microburst Sounding

Accompanied by precipitation

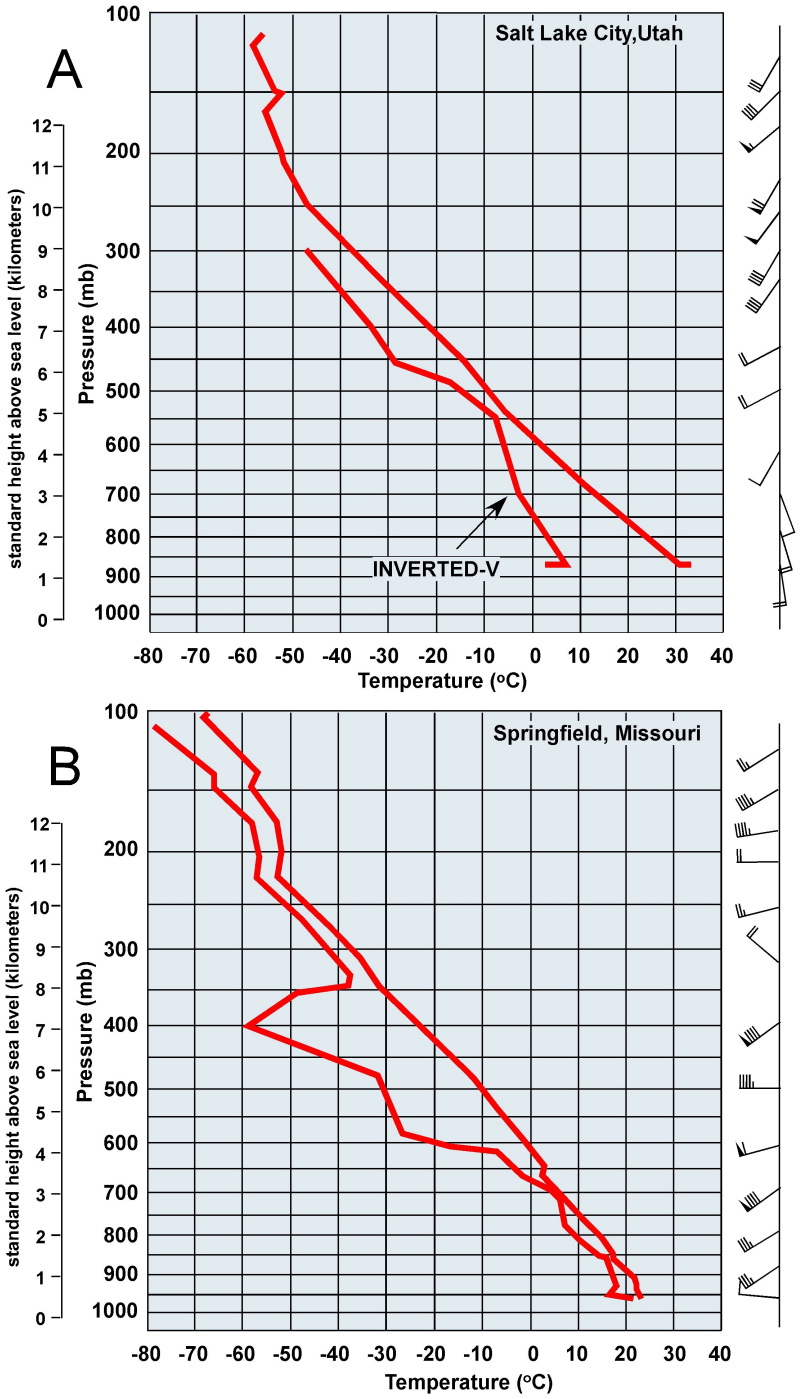

Wet Downbursts

- Mid-level dry air
- Dry adiabatic lapse rate but with moisture & higher precipitable water in sounding
- Evaporation and melting important below melting level; sublimation of ice/snow important above that.
- Entrainment of dry mid-level air into the downdraft may cause evaporative cooling (which will increase with vertical wind shear and storm-relative winds).
- This increases the negative buoyancy and can result in microbursts and macrobursts

Downbursts and Dry Air

- Evaporative cooling occurs as downdraft descends and warms due to compression.
- Downdraft intensity depends on depth of subcloud layer, lapse rate in subcloud layer, and rain water conent at cloud base.
- RH at surface determines LCL and mixed layer depth.
- Mixing ratio at surface determines (to some extent) the rain water content at cloud base.

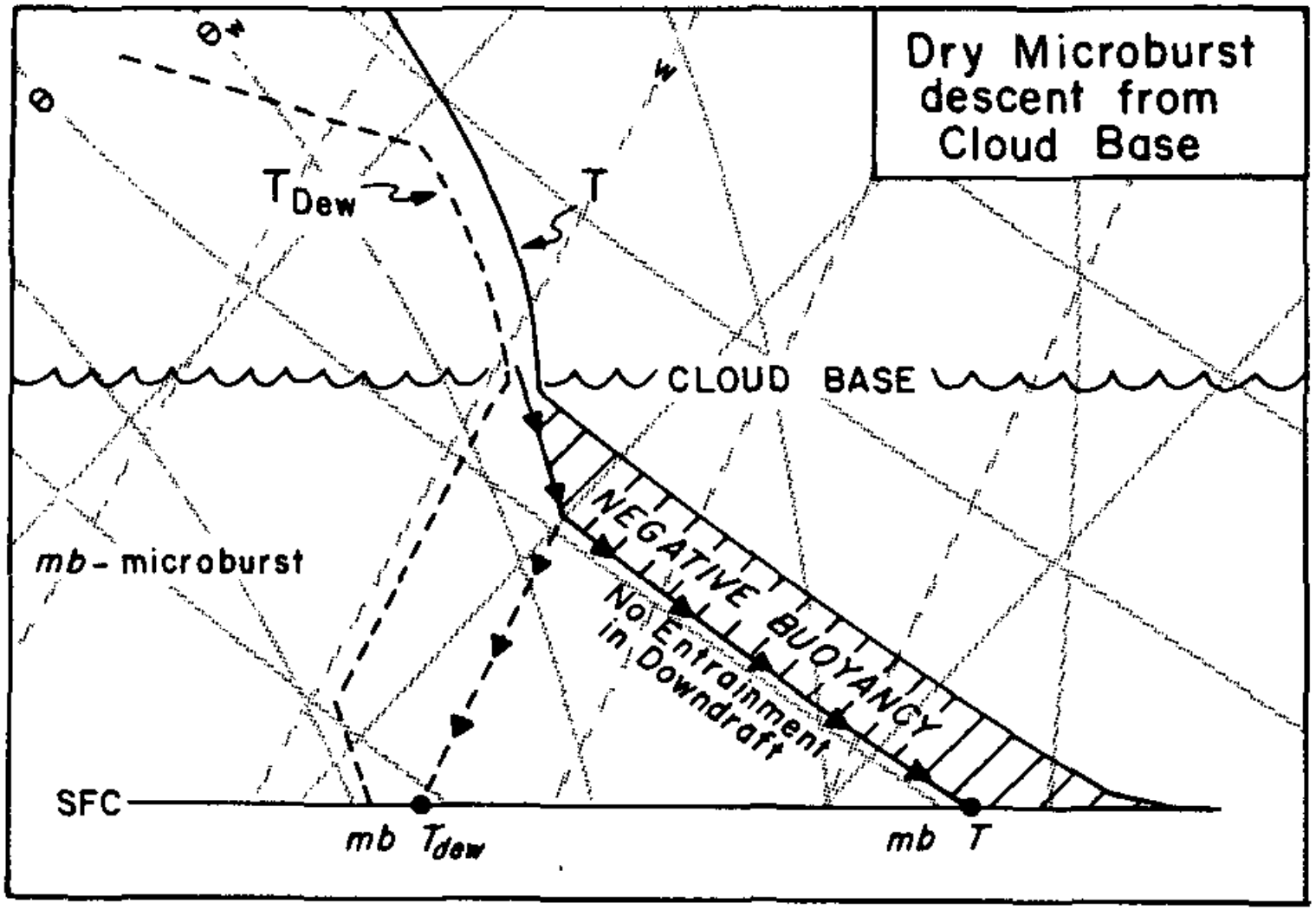

FIG. 10. Model of the thermodynamic descent of a dry microburst from cloud base. Surface temperature and dew-point temperature within the microburst are determined from PAM data. No entrainment into the downdraft is assumed.

Table 1. Maximum surface horizontal air velocity (m/s).

-dT/dz (K/km)	Maximum rainwater mixing ratio (g/kg) 1/8	1/4	1/2	1	2	4	8
9.6	10.3	12.9	16.4	20.4	24.6	29.3	35.3
9.2	1.3	2.5	8.6	14.4	19.7	25.2	31.3
8.8		1.4	2.6	8.8	15.0	21.1	27.7
8.3		1.1	1.6	5.2	11.2	17.1	24.1
7.9			1.3	3.0	8.0	14.0	20.5
7.4						11.3	17.2

10 m/s

20

30 m/s

Table 2. Maximum downward vertical air velocity (m/s)

-dT/dz (K/km)	Maximum rainwater mixing ratio (g/kg)						
	1/8	1/4	1/2	1	2	4	8
9.6	8.7	10.4	12.3	14.4	16.6	19.2	22.6
9.2	3.4	6.0	9.0	11.8	14.4	17.3	20.9
8.8		3.3	6.0	9.2	12.3	15.5	19.3
8.3		2.2	4.1	7.0	10.2	13.6	17.6
7.9			3.0	5.4	8.4	11.9	16.0
7.4						10.3	14.5

10 m/s

20 m/s

Microbursts and Snow?

- Cloud-resolving model simulations have shown that hydrometeors in the form of snowflakes are effective at producing microbursts.

- The sublimation of snowflakes is particularly effective because:

  – the numerous low-density, snow particles readily sublimate, with much of the snow content depleted before melting to rain,
  – the latent heat of sublimation is greater than the latent heat of either evaporation or melting, and
  – the cooling from sublimation takes place at a relatively high altitude within the deep adiabatic layer, allowing the downdraft to accelerate through a deep column.

From Wilson and Wakimoto, 2001

Numerical Simulations

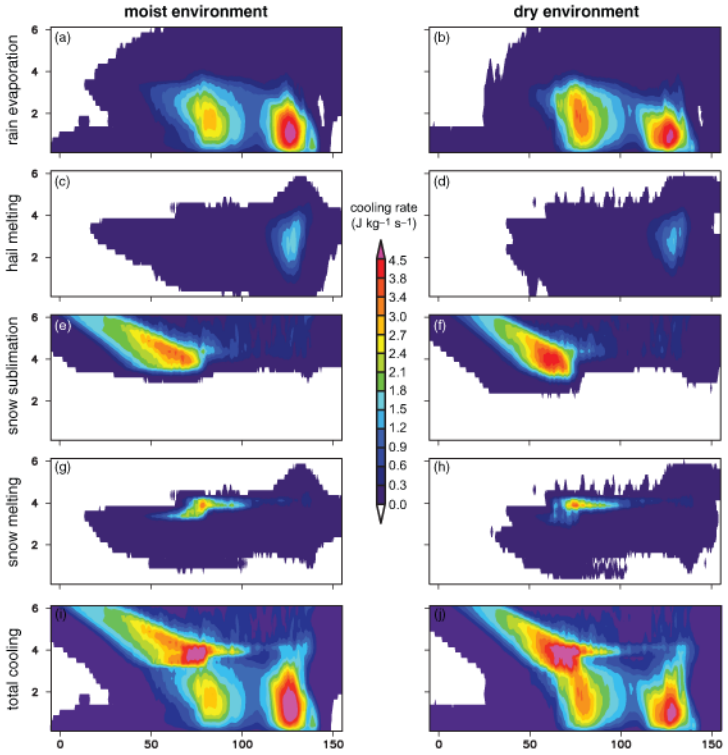

see next slide
for larger graphics

Figure 10.29

Vertical cross-sections of line-averaged latent cooling rates in a pair of numerical simulations of a long-lived MCS. The panels in the left column (a, c, e, g, i) are from a simulation in which the environment has a relatively high relative humidity throughout the troposphere (the relative humidity decreases from 95% at the top of the boundary layer to 50% at the tropopause), whereas the panels in the right column (b, d, f, h, j) are from a simulation in which the midtropospheric environment has a 1.5 km-deep dry layer with relative humidity of only 10%. The CAPE in both simulations is 4000 J kg^{-1}. The melting level in both simulations is at approximately 4 km. The x and z axis labels are in kilometers. The latent cooling rates (J kg^{-1} s^{-1}) from (a, b) rain evaporation, (c, d) hail melting, (e, f) snow sublimation, and (g, h) snow melting are shown 4 h into the simulations, as is (i, j) the total latent cooling rate. The evaporative cooling (and total latent cooling) in the moist environment immediately behind the gust front (the gust front is at x = 150 km) exceeds that in the dry environment (the domain-wide evaporative cooling and total latent cooling are also greater in the moist environment, although this is not as obvious from the panels above). Image courtesy of Richard James.

Moist Environment Dry Environment COOLING RATES

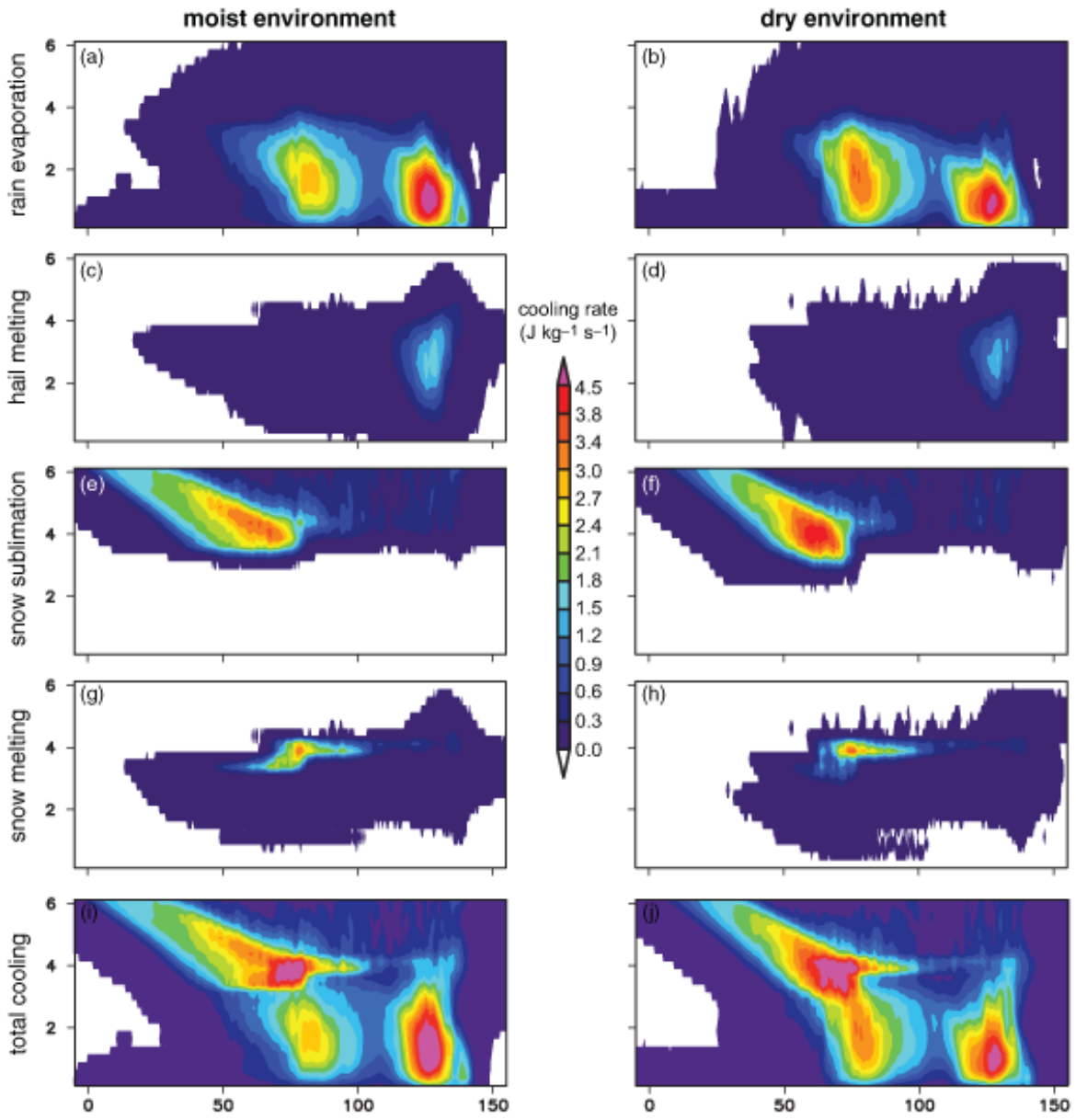

rain evaporation

hail melting

snow sublimation

snow melting

Total cooling

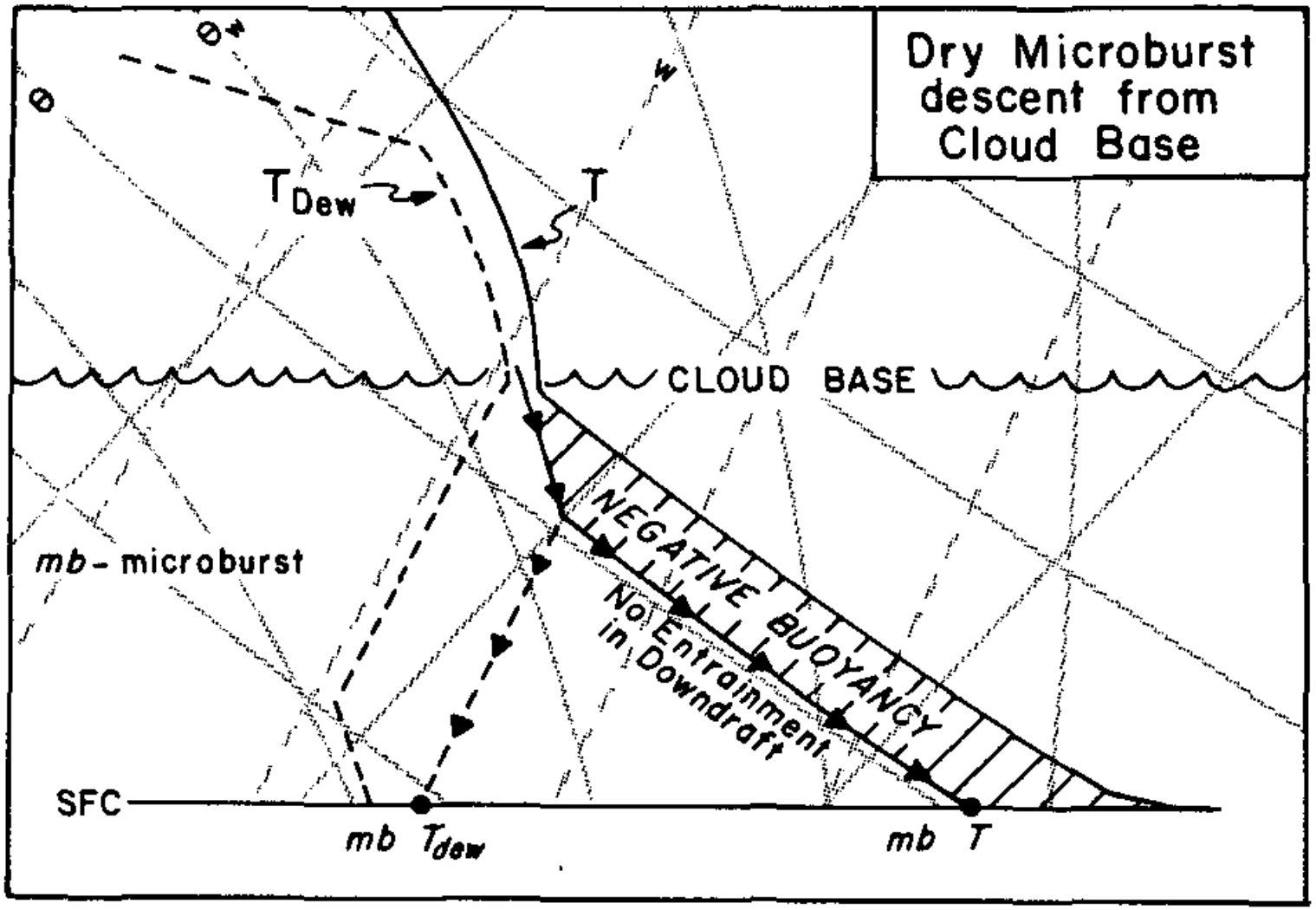

FIG. 10. Model of the thermodynamic descent of a dry microburst from cloud base. Surface temperature and dew-point temperature within the microburst are determined from PAM data. No entrainment into the downdraft is assumed.

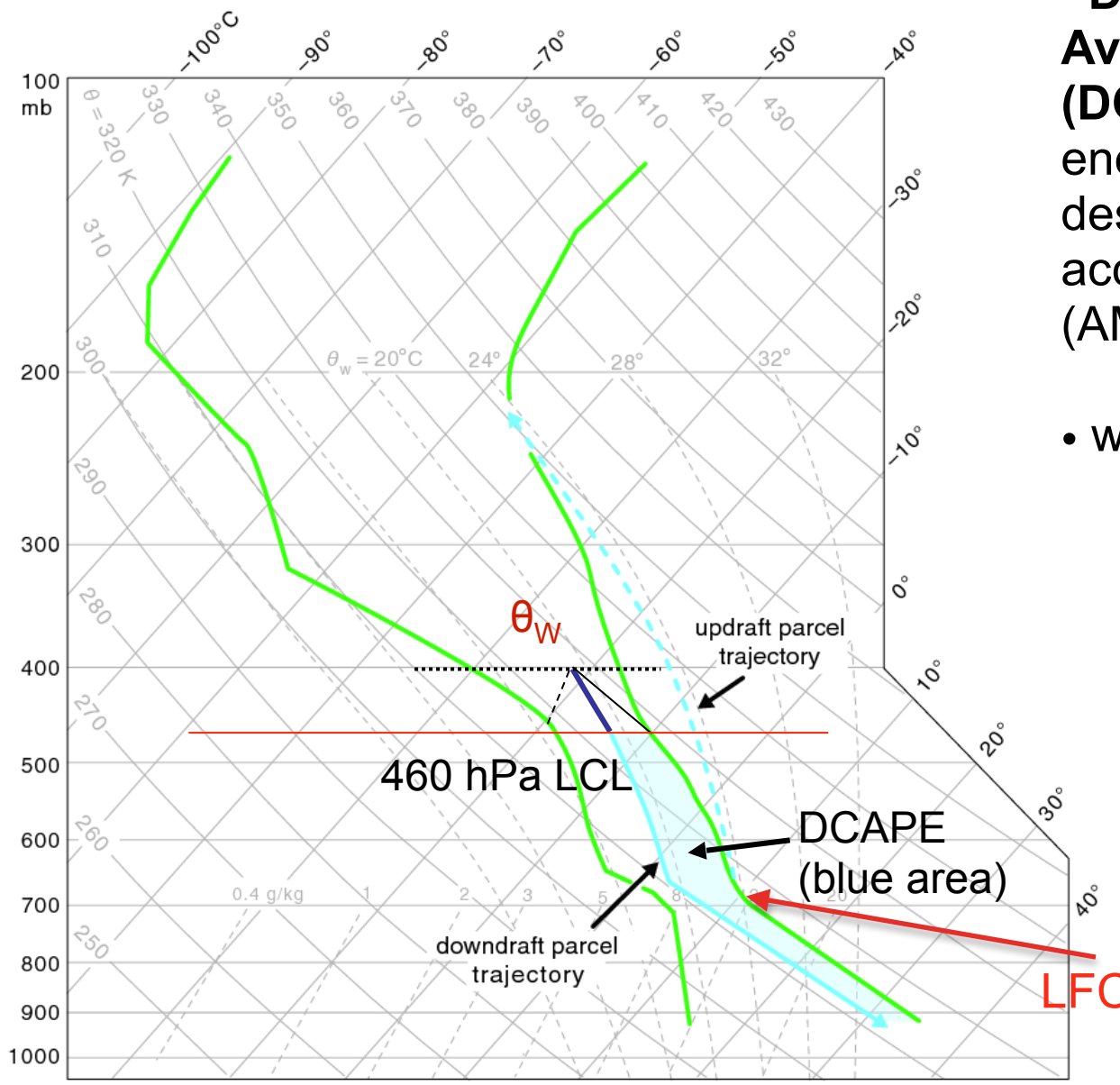

- **Downdraft Convective Available Potential Energy (DCAPE)**: The maximum energy available to a descending parcel, according to parcel theory (AMS Glossary)

- $w_{max} = (2*DCAPE)^{1/2}$ m s^{-1}

  - Downburst typically develops in lower part of cloud, so cloud does not need to be deep
  - In some cases, just showers are present
  - WINDEX, MDPI, etc. also predict downdraft wind speed

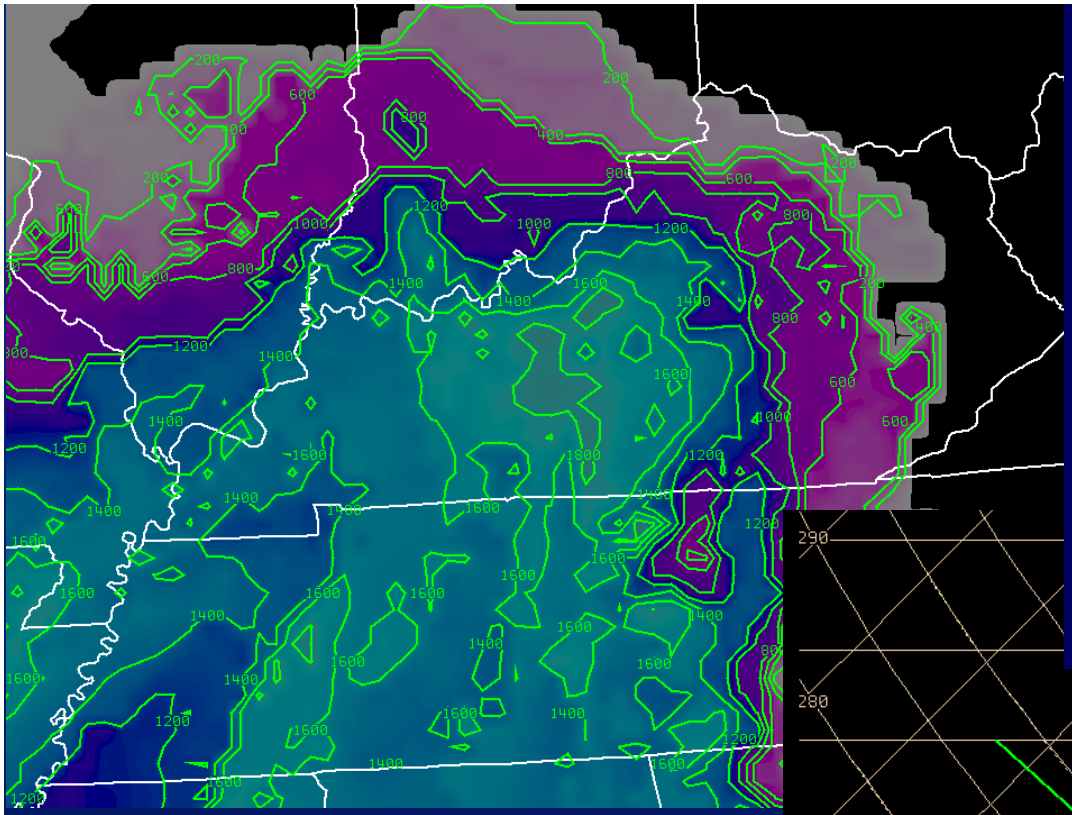

DCAPE – 18Z Mar 2, 2012

High DCAPE (above) resulted in outflow-dominated and wind-producing storms in central Kentucky. Tornadic supercells occurred in parts of southern Indiana.

This downdraft parcel is assumed saturated for all of its descent.

Finding DCAPE on a Sounding:

1. *From 700 mb, find the Lifting Condensation Level (LCL) (600 mb or average wet bult temp from 500-700 mb are used at times). LCL = level where dotted yellow and dashed red lines meet (where saturation occurs)*
2. *Follow moist adiabat on sounding down to surface (solid blue line)*
3. *The area between the blue line and environmental temperature curve (green line) equals DCAPE*

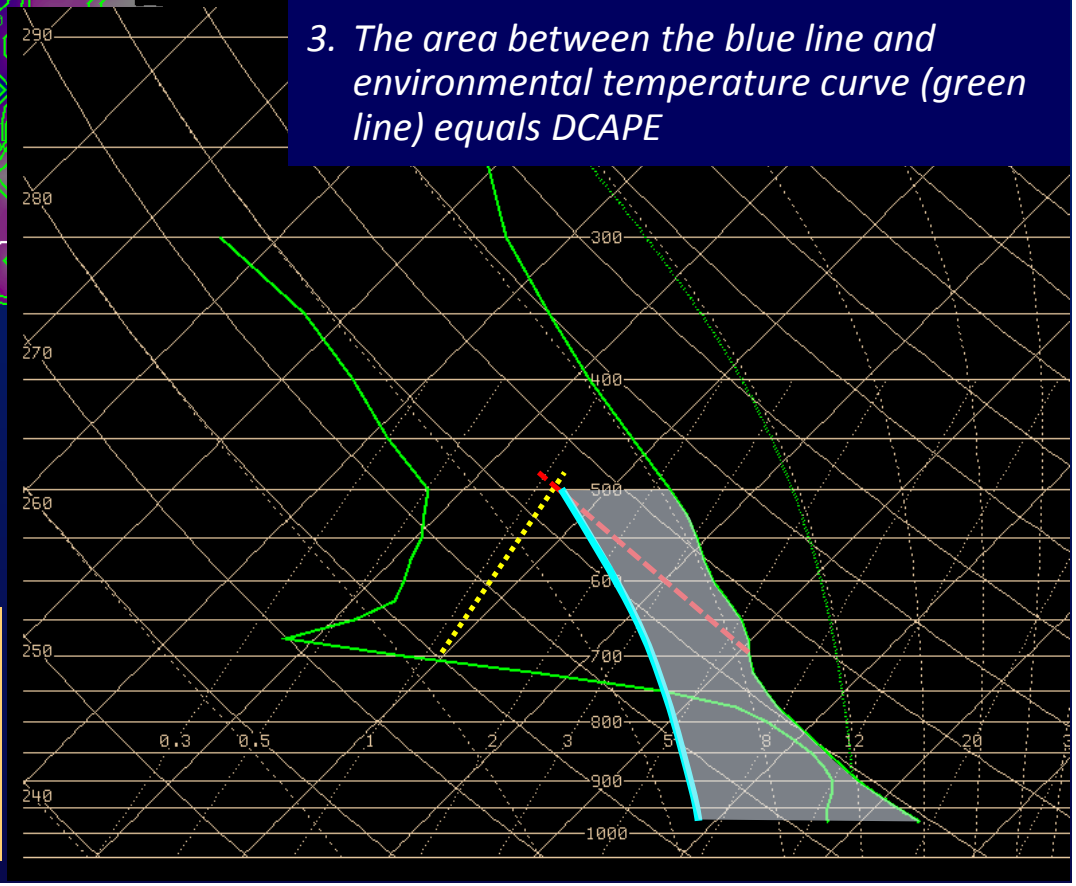

Microburst Climatology

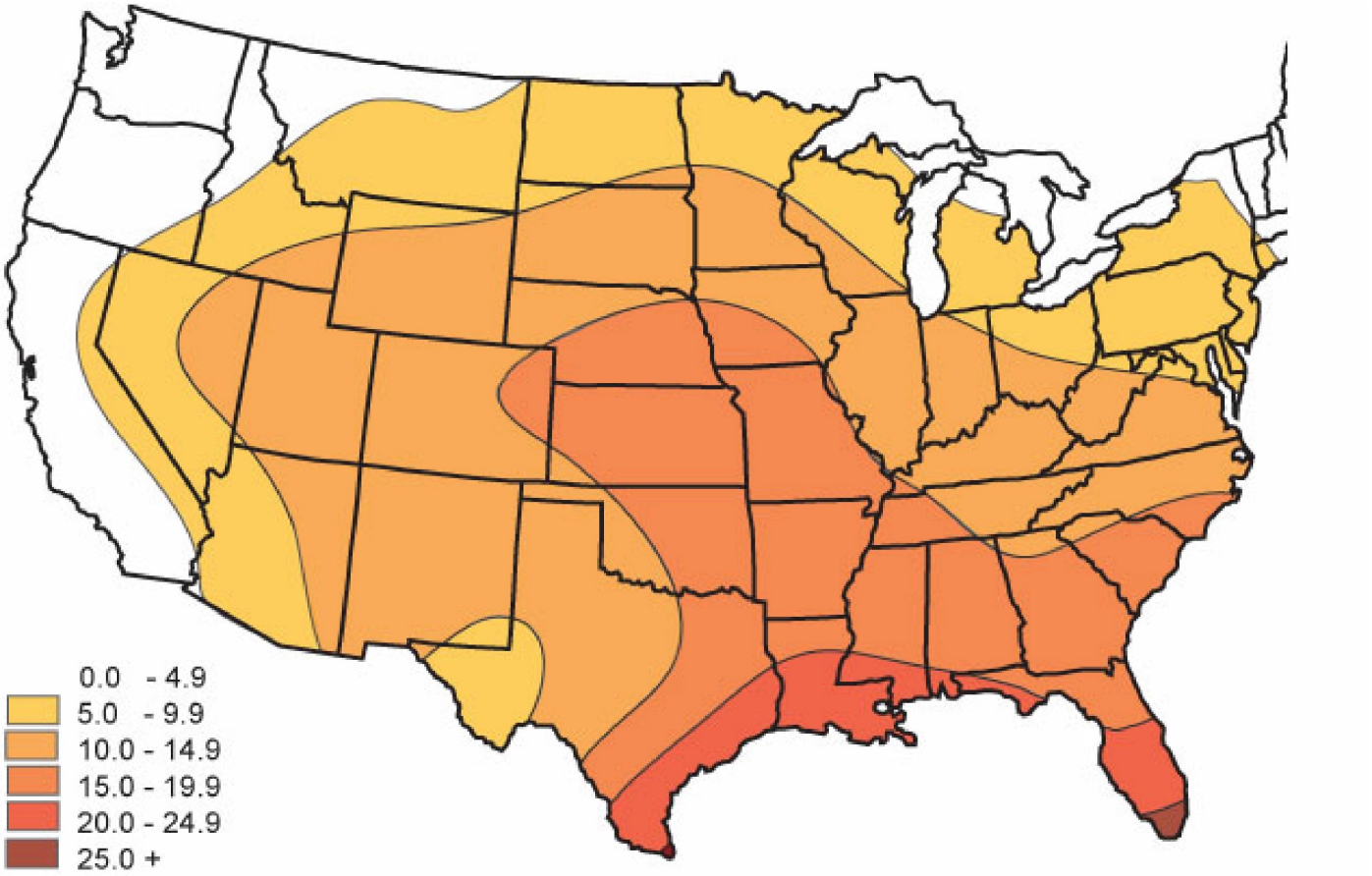

Courtesy of James C. Walter, Salt River Project, Tempe, Arizona

Average number of potential microburst days for the months of July and August based on 30 years of 00Z rawinsonde data

Diurnal Cycle

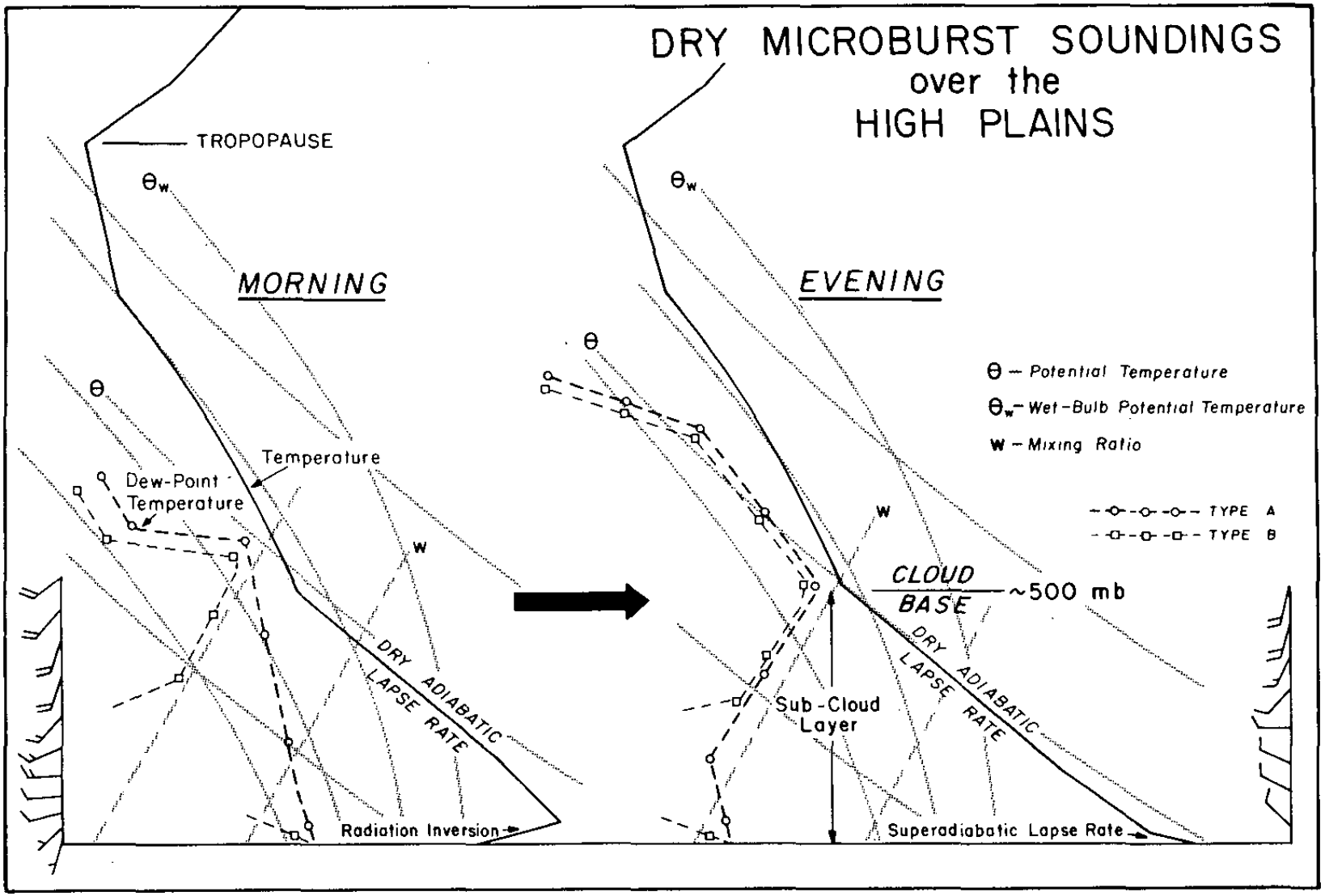

FIG. 8. Model of the characteristics of the morning and evening soundings favorable for dry-microburst activity over the High Plains.

DIURNAL VARIATION OF MICROBURSTS

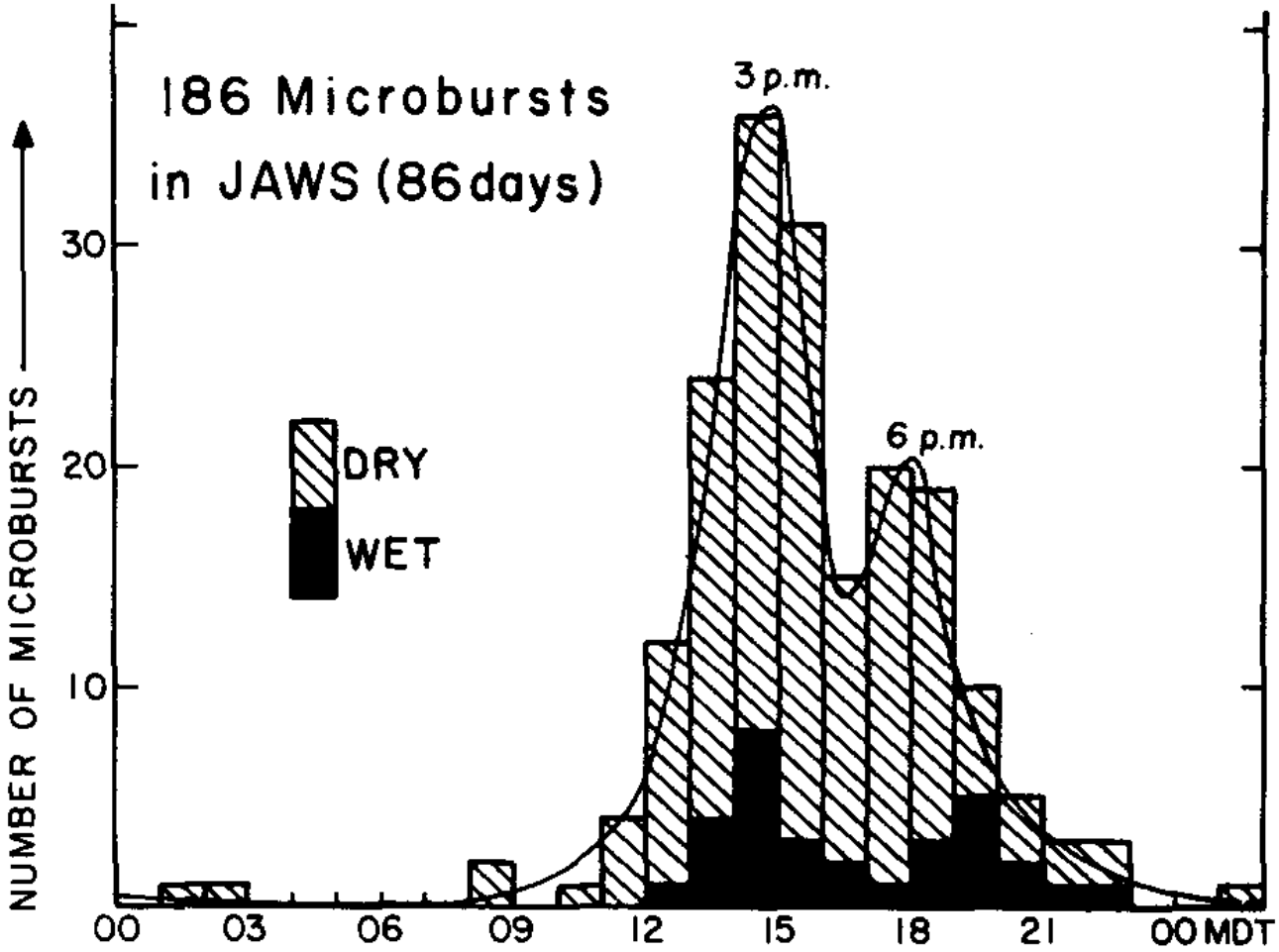

FIG. 4. Diurnal variation of the 186 microbursts during the JAWS Project. Most of the activity occurs during daylight hours with two peak periods at 1500 and 1800 MDT (MDT + 6 h = GMT).

Heat Burst!

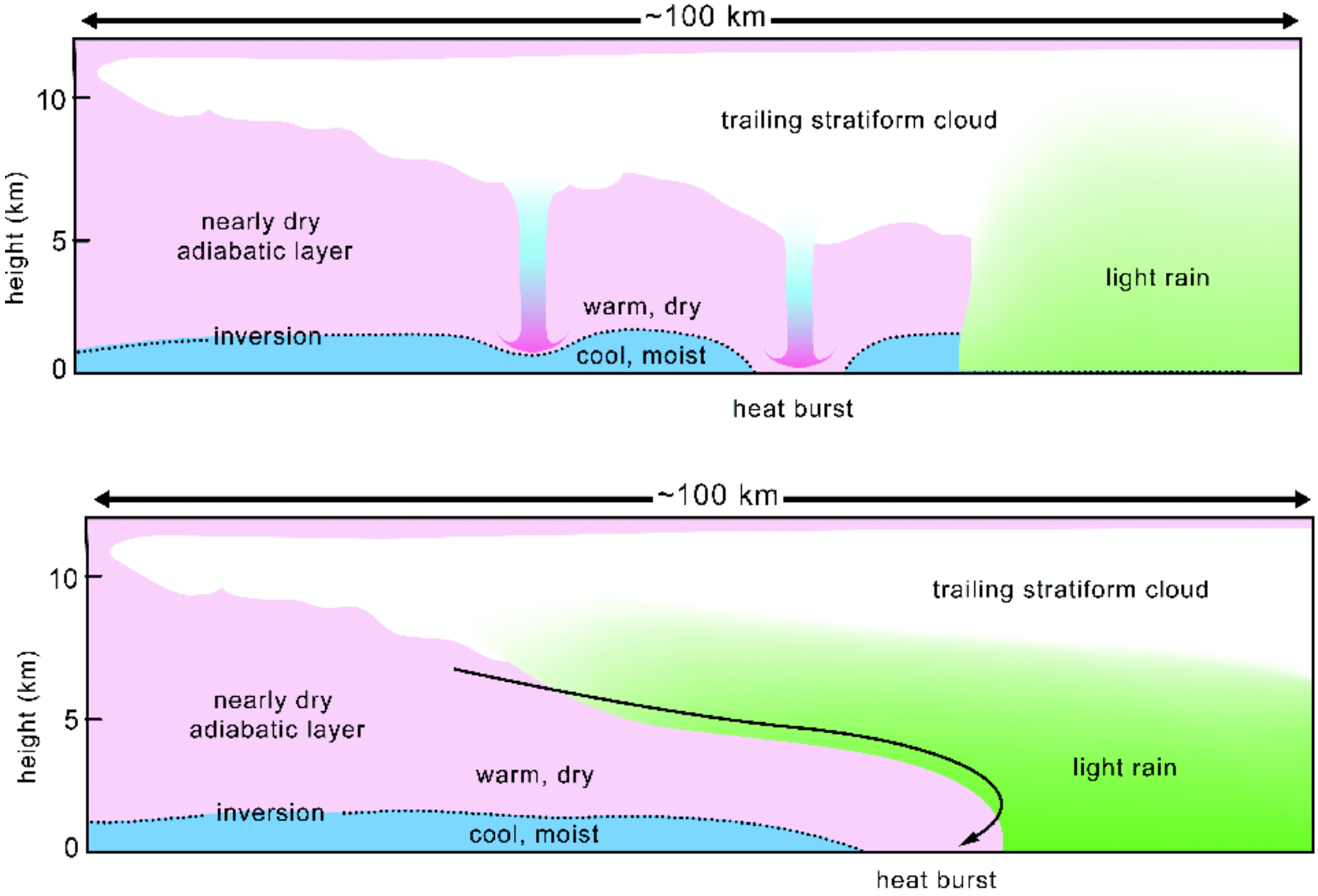

Markowski and Richardson (2010)

Heat Burst!

- A special, and much rarer, kind of downburst
- Results from precipitation-evaporated air
  - compressionally heating as it descends from very high altitude, usually on the backside of a dying squall line or outflow boundary.
- Heat bursts are chiefly a nocturnal occurrence
- can produce winds of up to 160 km/h
- are characterized by exceptionally dry air
- and can suddenly raise the surface temperature to 38 °C or more,
- sometimes persisting for several hours

Downbursts on Radar

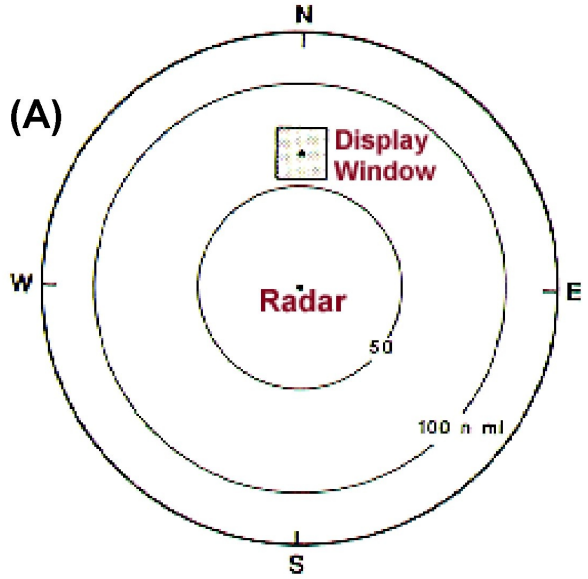

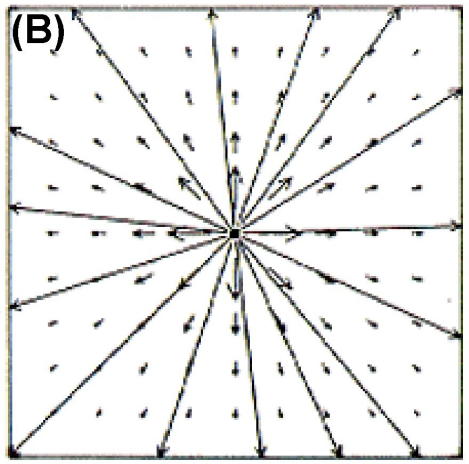

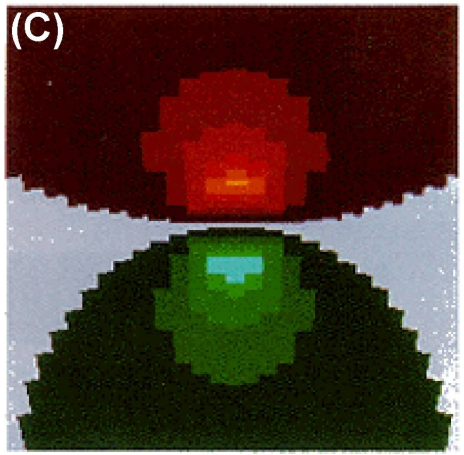

Courtesy of NOAA

Downbursts on Radar

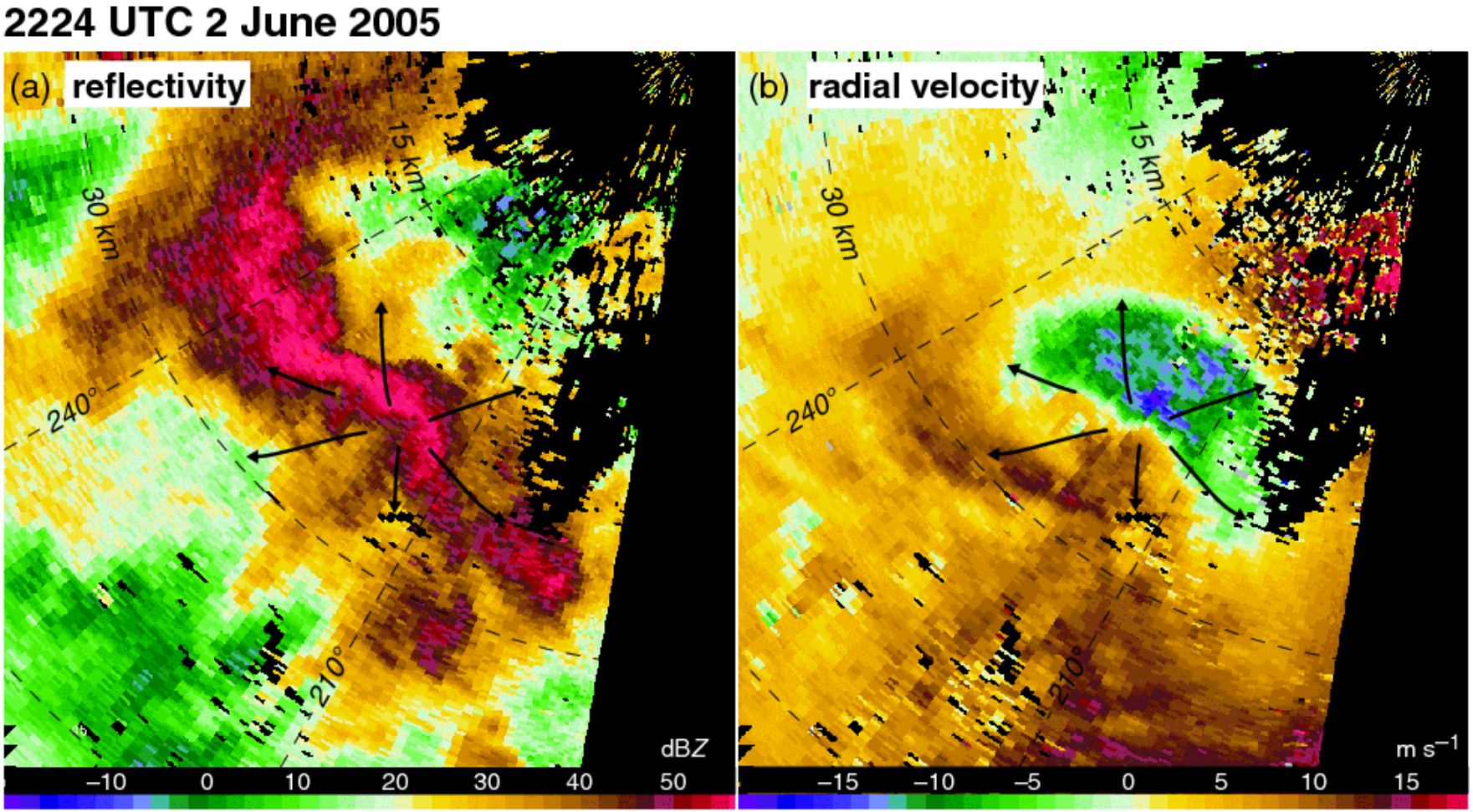

Downburst Radar Algorithms

- EC MICRO algorithm
  - Looks for regions of divergent shear along radial and matches these to form a 2D pattern
  - Provides no lead time
- EC WDRAFT algorithm
  - Based on empirical relationship between VIL (Vertically Integrated Liquid) and resulting downdraft intensity
  - Can provides 10-15 min lead time
- Airports also have TDWR (Terminal Doppler Weather Radar; n.wikipedia.org/wiki/Terminal_Doppler_Weather_Radar) and various algorithms for microburst detection

Dual-Doppler Downburst Winds

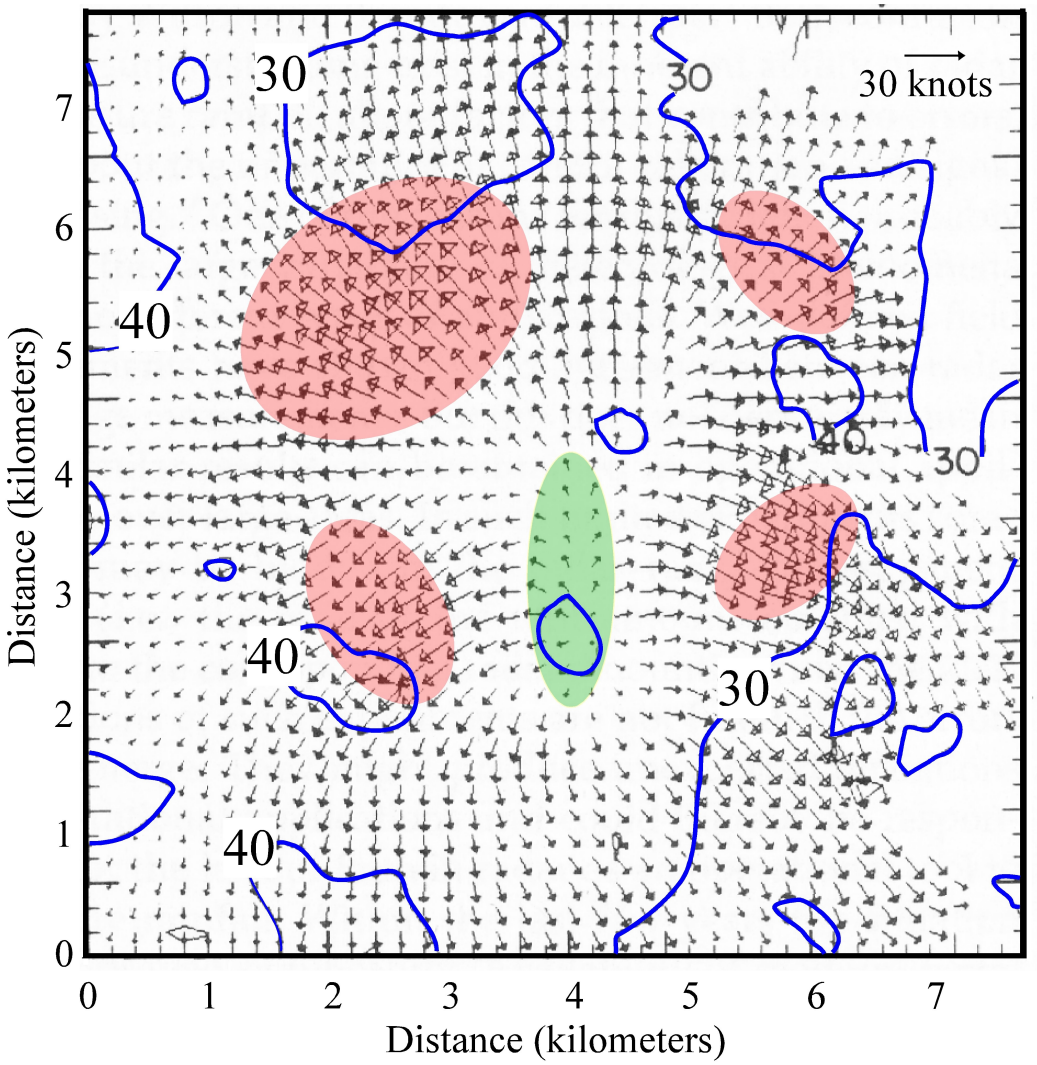

Courtesy of Jim Wilson and the American Meteorological Society

Derechoes

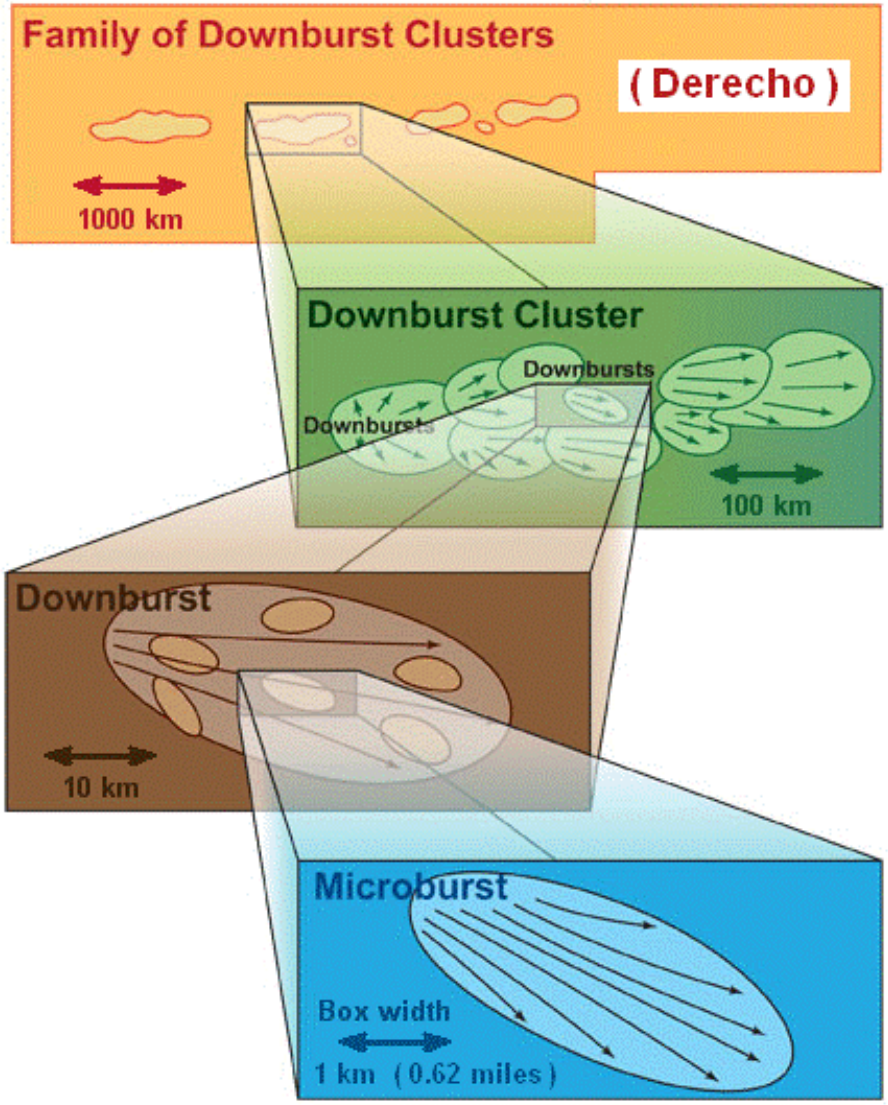

www.spc.noaa.gov

- Johns and Hirt (1987) defined a derecho as a concentrated area of damaging downburst winds having a major axis length of at least 400 km
- The graphic at left suggests much larger major axis lengths – appears that more refinement of definition is required!

Derecho Climatology

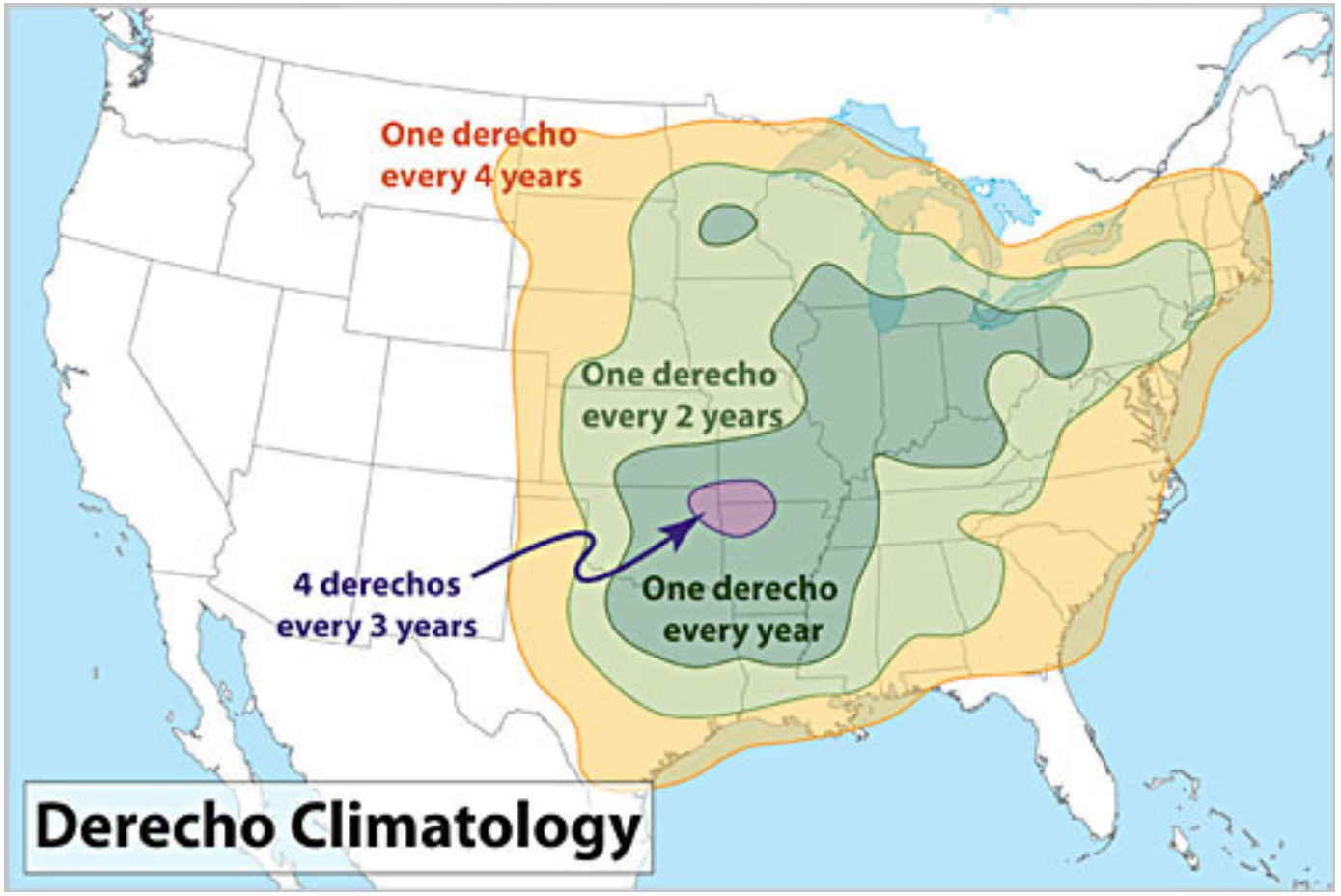

www.spc.noaa.gov

Sting Jets

- Mesoscale phenomenon associated with rapidly deepening synoptic-scale extra-tropical system

- Damaging winds can reach 50 m/s and affect an area ~50 km wide and several hundred km long

- Conceptual model of sting jet first formally developed by Keith Browning in 2004 during his re-analysis of the Britain's 'Great Storm' of October 15-16, 1987

- Still a very active area of research

GREAT STORM OF OCTOBER 1987

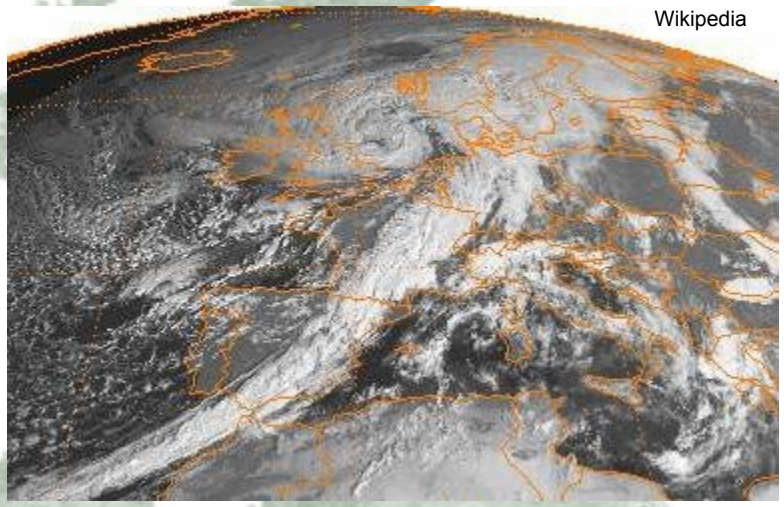

Wikipedia

1 1am 16th Oct

2 4am 16th Oct

3 7am 16th Oct

4 10am 16th Oct

Gorleston

London

Langdon Bay

Herstmonceux

Southampton

IMPACTS

Most damaging storm since 1703

Fatalities 18

Damage £1.4bn

Trees blown over 15m

STRONGEST GUSTS

Gorleston	122mph
Langdon Bay	108mph
Herstmonceux	104mph
London	94mph
Southampton	86mph

http://www.channel4.com/news/the-great-storm-of-1987-infographic

Map Google | Data Met Office

The famous ‘Great Storm’ cut a swathe of damage across South-east England in the early hours of the 16th October 1987. It was a good example of a storm with a ’Sting Jet’.

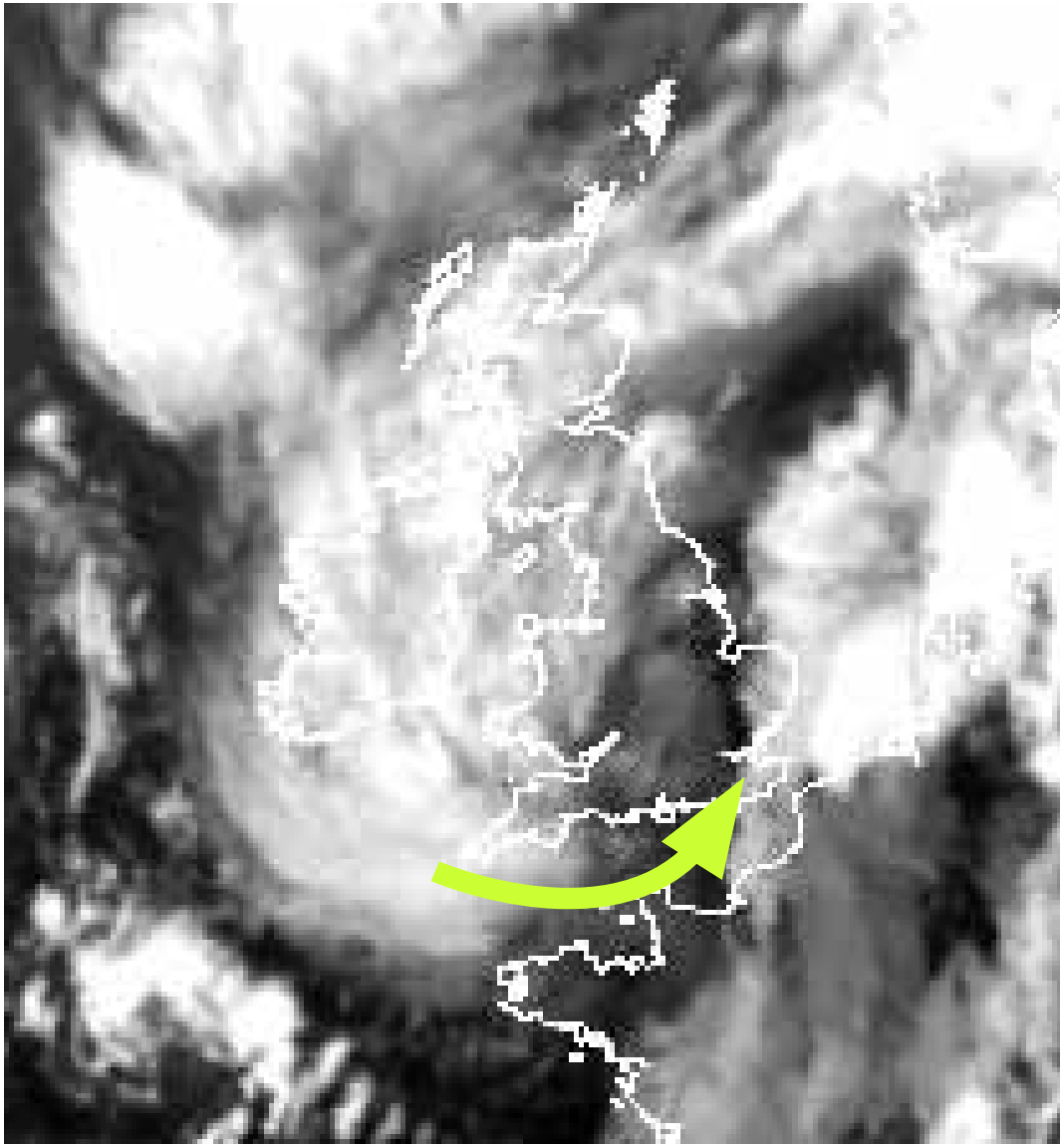

The satellite image above shows the pattern of the cloud just before the strongest winds hit the south coast of Kent and Sussex near the ‘tail’ of the hook-shaped cloud wrapping round the cyclone.

The green arrow shows the approximate path of the Sting Jet.

Frontal Fracture

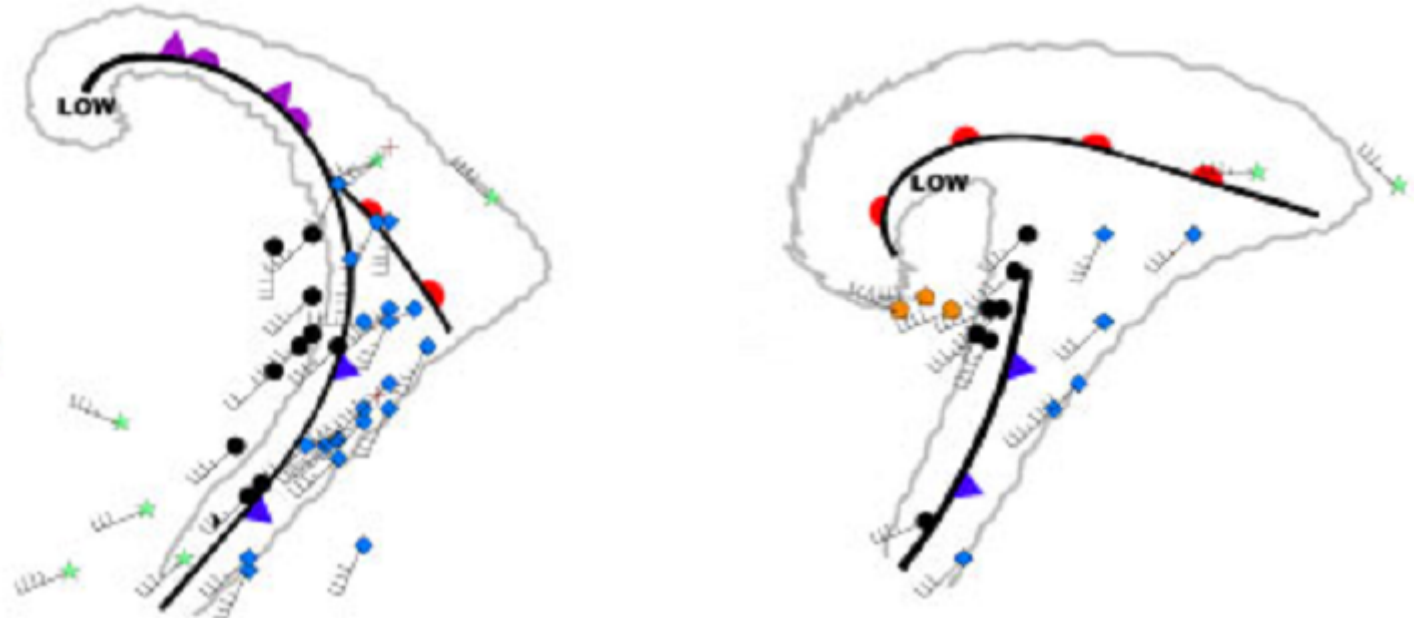

Shapiro and Keyser (1990)

• Classic ‘Norwegian’ and Shapiro-Keyser conceptual models for evolution of extra-tropical cyclones: ‘occluded front’ vs. ‘frontal fracture’

Sting Jet Development

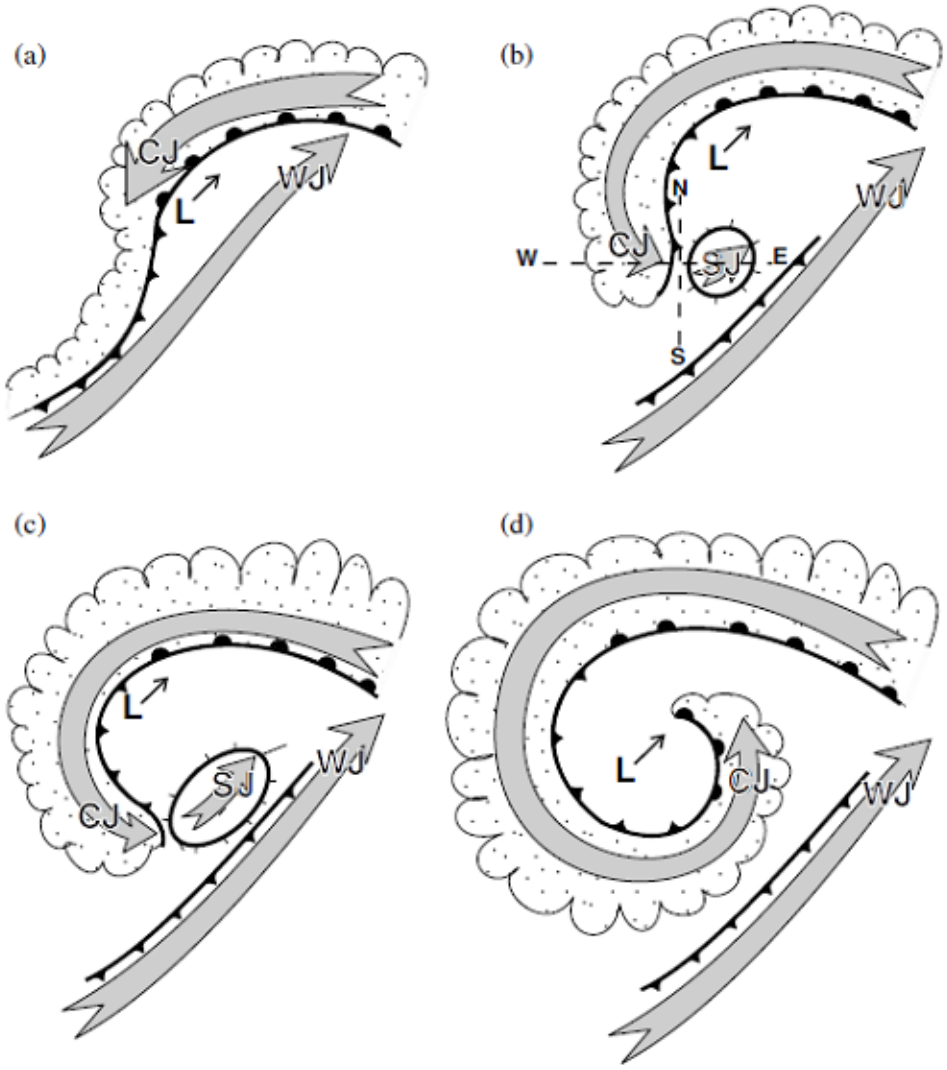

Clark et al. (2005)

1.

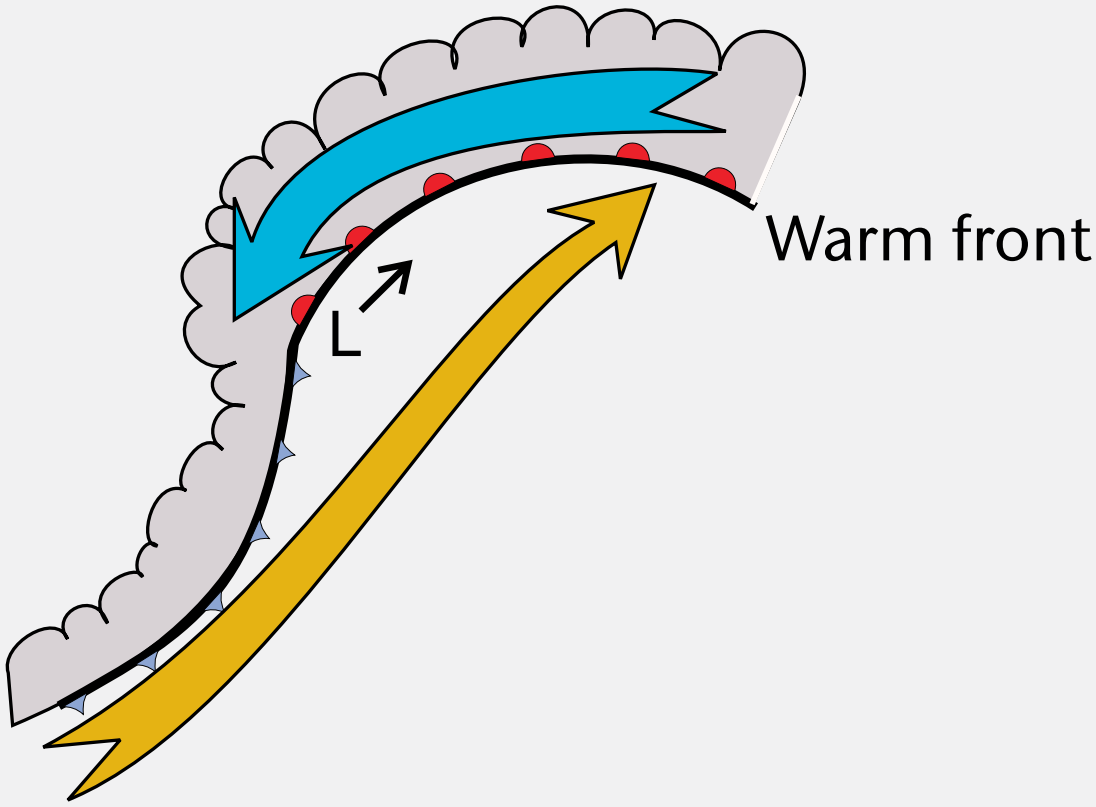

As the pressure starts to drop, two narrow jets of air form near the surface, one cold (blue) the other warm (orange). The low pressure centre (L) is usually moving with the warm jet, so the warm jet produces stronger winds.

2.

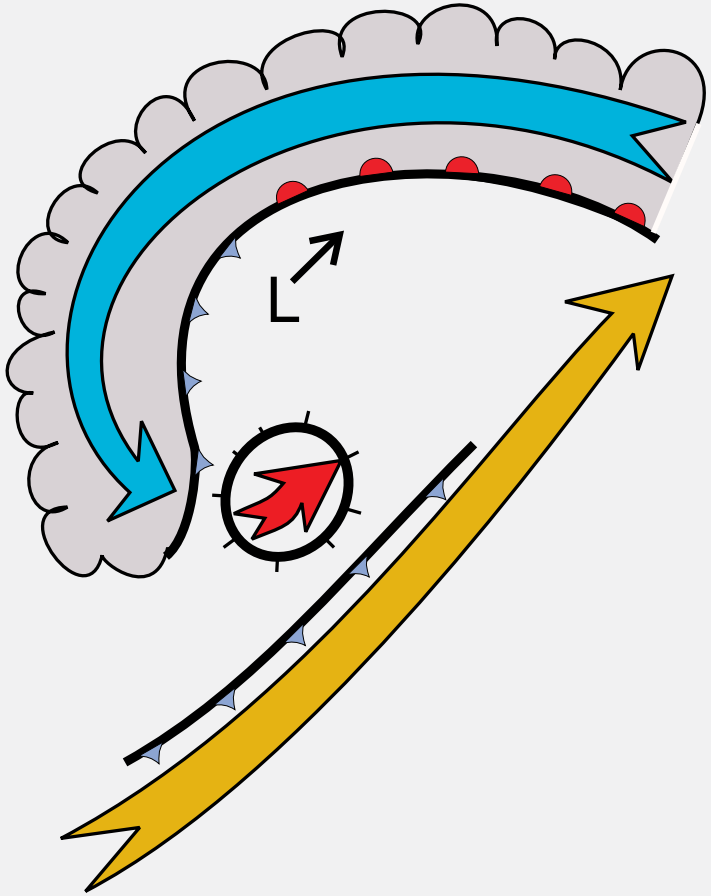

The weather front ‘fractures’, shortly afterwards the Sting Jet reaches the ground near the break (red). The most damaging winds occur here.

3.

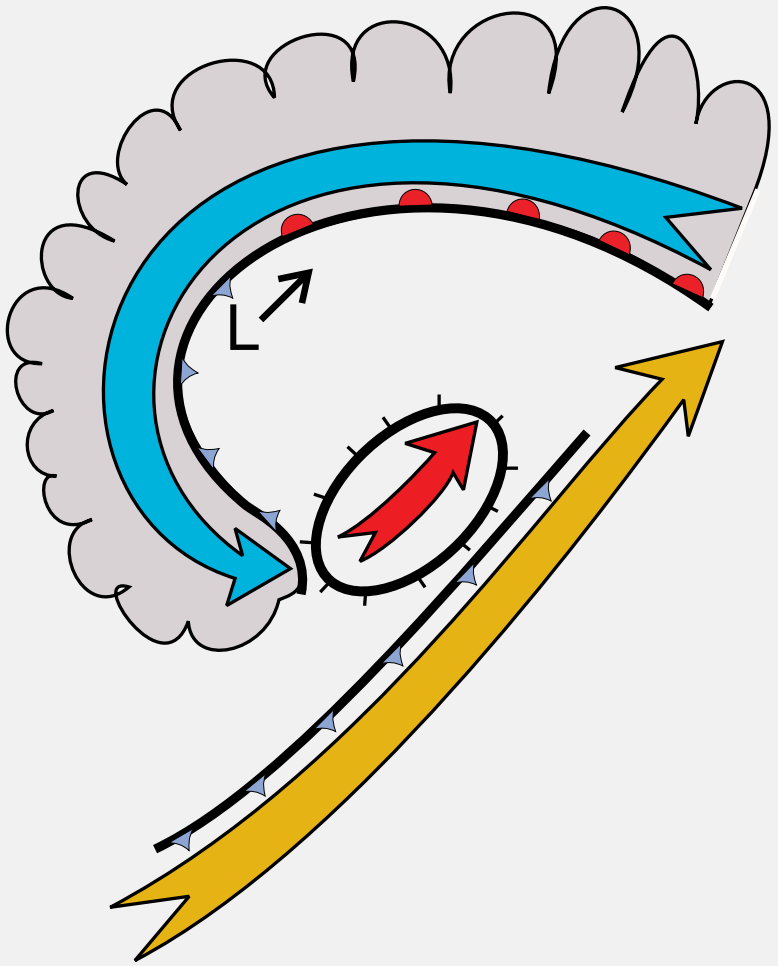

The Sting Jet region enlarges over a few hours.

4.

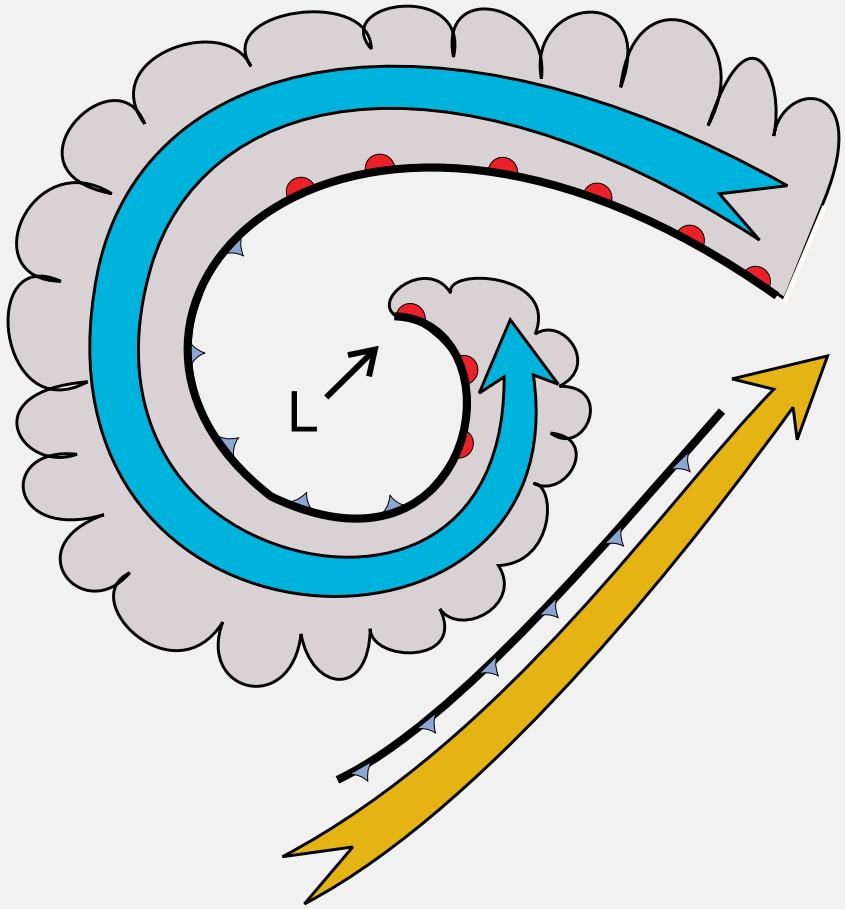

The cold jet eventually wraps round the low centre and catches up with the Sting Jet. Strong winds may still occur, but the most damaging are over.

The sting at the end of the tail..

Browning (2004) defined the sting jet as follows:

"The most damaging extra-tropical cyclones go through an evolution that involves the formation of bent-back front and cloud head separated from the main polar front cloud band by a dry slot. When the cyclone attains its minimum central pressure, the trailing tip of the cloud head bounding the bent-back front forms a hook which goes on to encircle a seclusion of warm air. The most damaging winds occur near the tip of this hook – the sting at the end of the tail."

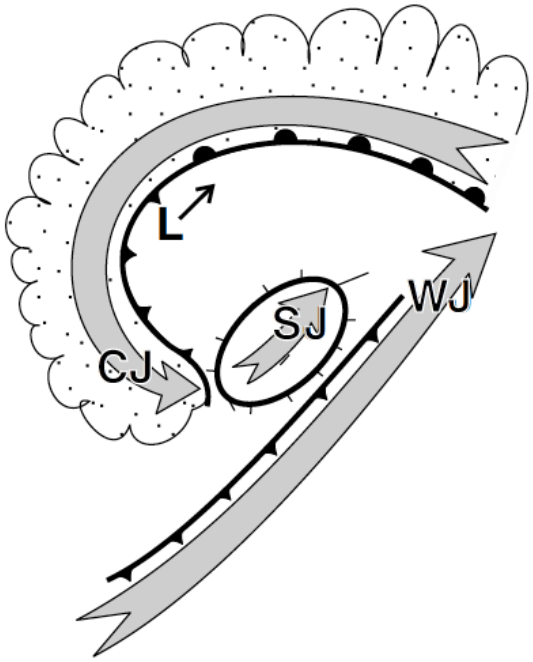

Clark et al. (2005)

Sting Jet Development

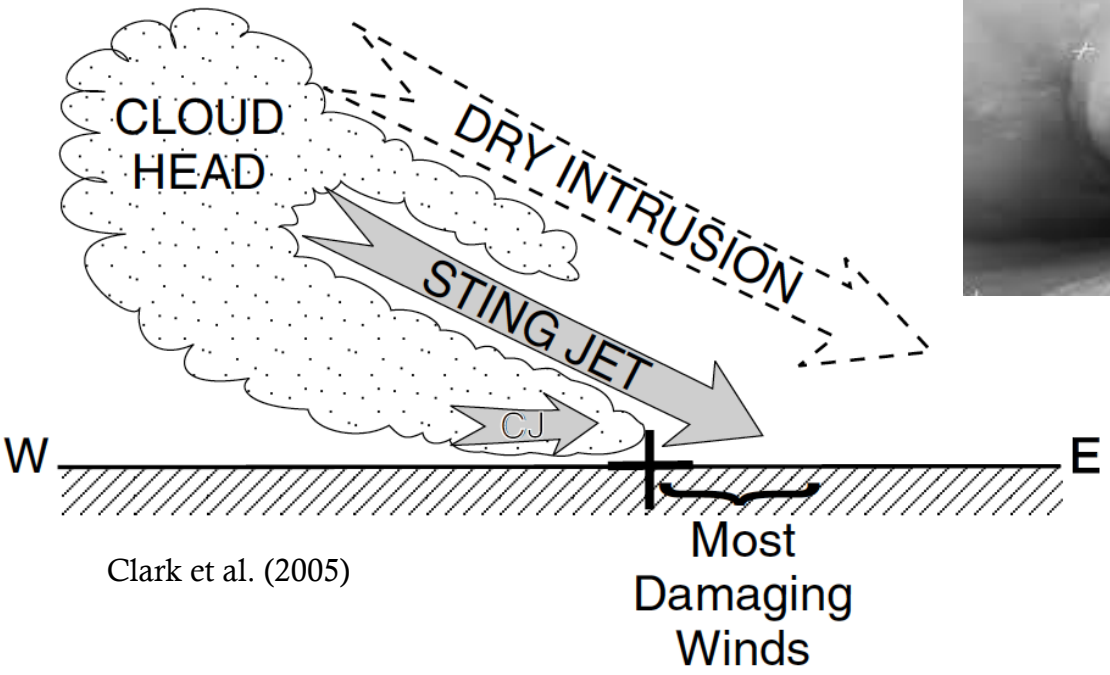

Clark et al. (2005)

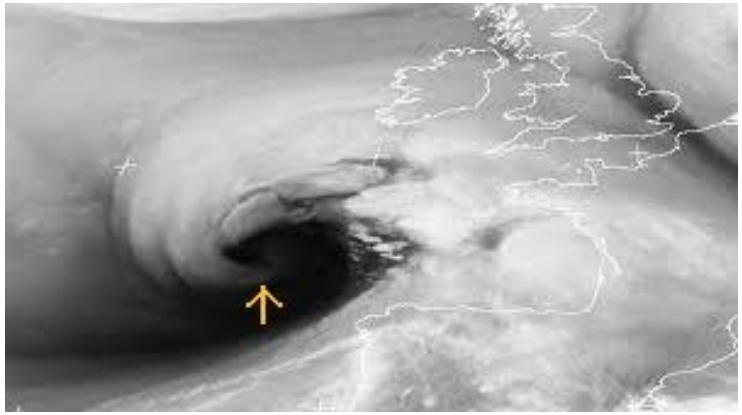

http://hydrometeo.e-monsite.com

- Sting Jet starts 3-4 km above ground level and descends over several hours
- 'Slantwise convection' and rapid evaporative cooling thought to be important, but exact processes remain uncertain.
- Slantwise convection: more details http://www.meted.ucar.edu/norlat/slant/

Modelling the Sting Jet

What we see at the ground

These results are from a simulation of the 16 October 1987 'Great Storm' using a version of the Met Office's forecast model (as at Autumn 2002). It was started using a re-analysis of the atmospheric state at 12 UTC 15 October 1987 by the European Centre for Medium Range Weather Forecasting (ECMWF).

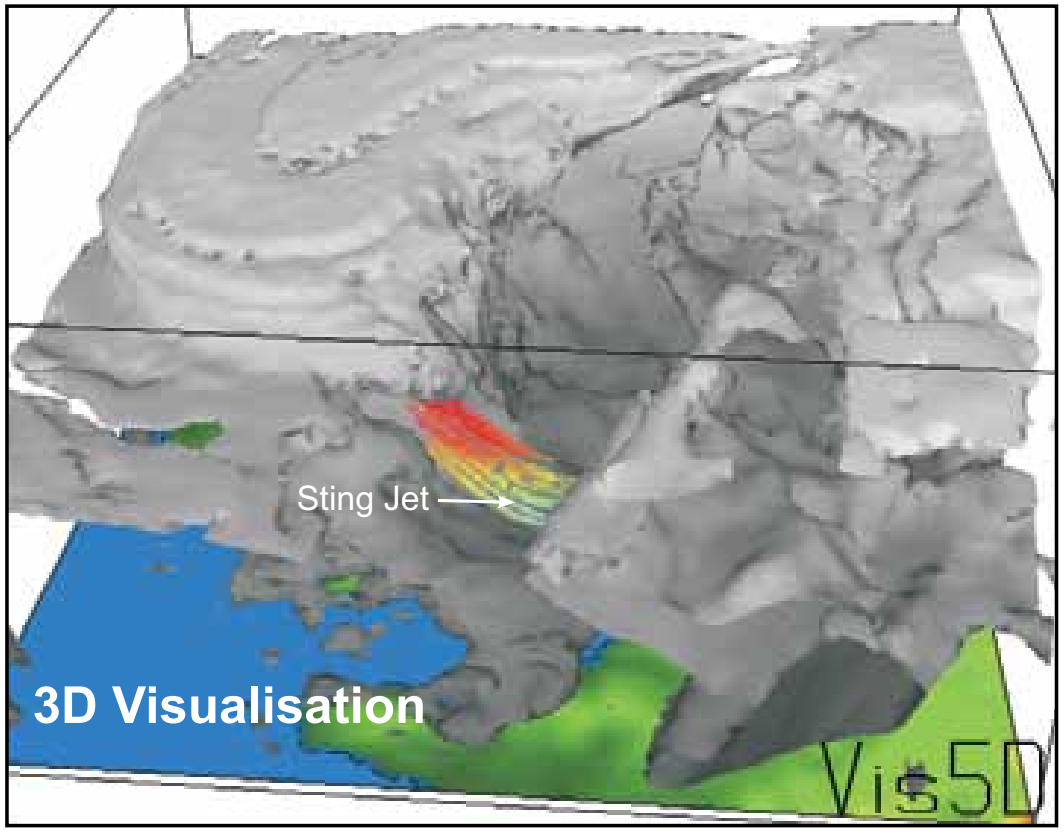

The modelled sea level pressure pattern (left) and a 3D representation of the model cloud (right) corresponding. The cloud is shaded according to the height above the surface - lighter gray is higher up.

The coloured streaks show the track of air in the Sting Jet leading to the strongest surface winds for 4 hours back from the time shown. The tracks are coloured by altitude - red is about 4 km above the surface, yellow 3 km, green 2 km, blue 1 km. Strong surface winds are shown circled in red (left).

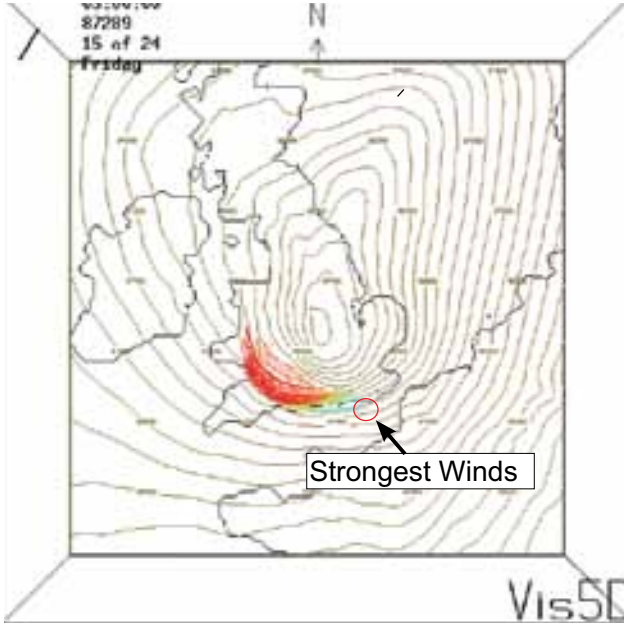

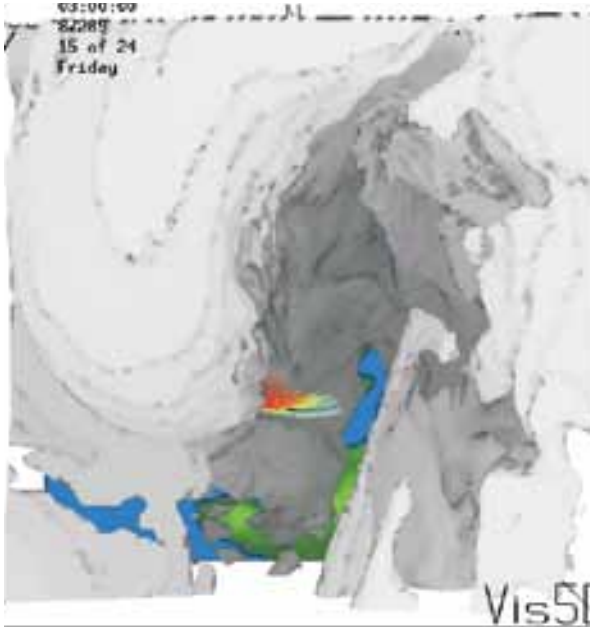

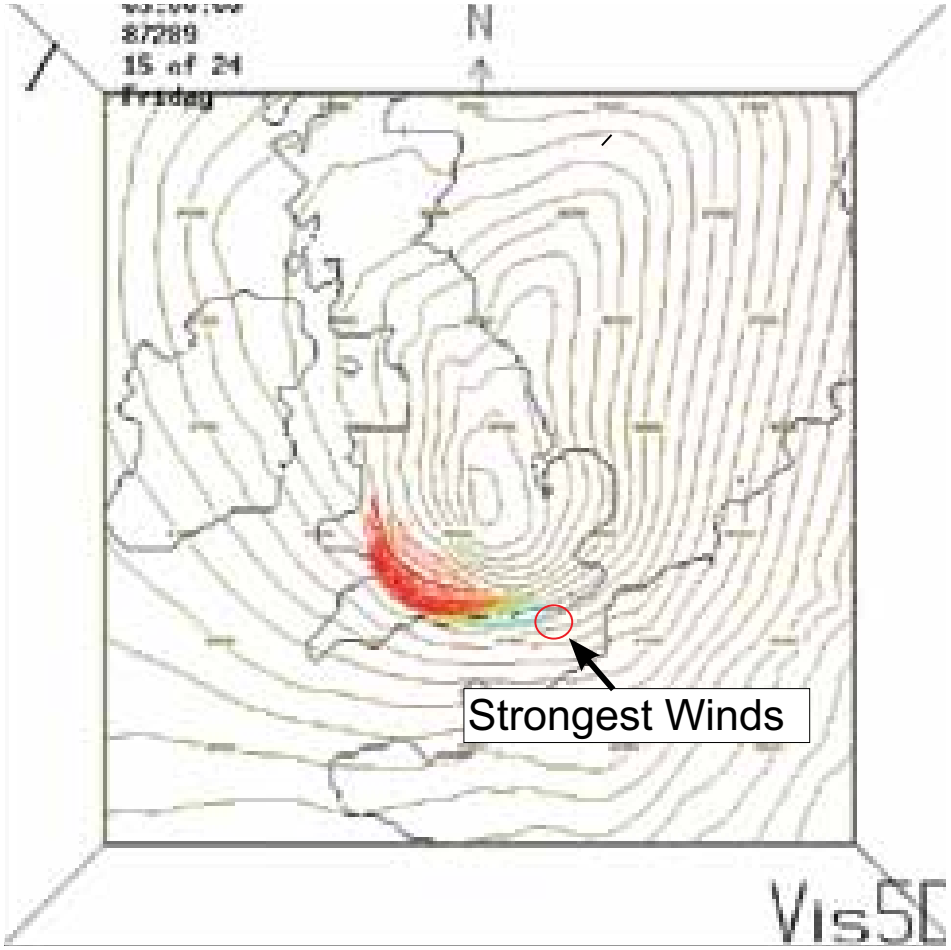
N
15 of 24
Friday
Strongest Winds

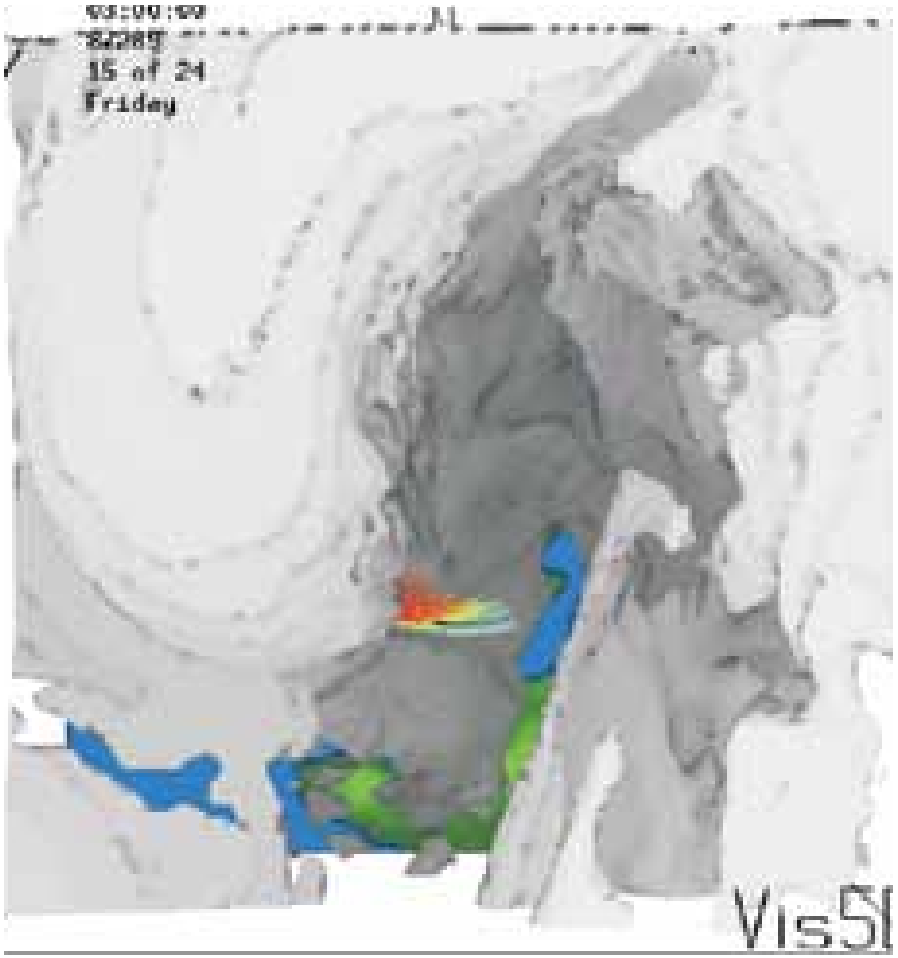
15 of 24
Friday

Simulated image from Met Office Unified Model 15 hour forecast from 12UTC 15 October 1987.

If we simulate what a satellite would see of our model results and compare with a satellite image we find a remarkably similar pattern in the cyclone cloud. However, it is not perfect; in particular the model cloud is not so 'hooked', suggesting that the real cyclone may have been more intense.

The green box shows the area on the 3D pictures (above).

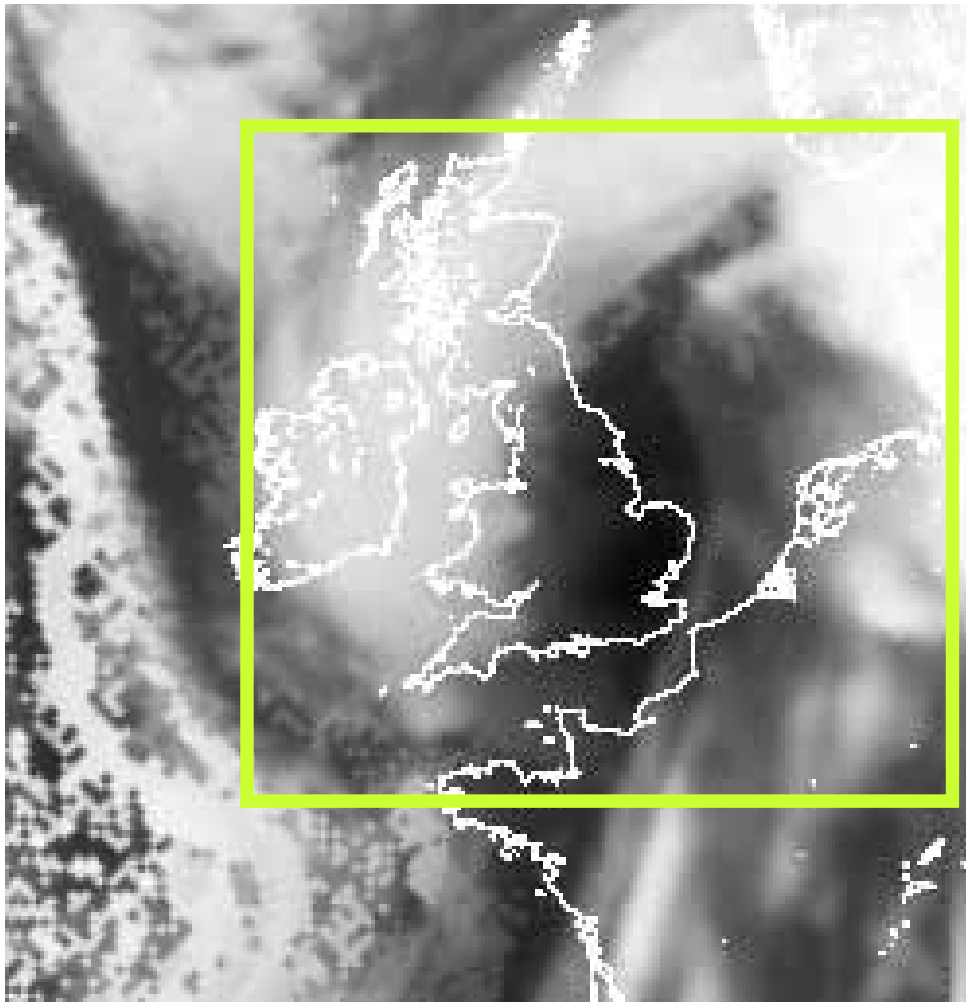

Why do we need to understand the Sting Jet?

We need to understand why the Sting Jet forms to make sure our model can represent it well.

We now know that we need:

1) To capture the width of the Sting Jet (about 50 km)

2) To capture the depth of the Sting Jet (about 1 km)

3) To capture the evaporation of snow (as it falls about 500 m).

4) To capture the interaction of the Sting Jet with the air flowing near the surface.

Our current global forecast model has a horizontal gridlength of about 60 km over the UK and has 38 levels going up to nearly 40 km. It does a good job of warning of strong winds, but predicts peak gusts of only about 60 knots (70 mph) (right). It predicts no Sting Jet.

A version of the model run over a region of about 3000 km x 3000 km and with 90 levels produces a Sting Jet and does a much better job, predicting gusts above 80 knots (95 mph).

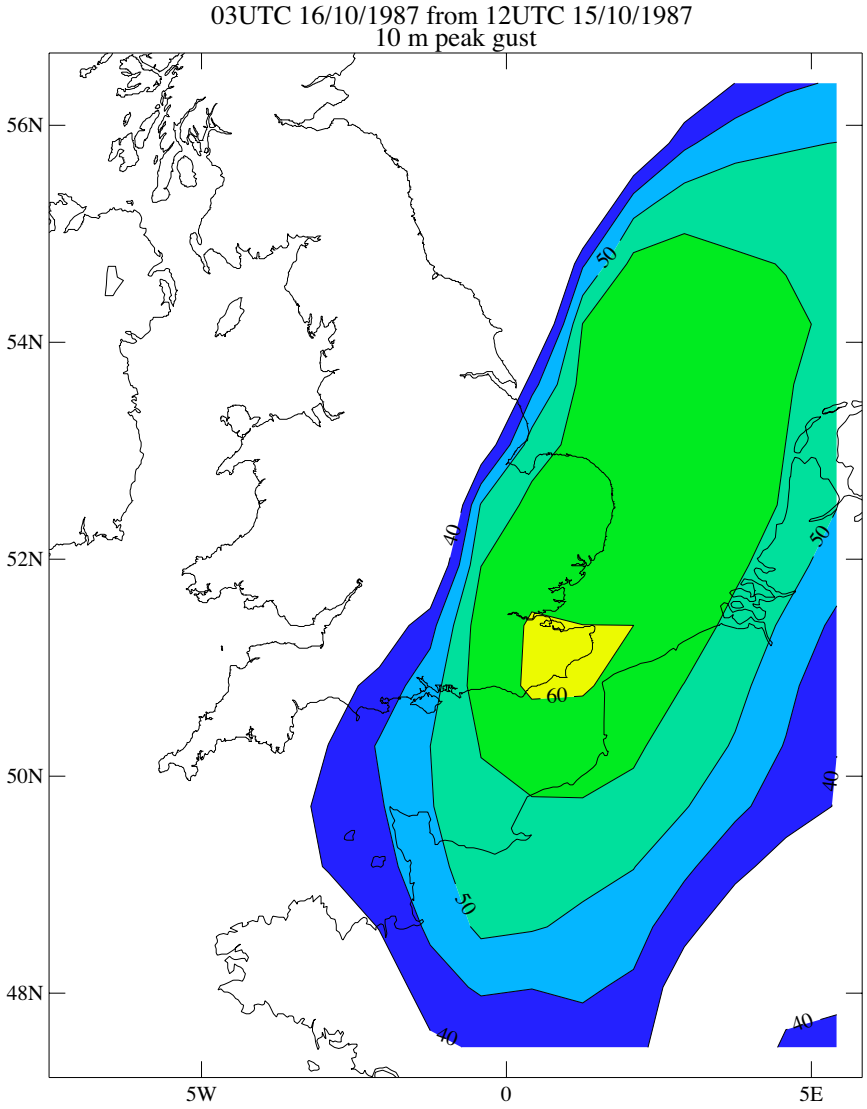

Predicted wind gusts at 03 UTC 16th October 1987 during the 'Great Storm' using a model with 60 km resolution, 38 levels. The model predicts a large area of strong winds peaking at more than 60 knots (about 70 mph) in a region just crossing the south coast.

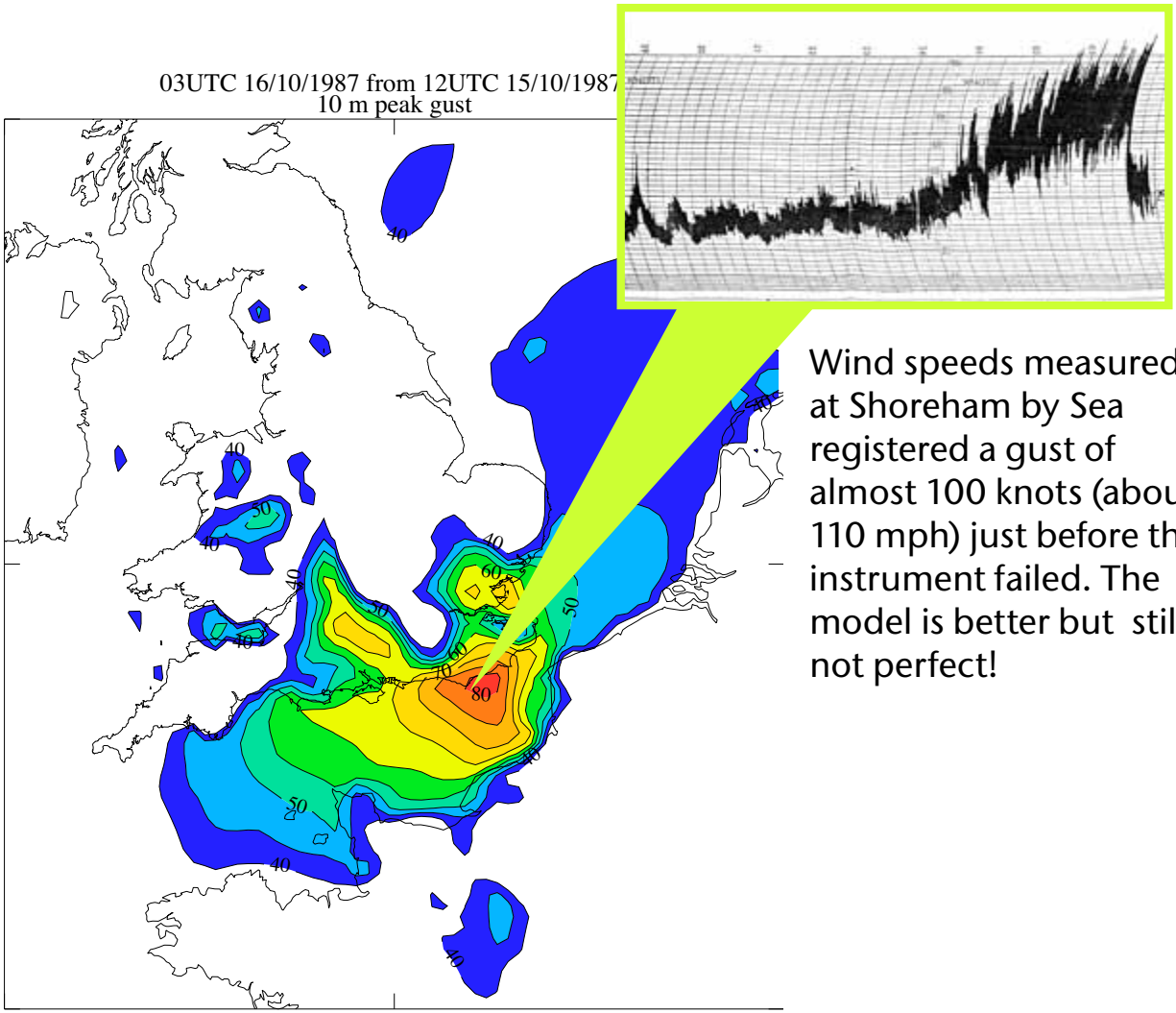

Wind speeds measured at Shoreham by Sea registered a gust of almost 100 knots (about 110 mph) just before the instrument failed. The model is better but still not perfect!

Predicted peak wind gusts at 03 UTC 16th October 1987 during the 'Great Storm' using a model with 12 km resolution and 90 levels. The model predicts more than 80 knots (about 95 mph) in a region just crossing the south coast.

Using Frontogenesis to Identify Sting Jets in Extratropical Cyclones

DAVID M. SCHULTZ

Centre for Atmospheric Science, School of Earth, Atmospheric and Environmental Sciences, University of Manchester, Manchester, United Kingdom

JOSEPH M. SIENKIEWICZ

NOAA/NWS/NCEP/Ocean Prediction Center, College Park, Maryland

(Manuscript received 5 December 2012, in final form 13 March 2013)

Weather and Forecasting

- Case study of an intense cyclone over the North Atlantic Ocean that possessed a sting jet detected from the NASA Quick Scatterometer (QuikSCAT).

- A couplet of Petterssen frontogenesis and frontolysis occurred along the bent-back front.

- The direct circulation associated with the **frontogenesis led to ascent within the cyclonically turning portion of the warm conveyor belt, contributing to the comma-cloud head**.

- When the bent-back front became **frontolytic**, an indirect circulation associated with the frontolysis, in conjunction with along front cold advection, led to **descent within and on the warm side of the front, bringing higher-momentum air down toward the boundary layer**.

• Sensible heat fluxes from the ocean surface and cold-air advection destabilized the boundary layer, resulting in near-neutral static stability facilitating downward mixing.

• **Descent associated with the frontolysis reaching a near-neutral boundary layer provides a physical mechanism for sting jets**.

• The couplet of **frontogenesis and frontolysis** could explain

- **why sting jets occur at the end of the bent-back front and emerge from the cloud head,**
- why sting jets are mesoscale phenomena, and
- why they only occur within Shapiro–Keyser cyclones.

Frontal Fracture

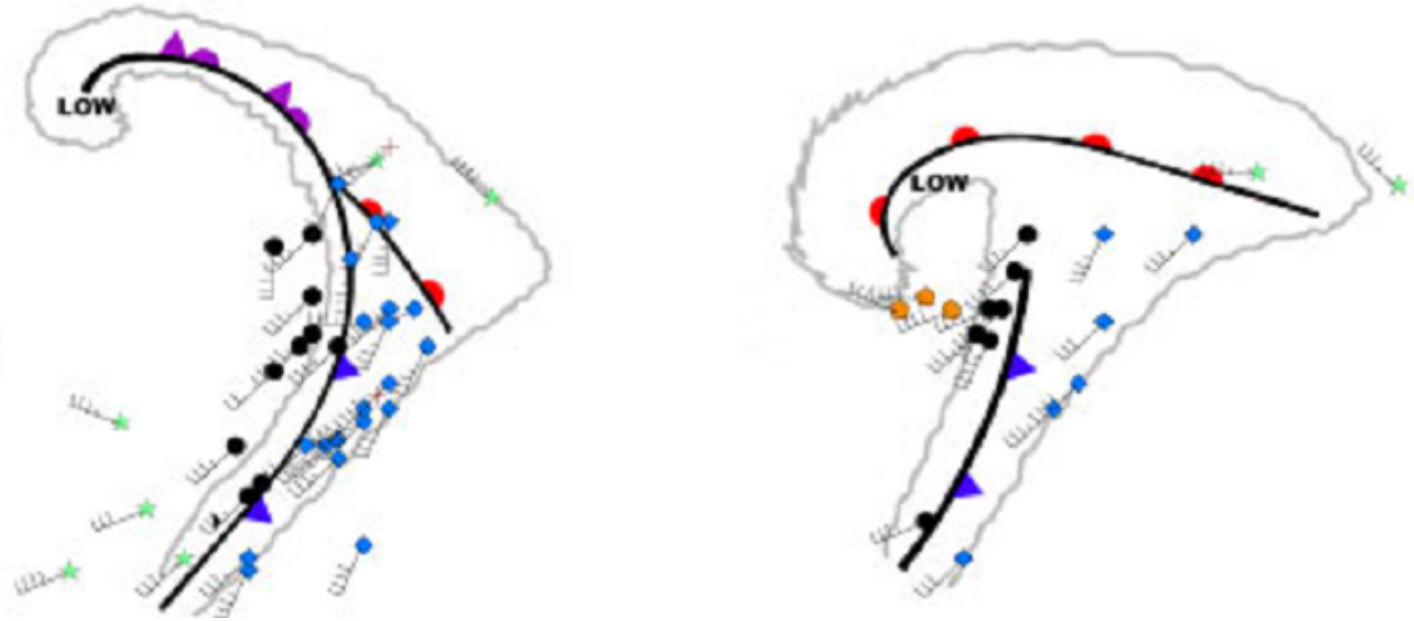

Shapiro and Keyser (1990)

• Classic ‘Norwegian’ and Shapiro-Keyser conceptual models for evolution of extra-tropical cyclones: ‘occluded front’ vs. ‘frontal fracture’

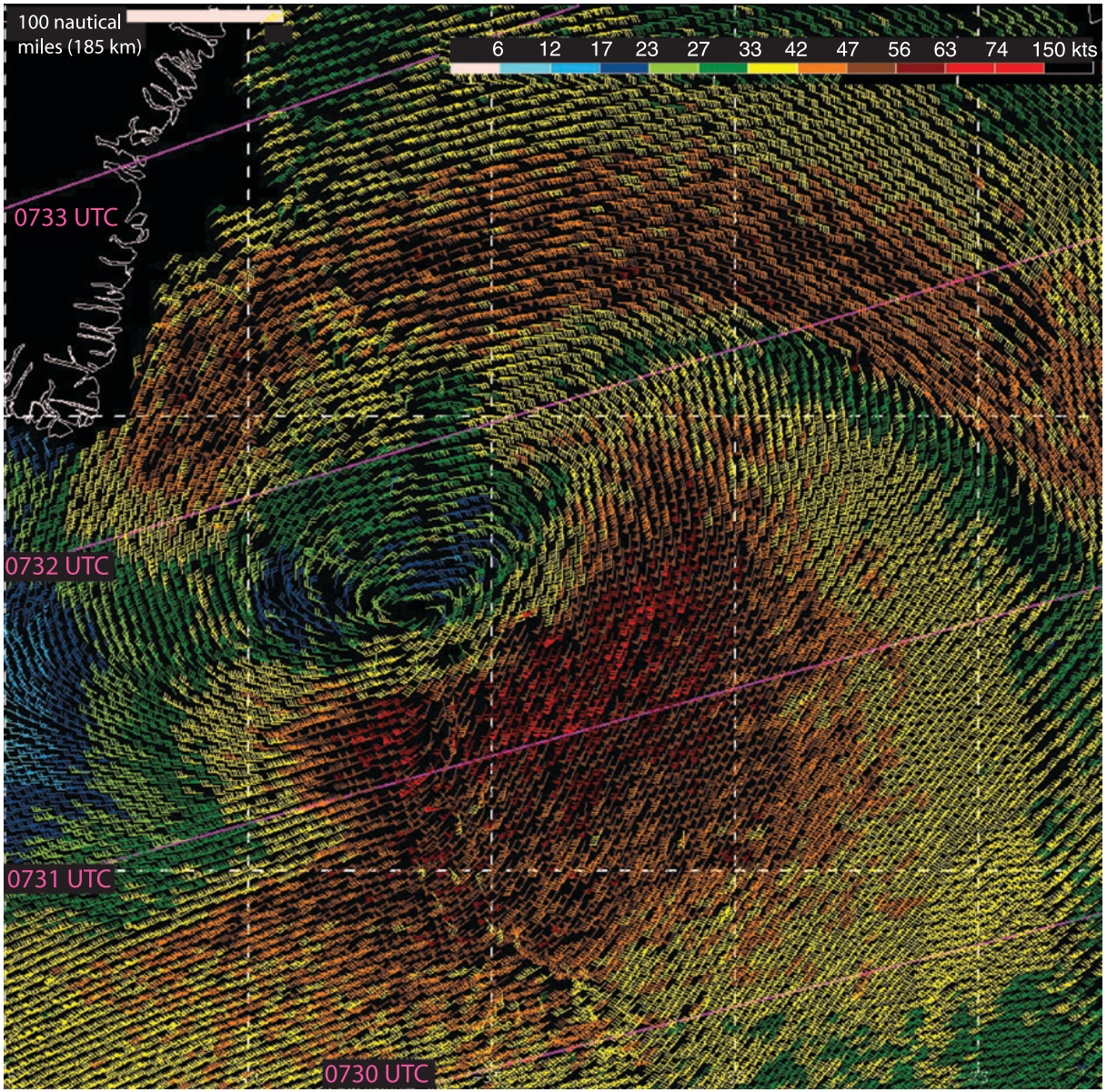

FIG. 1. QuikSCAT imagery of horizontal wind speed and direction at 0730–0733 UTC 8 Dec 2005 (pennant, full barb, and half-barb denote 50, 10, and 5 kt, respectively, where 1 kt = 0.514 m s^{-1}; separation between displayed wind vectors is 12.5 km). The colored wind barbs represent wind speed (kt) according to the scale in the top-right corner, the pink lines represent satellite overpass times, and the scale bar in the top-left corner represents 100 nautical miles (n mi, or 185 km).

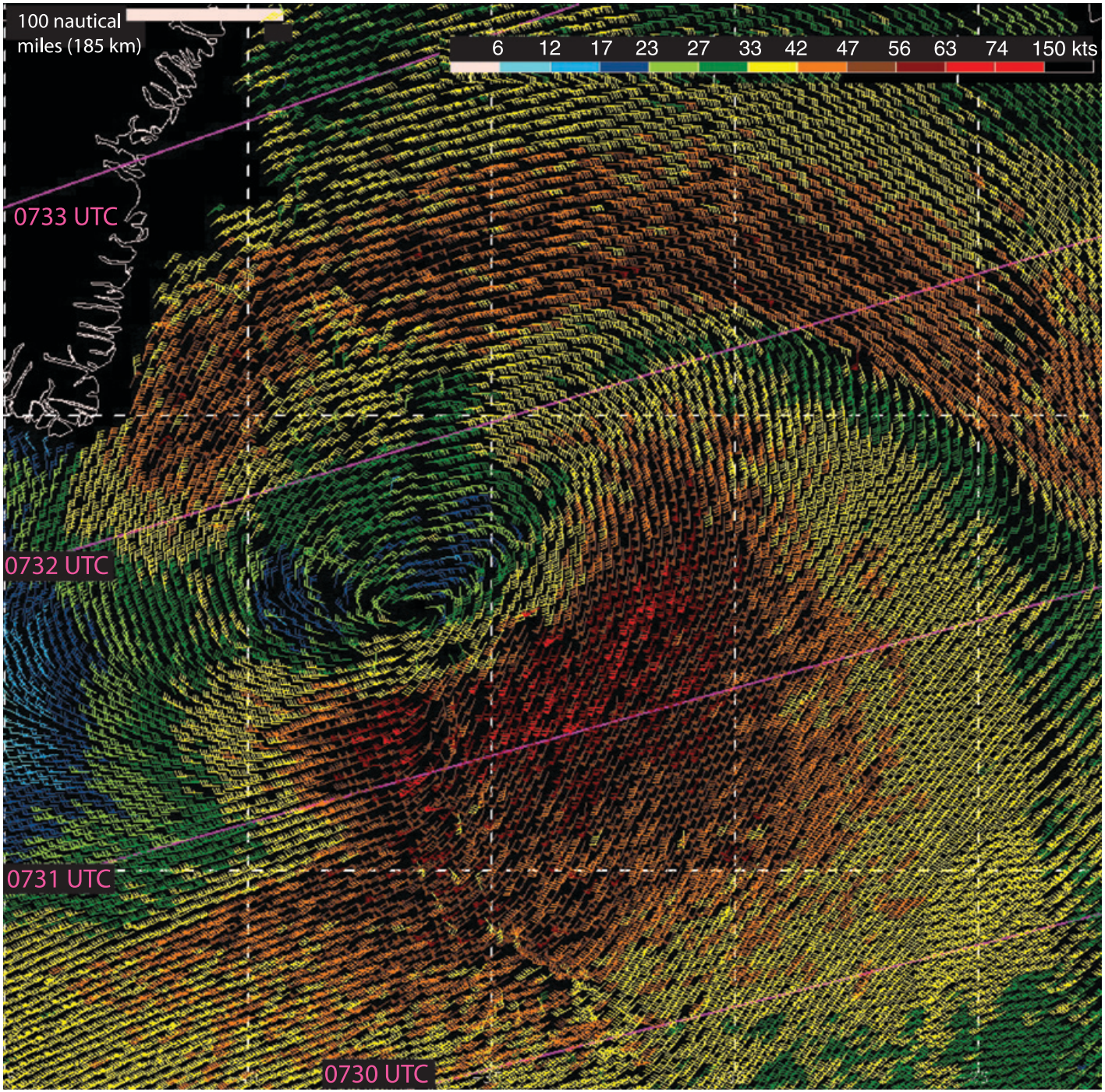
100 nautical
miles (185 km)
6 12 17 23 27 33 42 47 56 63 74 150 kts
0733 UTC
0732 UTC
0731 UTC
0730 UTC

WRF simulation

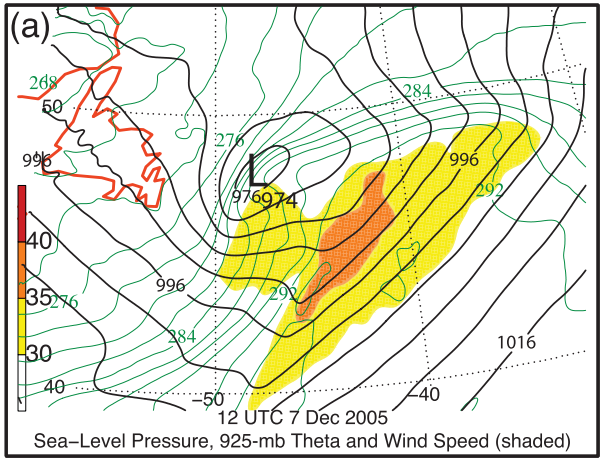

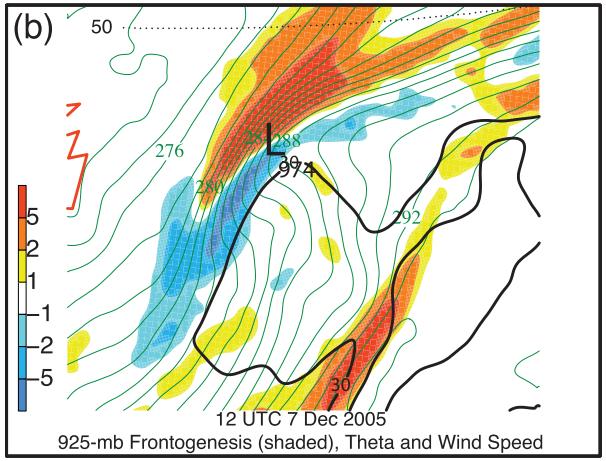

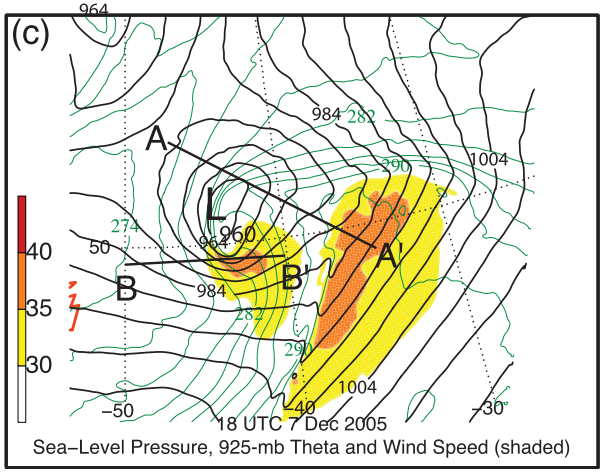

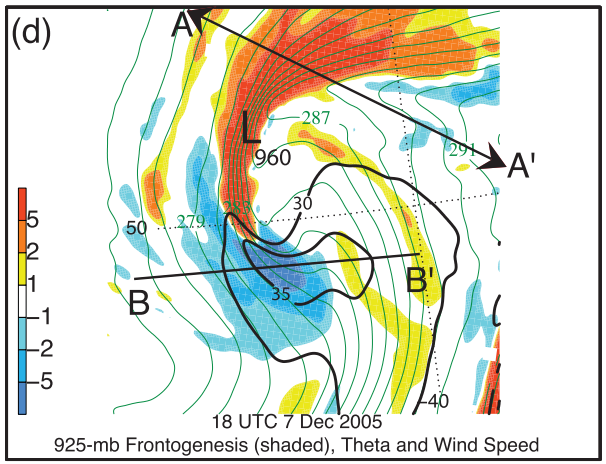

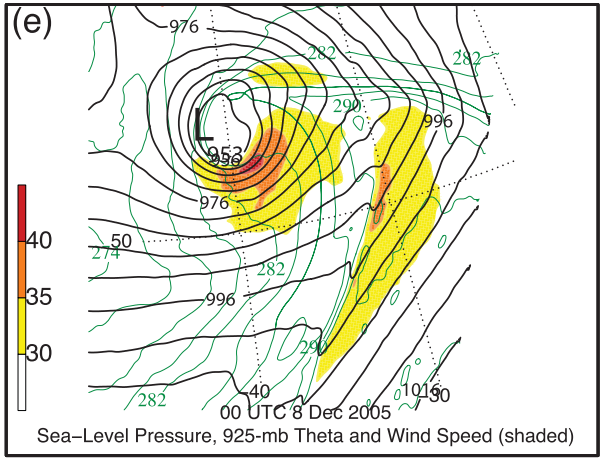

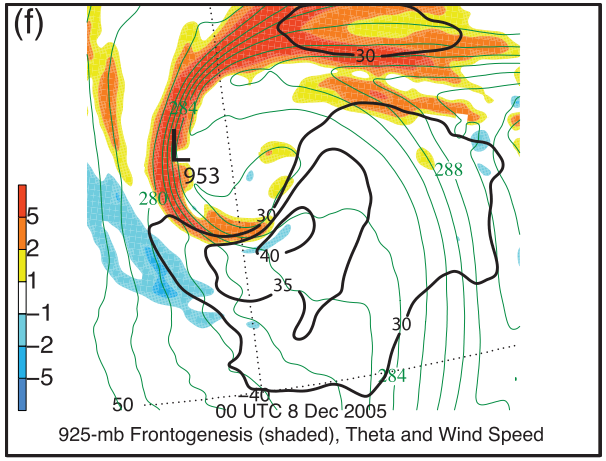

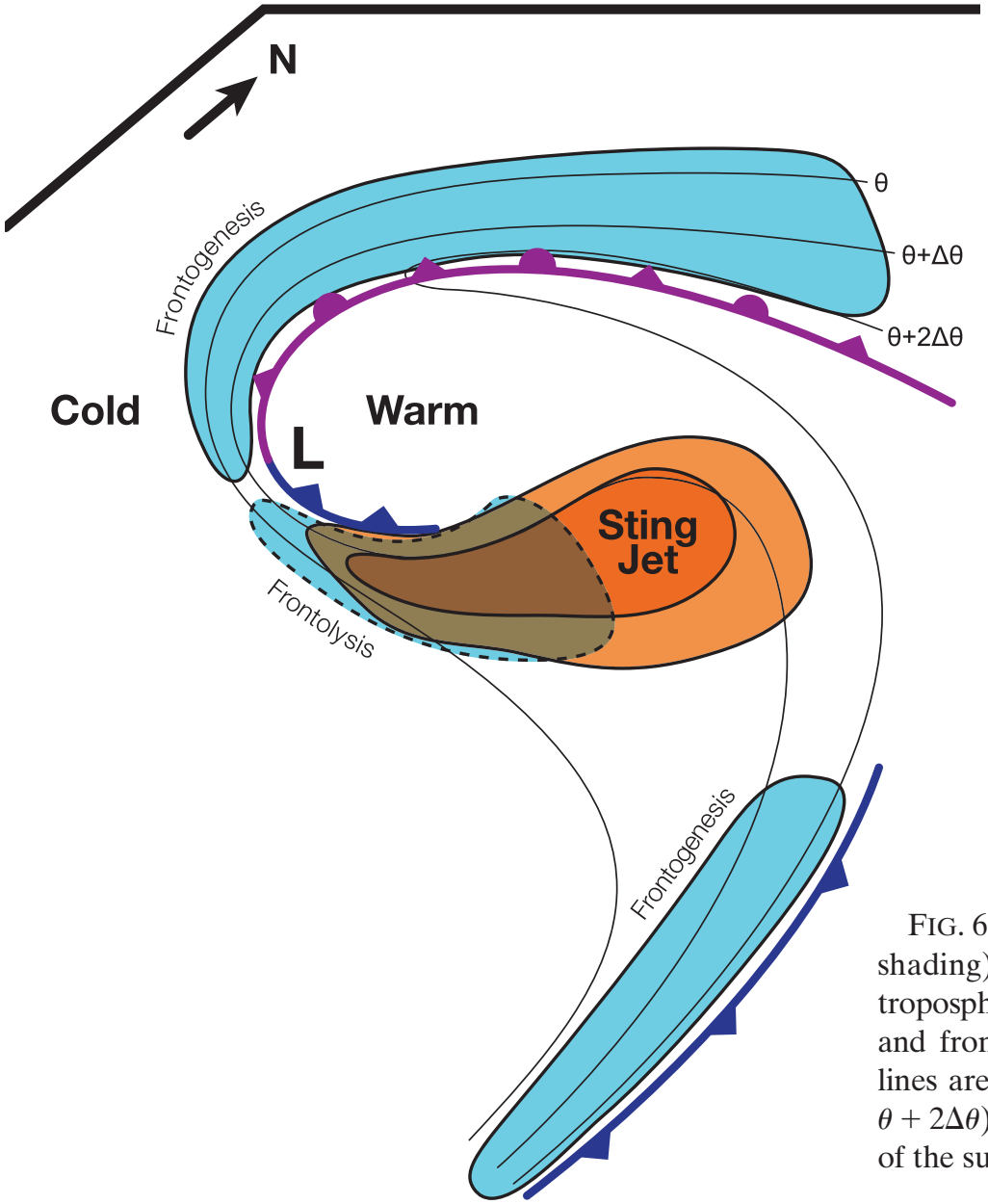

FIG. 6. Conceptual model for the location of a sting jet (orange shading) in a Shapiro–Keyser cyclone, highlighting regions of lower-tropospheric frontogenesis (blue shading surrounded by solid lines) and frontolysis (blue shading surrounded by dashed lines). Thin lines are lower-tropospheric (e.g., 925 hPa) isentropes (θ, $\theta + \Delta\theta$, $\theta + 2\Delta\theta$), frontal symbols are conventional, and L marks the position of the surface low center.

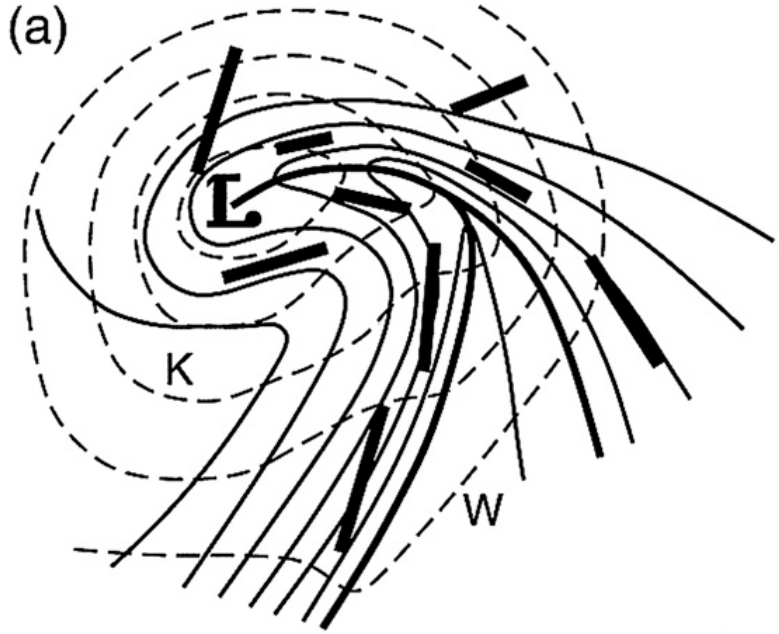

FIG. 7. Schematic comparison of the lower-tropospheric (e.g., 850 hPa) structures of the (a) Norwegian occlusion and (b) Shapiro–Keyser frontal fracture. Dashed lines denote geopotential height, thin solid lines denote potential temperature, thick solid lines represent fronts, and thick line segments represent axes of dilatation of total horizontal wind with segment length proportional to the resultant deformation. Areas surrounded by dotted lines labeled FL in (b) represent regions of frontolysis, and K and W in (a) and (b) denote the cold and warm regions of the cyclones, respectively. The characteristic scale of the cyclones based on the distance from the geopotential height minimum, denoted by L, to the outermost geopotential height contour is 1000 km. [Figure and caption from Fig. 10 in Schultz et al. (1998).]

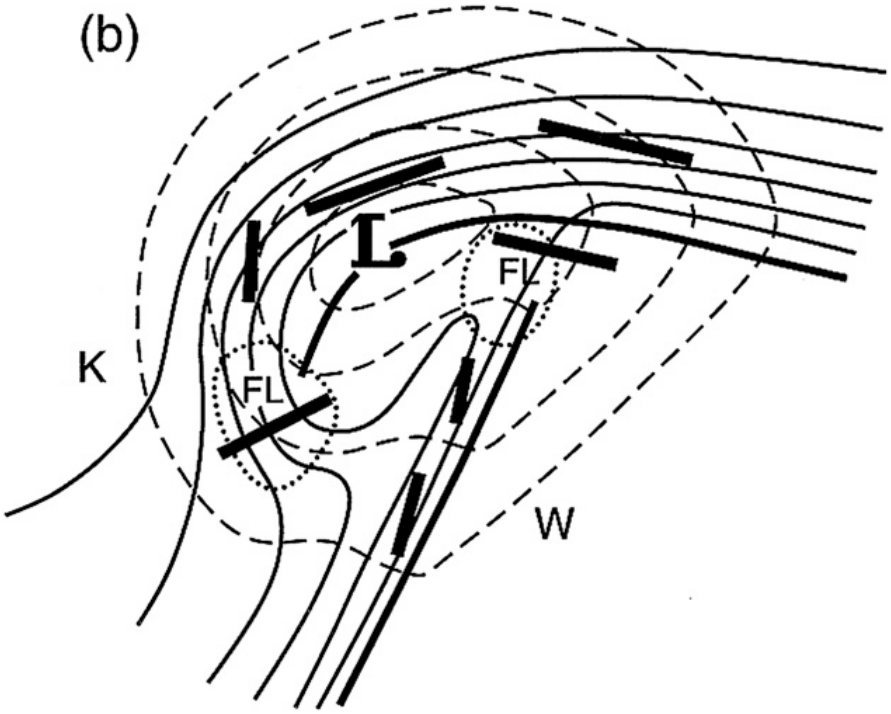

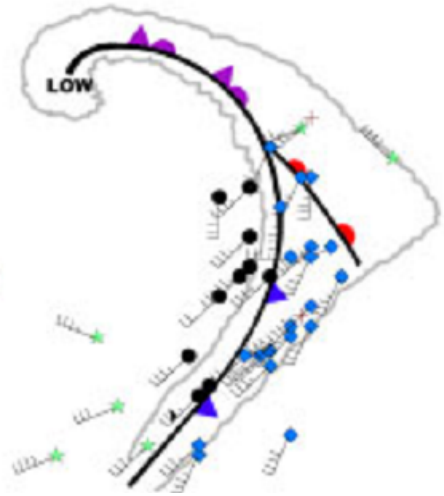

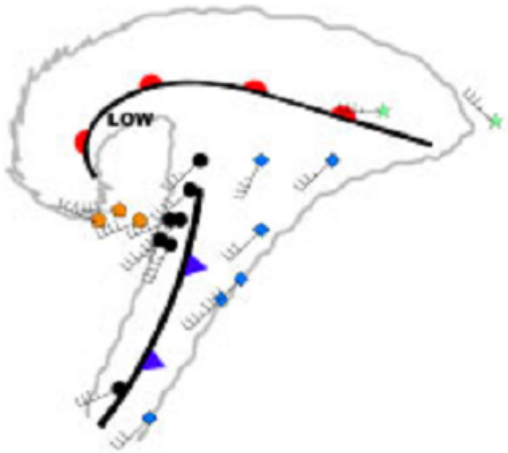

Sting Jet Occurrences

- Most documented Sting Jets have been over European countries bordering Atlantic Ocean.
    - *Oct 1987, Jan 1990, Feb 1990, Jan 1992, Sep 1996, Dec 1999, Oct 2000, Feb 2002, Oct 2002, Jan 2005, etc.*
- Occur most often fall through spring when intense extra-tropical systems are most frequent.
- Have been events over North America that appear to be related to Sting Jets.
    - bordering Pacific Ocean and Great Lakes
- Marine connection not clear…

Sting Jet Occurrences

• Sting Jet occurrence has yet to be formally confirmed in Canada.

- Sep 2003: gusts > 30 m/s in Lake Superior area
- Sep 2006: gusts > 25 m/s in Muskoka region downed trees and cut power to over 90K customers
- Sep 2007: gusts > 25 m/s NE of Lake Superior
- Apr 2011: gusts > 35 m/s in Niagara region, tree damage like ‘war zone’ (and before full foliage!) + two fatalities



Images from 28 Apr 2011 event - http://niagara-gazette.com

24 Sep 2006 Sting Jet?

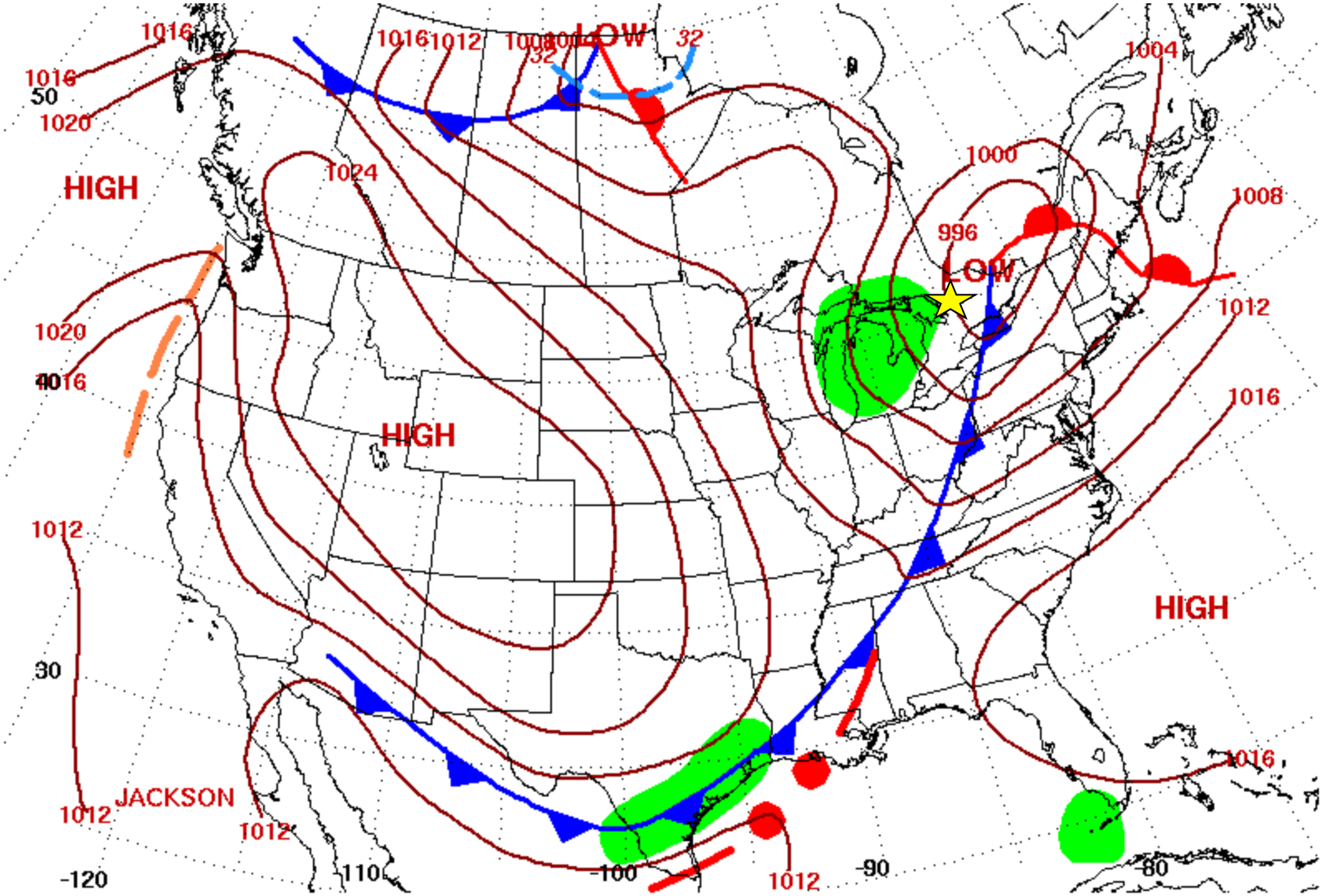

Surface Weather Map at 7:00 A.M. E.S.T.

24 Sep 2006 Sting Jet?

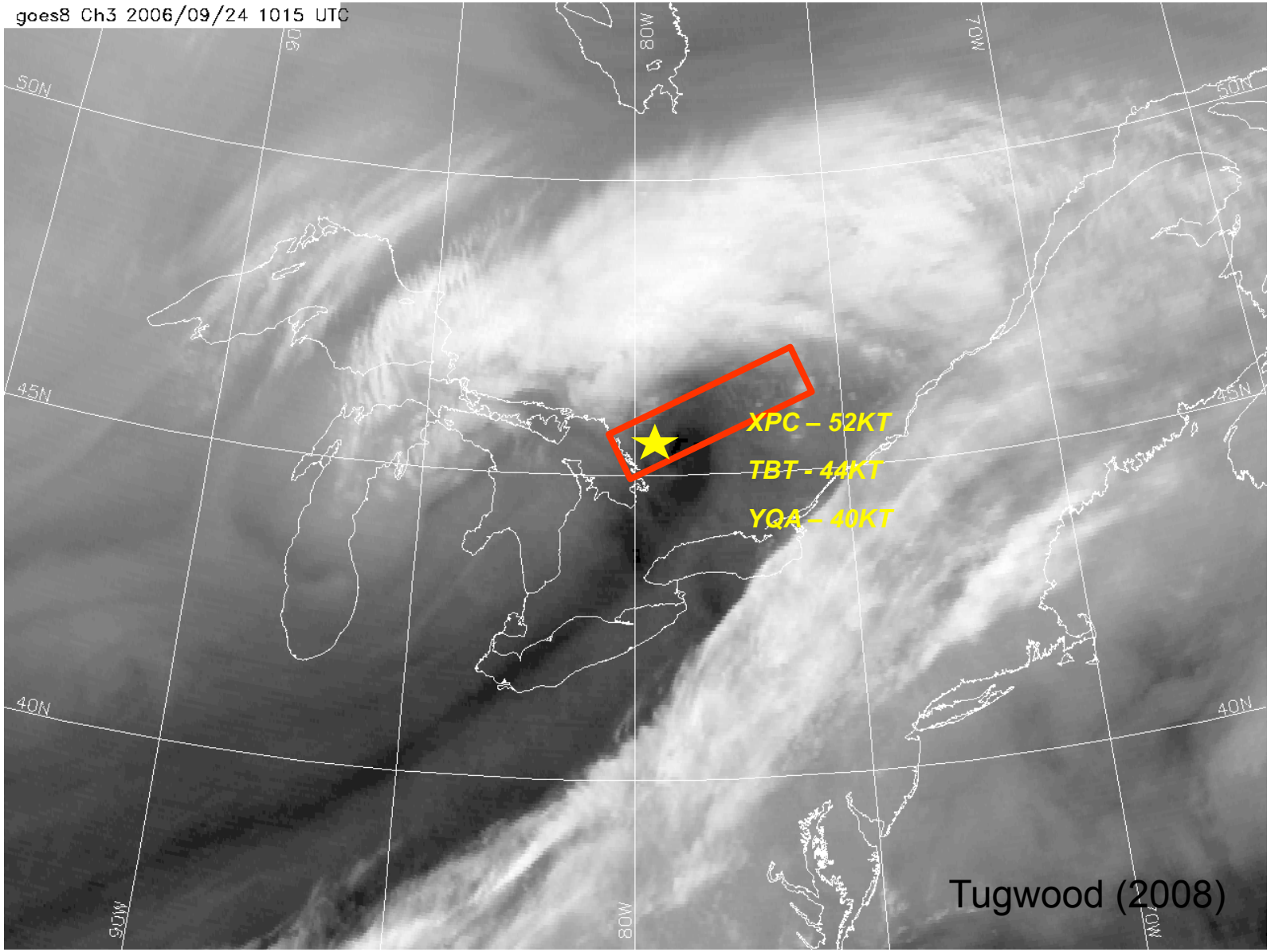

24 Sep 2006 Sting Jet?

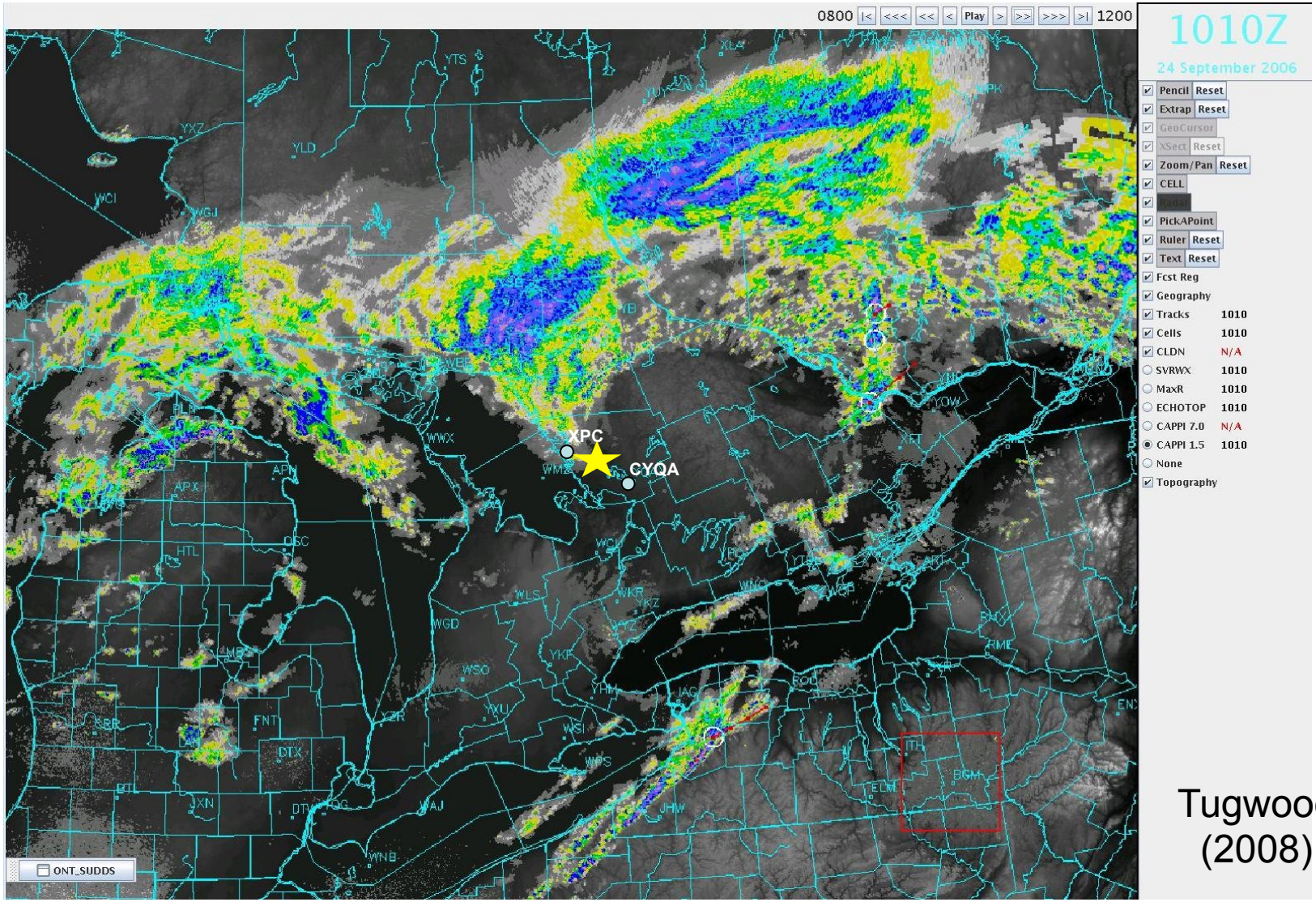

Tugwood (2008)

24 Sep 2006 Sting Jet?

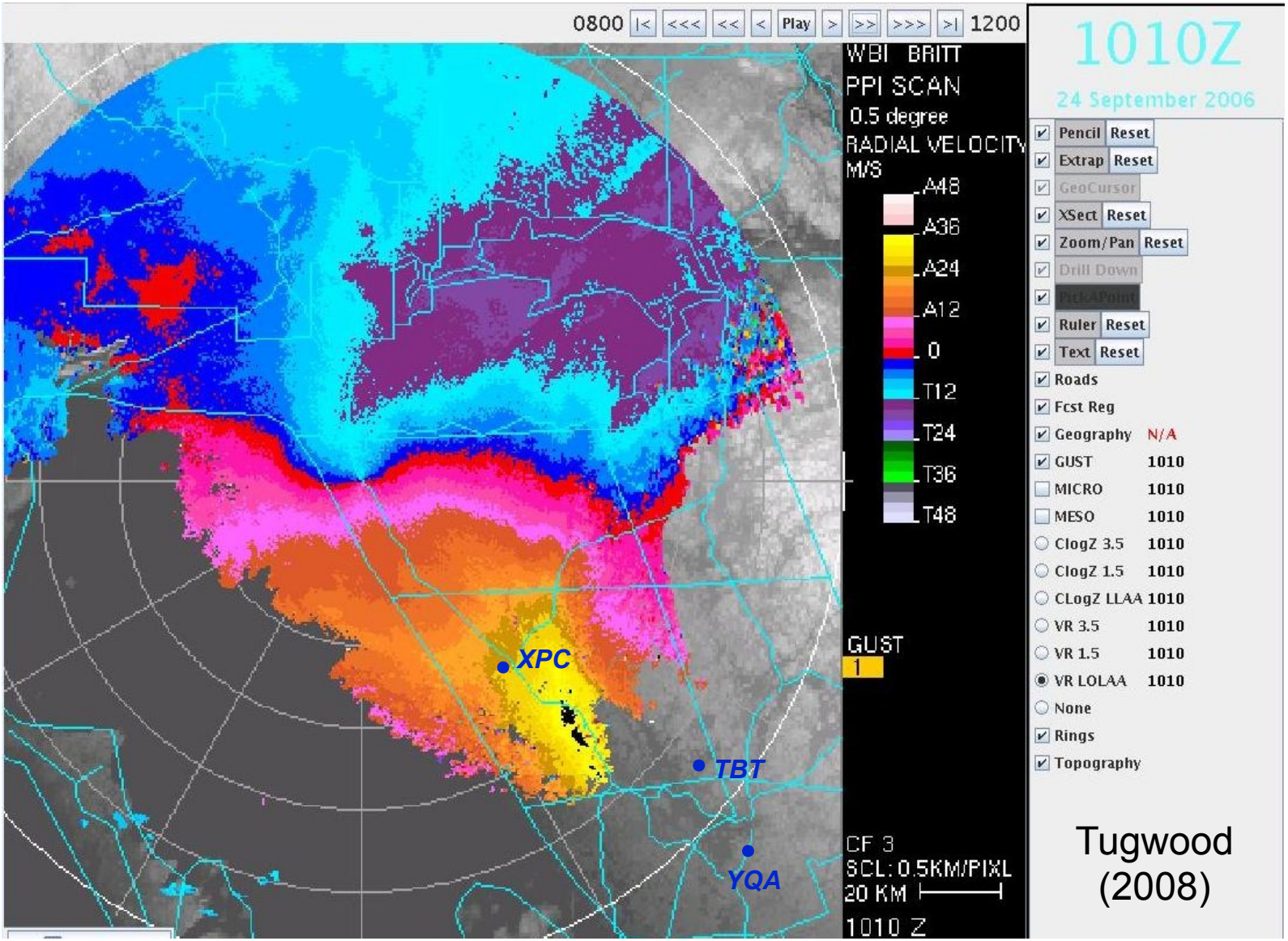

Tugwood (2008)

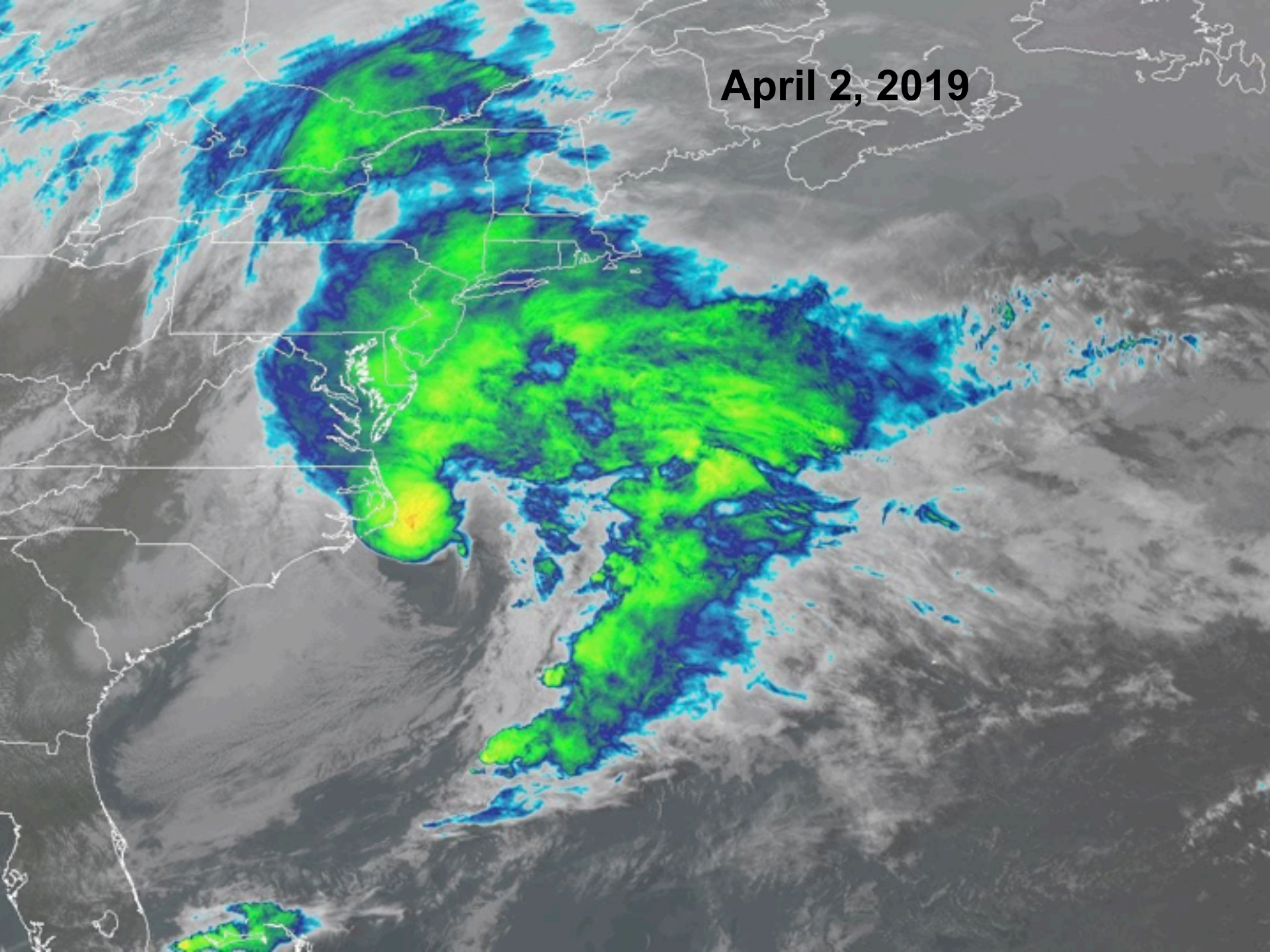
April 2, 2019

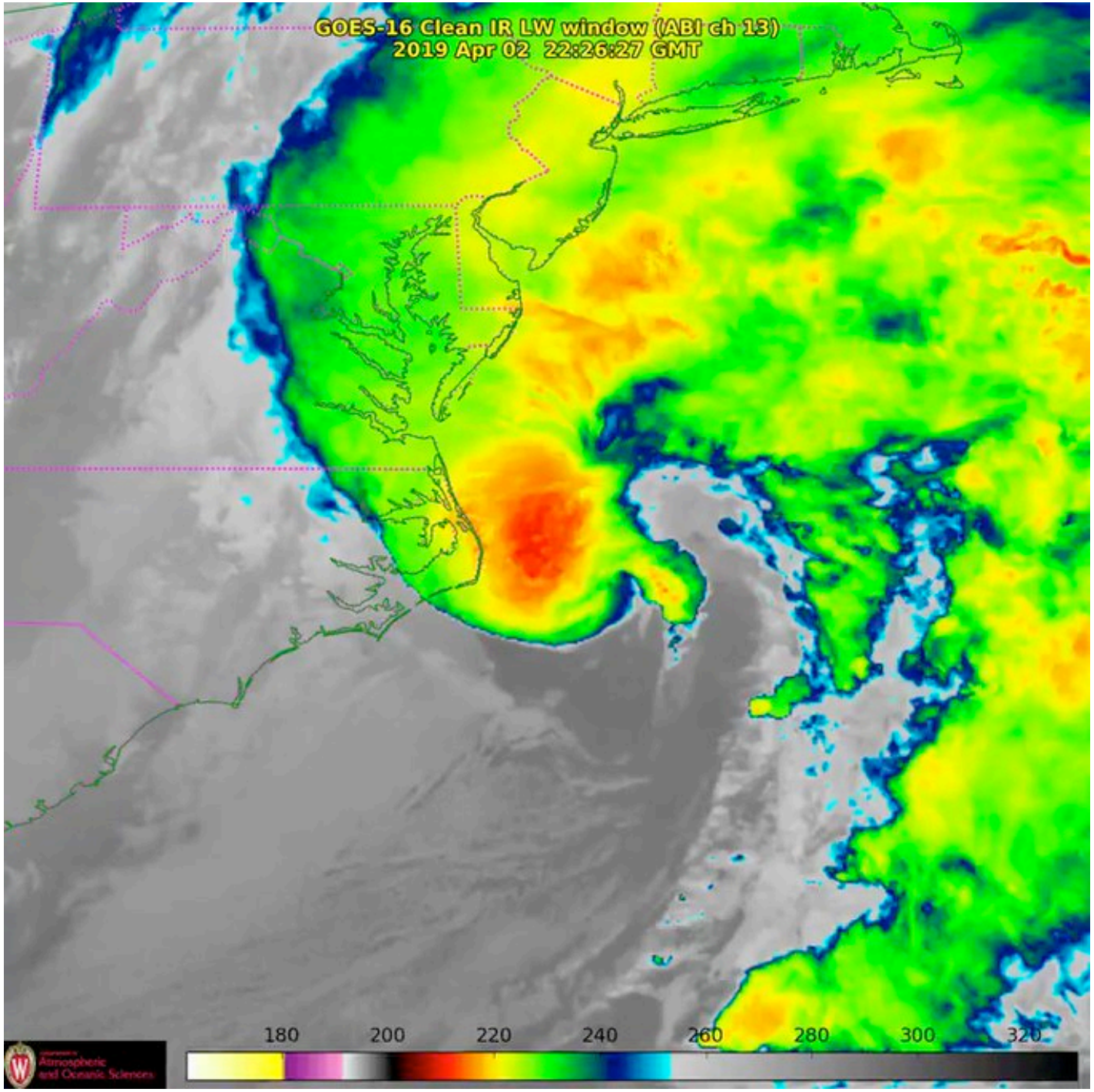
GOES-16 Clean IR LW window (ABI ch 13)
2019 Apr 02 22:26:27 GMT
180
200
220
240
260
280
300
320

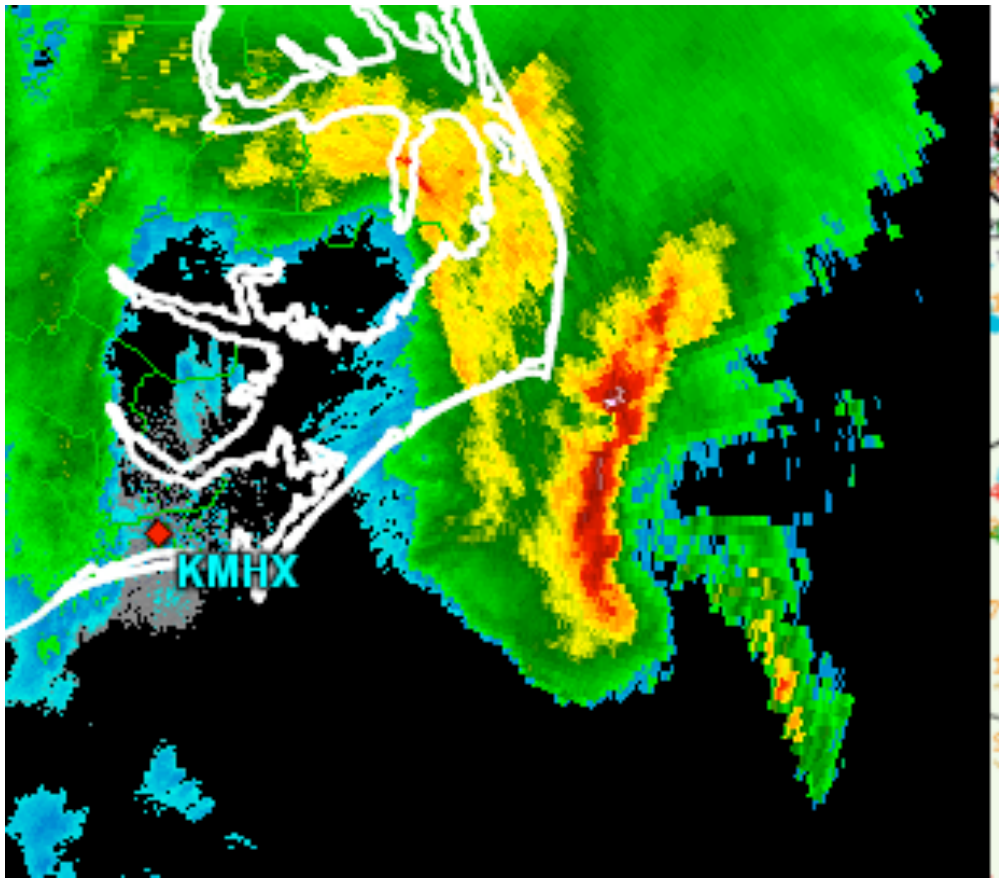

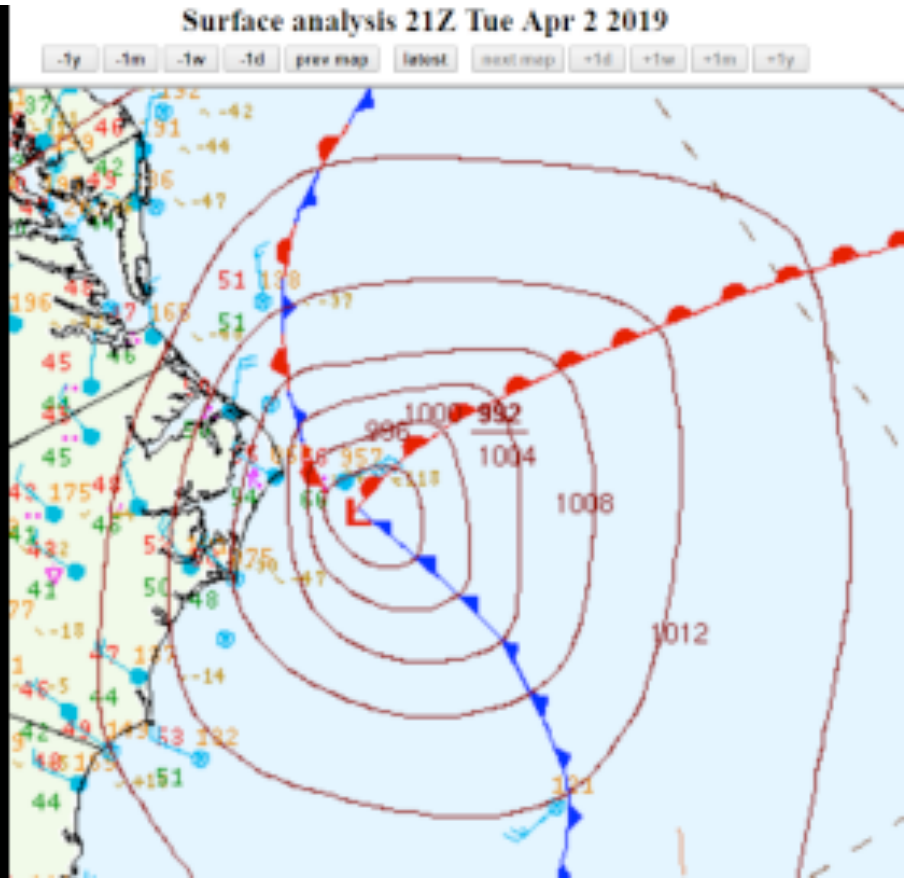

Radar-derived winds aloft have been close to 115 mph

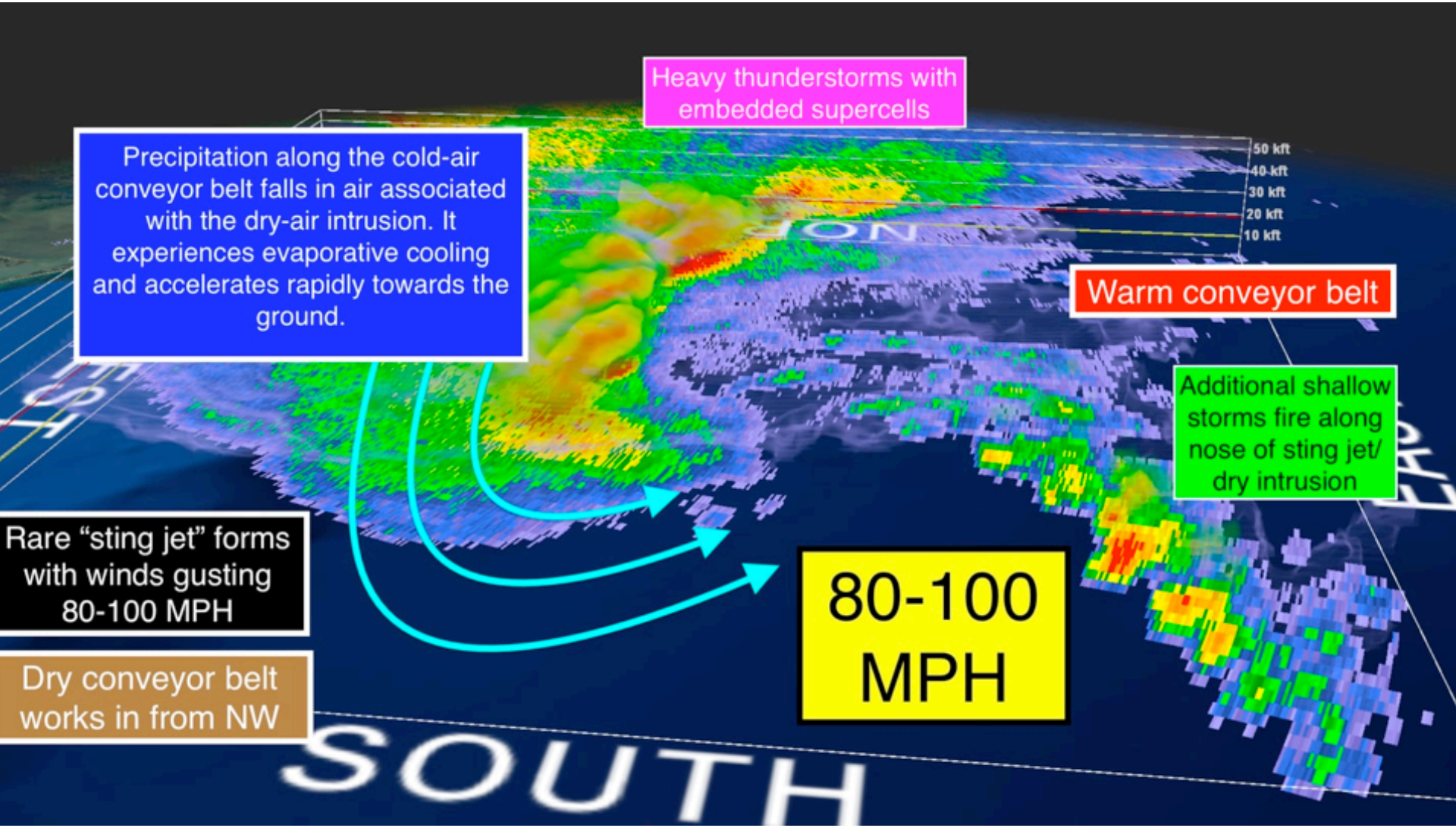
Heavy thunderstorms with embedded supercells
Precipitation along the cold-air conveyor belt falls in air associated with the dry-air intrusion. It experiences evaporative cooling and accelerates rapidly towards the ground.
50 kft
40 kft
30 kft
20 kft
10 kft
Warm conveyor belt
Additional shallow storms fire along nose of sting jet/ dry intrusion
Rare "sting jet" forms with winds gusting 80-100 MPH
Dry conveyor belt works in from NW
80-100 MPH
SOUTH